



NextGEM

Next Generation Integrated Sensing and Analytical System for Monitoring and Assessing Radiofrequency Electromagnetic Field Exposure and Health

D3.8: Analysis of 5G architecture modelling and mapping - Final version

Document Summary Information

Start Date	01/07/2022	Duration	48 months
Project URL	https://www.nextgem.eu/		
Deliverable	D3.4: Analysis of 5G architecture modelling and mapping - Initial version		
Work Package	WP3	Task	T3.4
Contractual due date	31/01/2025	Actual submission date	31/01/2025
Type	Report	Dissemination Level	PUB - Public
Lead Beneficiary	TIM	Deliverable Editor	Alberto Galati, Andrea Schiavoni (FIBER), Maurizio Crozzoli (TIM)



Contributors and Peer Reviewers

Contributors
Daniele Pinchera, Fulvio Schettino, Marco Donald Migliore (UCAS), Alberto Galati, Andrea Schiavoni, Giorgio Calochira, Simone Piacco (FIBER), Maurizio Crozzoli (TIM), Nikolaos Petroulakis (FORTH), Eduardo Soudah (CIMNE)
Peer Reviewers
Marco Spirito (TUD), Fulvio Schettino (UCAS)

Revision history (including peer-reviewing and quality control)

Version	Issue Date	Changes	Contributor(s)
v0.1	08/11/2024	Table of Contents provided	FiberCop
v0.2	11/11/2024	Sections populated with the Task leaders	Alberto Galati, Andrea Schiavoni (FIBER), Maurizio Crozzoli (TIM)
v0.3	26/11/2024	Section defined, assigned, and agreed	Alberto Galati, Andrea Schiavoni (FIBER), Maurizio Crozzoli (TIM)
v0.4	12/12/2024	First contributions	All partners
v0.5	03/01/2025	Integration and harmonization	Alberto Galati, Andrea Schiavoni (FIBER), Maurizio Crozzoli (TIM)
v0.6	10/01/2025	Second contributions and updates	All partners
v0.7	17/01/2025	Complete version ready for peer review	Alberto Galati, Andrea Schiavoni (FIBER), Maurizio Crozzoli (TIM)
v0.8	24/01/2025	Peer review and comments addressed	Marco Spirito (TUD), Fulvio Schettino (UCAS)
v0.9	29/01/2025	Technical and quality assurance review and comments addressed	Mats-Olof Mattsson (SPi), Nicolas Louca (EBOS)
v1.0	31/01/2025	Final review and submission	Nikolaos Petroulakis (FORTH)

Disclaimer

Funded by the European Union. Views and opinions expressed are however those of the author(s) only and do not necessarily reflect those of the Euro pean Union or the European Commission. Neither the European Union nor the granting authority can be held responsible for them.”

While the information contained in the documents is believed to be accurate, the authors(s) or any other participant in the NextGEM consortium make no warranty of any kind with regard to this material including, but not limited to the implied warranties of merchantability and fitness for a particular purpose.

Neither the NextGEM Consortium nor any of its members, their officers, employees, or agents shall be responsible or liable in negligence or otherwise howsoever in respect of any inaccuracy or omission herein.

Without derogating from the generality of the foregoing neither the NextGEM Consortium nor any of its members, their officers, employees, or agents shall be liable for any direct or indirect or consequential loss or damage caused by or arising from any information advice or inaccuracy or omission herein.

Copyright message

© NextGEM Consortium. This deliverable contains original unpublished work except where clearly indicated otherwise. Acknowledgement of previously published material and of the work of others has been made through appropriate citation, quotation, or both. Reproduction is authorised provided the source is acknowledged.

Table of Contents

Executive Summary.....	12
1 Introduction.....	13
1.1 Mapping NextGEM Outputs	13
1.2 Deliverable overview and report structure	14
1.3 Updates from previous Deliverable D3.4 “Analysis of 5G architecture modelling and mapping - Initial version”.....	14
2 International Guidelines and Standards.....	15
2.1 Whole body vs localized exposure: different approaches.....	17
2.2 Status of standards.....	17
3 Mobile network planning: exposure to EMF, coverage, and performances requirements need to be matched at the same time.	19
4 MaMIMO antennas require a new approach for evaluating exposure to EMF.....	21
4.1 MaMIMO Antennas in 5G NR.....	21
4.1.1 The envelope radiation pattern	24
4.1.2 Power associated with Broadcast and power associated with Traffic beams: the 5G NR frame	24
4.2 A change of paradigm in radiation: from a deterministic to a statistical approach	26
4.2.1 Exposure at location.....	28
4.2.2 SINR at location	29
5 Activities planned in Task 3.4.....	30
5.1 Background.....	30
5.2 Structure and Expected Results	30
6 Requirements for Simulations.....	32
6.1 The Scenario.....	32
6.1.1 General	32
6.1.2 The Modified Madrid Grid Scenario	32
6.1.3 The Real Town Scenario.....	38
6.1.4 The Indoor Scenario	39
6.1.5 The Scenario in FR2.....	40
6.2 Transmitter.....	41
6.2.1 Position and height.....	41
6.2.2 Frequencies.....	41
6.2.3 Power.....	42
6.2.4 Radiation pattern	42
7 Description of the Computational Tools	44
7.1 UNICAS simulation tool.....	44
7.2 TIM - FiberCop simulation tool (T3D e FIA)	45
7.2.1 General	45
7.2.2 Intelligent Ray Tracer	45

7.2.3	Fast Indoor Analysis.....	46
8	Evaluation of the exposure to EMF	47
8.1	Users Distribution manages the exposure	48
8.1.1	Amount of data assigned to each user.....	48
8.1.2	Capacity of each 5G NR BTS equipped with MaMIMO antenna.....	49
8.1.3	SINR to Throughput.....	49
8.1.4	Users time and Space distribution.....	50
8.1.5	Power level assigned to each beam.....	50
9	Simulations and Results.....	51
9.1	UNICAS Simulations and Results.....	51
9.1.1	Antenna model.....	51
9.1.2	Generated pattern for FR1	52
9.1.3	Generated pattern for FR2	53
9.1.4	Generated pattern for INDOOR.....	55
9.1.5	Simulations in MMGS.....	57
9.2	TIM - FiberCop Simulations.....	62
9.2.1	Simulations in MMGS Scenario	62
9.2.2	Simulations in Real Town Scenario	74
9.2.3	Simulations in Indoor Office (IO) Scenario	80
9.2.4	Simulations in Indoor Industrial Hangar (IIH) Scenario.....	83
9.2.5	Simulations in FR2 reduced MMGS scenario.....	88
10	Conclusion.....	91
	References	93

List of Figures

Figure 1: Basic restrictions as defined in ICNIRP2020 for time intervals ≥ 6 min [1].....	15
Figure 2 : Basic restrictions as defined in ICNIRP2020 integrated over < 6 min time interval [1].....	15
Figure 3: Reference levels as defined in ICNIRP2020 per whole body exposure, averaged over a 30-minute time interval [1].....	16
Figure 4: Reference levels as defined in ICNIRP2020 per local exposure, averaged over a 6 minutes time interval [1]	16
Figure 5: Reference levels as defined in ICNIRP2020 per local exposure, integrated over <6 minutes time interval [1]	17
Figure 6: The design process of a mobile telecommunication network.....	19
Figure 7: a) Passive antennas radiation pattern coverage. b) MaMIMO antennas coverage.....	20
Figure 8: The time dependent beam arrangement to serve users located in the scenario.	21
Figure 9: The configuration structure for a generic MaMIMO antenna.....	22
Figure 10: Broadcast fixed beam coverage (a) and sweeping beam (b) coverage area definition.	22
Figure 11: Traffic beams of a GoB MaMIMO antenna (a) and Traffic beam for an EBB MaMIMO antenna (b).	23
Figure 12: Time Traffic Radiation Pattern of a GoB MaMIMO antenna (a) and Time Traffic Radiation Pattern for an EBB MaMIMO antenna (b).	23
Figure 13: Example of Envelope Elevation Radiation Pattern: the red curve identifies the maximum gain in each direction.....	24
Figure 14: 5G frame in the absence of users; on the left bottom 6 SSBs are visible; apart the SSB and some control signals, the frame is void.....	25
Figure 15: Full-loaded 5G frame; on the left bottom 6 SSBs are visible; the void area in the centre and at the end of the frame are the sections of the frame reserved for uplink data, almost all the remaining area is filled by PDSCH REs (users data).	25
Figure 16: The higher received power of the PDSCH REs compared to the SSB REs is due to the different beams used, broadcast beams for SSBs and traffic beams for PDSCH; traffic beams (used to send payload data to the UE) have a greater directivity than the broadcast.	26
Figure 17: Scenario coverage without any power control or beamsteering.	27
Figure 18: Scenario coverage with a technology implementing power control applied to a passive antenna.	27
Figure 19: Scenario coverage with a technology implementing power control applied to a MaMIMO antenna....	27
Figure 20: Exposure contributions to an observation point.	29
Figure 21: The simulation scheme adopted in task T3.4.	31
Figure 22: A schematic view of the simulation activities in task T3.4.....	32
Figure 23: The basic tile of the MMGS.....	33
Figure 24: The basic tile of the MMGS with building entrance. Building marked in the same way have building entrances in the same location.	34
Figure 25: The basic tile of the MMGS with metro entrance and bus stop.	34
Figure 26: The basic tile of the MMGS with crossing lanes.....	34
Figure 27: The basic tile of the MMGS with adopted cartesian coordinates.....	35
Figure 28: Example of the building represented by MMGS data file.....	35
Figure 29: a) the basic MMGS tile in 3D representation, b) the representation of a town.	37
Figure 30: a) Portion of real town. b) reconstructed model.	38

Figure 31: a) Portion of real town. b) reconstructed model.	39
Figure 32 Example of a real environment model with planimetric info.	39
Figure 33: Example of an office indoor modelling proposed to partners.	40
Figure 34: Example of an industrial hangar modelling proposed to partners.	40
Figure 35: Scenario adopted in FR2.....	40
Figure 36: example of installed BTS in the MMGS.	41
Figure 37: Scheme of the regular array (red elements) organized into subarrays (yellow rectangles) with a ground plane (cyan).	43
Figure 38: example of BASTA 2.0 .3drp standard	43
Figure 39: Example of the calculated rays (Blue) for the connection to a user (red) and the pattern used by the base station for the connection (cyan).	45
Figure 40: example of 3D scenario in TP3D.	45
Figure 41: example of connection between element of the scenario.....	46
Figure 42: Field calculation at receiving point.	46
Figure 43: Example of a FIA simulation.	46
Figure 44: A schematic view of the computation process.	47
Figure 45: Downloaded data per quarter of hour by the cell.	49
Figure 46: Downlink link level throughput.....	50
Figure 47 Array scheme: a) x, z view; b) perspective view; c) spherical coordinate system employed.	51
Figure 48 Example pattern for the FR1 antenna synthesized, relative to the file UNICAS_REF02_3600_B1309_+45_Pencil_Generic_draft.3drp.....	53
Figure 49 envelope Patten for the FR1 antenna synthesized, relative to the file UNICAS_REF02_3600_E425_+45_Envelope_Generic_draft.....	53
Figure 50 Example pattern for the FR2 antenna synthesized, relative to the file UNICAS_REF03_26000_B2107_+45_Pencil_Generic_draft.....	54
Figure 51 envelope Patten for the FR2 antenna synthesized, relative to the file UNICAS_REF03_26000_E533_+45_Envelope_Generic_draft.....	55
Figure 52 Example pattern for the INDOOR antenna synthesized, relative to the file UNICAS_REF04_3700_B401_-45_Pencil_Generic_draft.....	56
Figure 53 envelope Patten for the INDOOR antenna synthesized, relative to the file UNICAS_REF04_3700_E8_+45_Envelope_Generic_draft.....	56
Figure 54 Examples of the paths calculated with the Ray Launching Software.....	57
Figure 55 Analysis of square A.....	58
Figure 56 Analysis of Square B.....	58
Figure 57 Analysis of Square C.....	59
Figure 58 Analysis of square D.....	59
Figure 59 Summary of the difference in power level achieved in the four squares.....	60
Figure 60: Analysis of street E.....	61
Figure 61 Analysis of street F.....	61
Figure 62: a) a scheme representing the positions of the cells in the MMGS and b) a 3D portion of the MMGS scenario radiated by 1 beam; c) exposure along a street surrounded by buildings.....	62
Figure 63: Schematic representation of the beams each MaMIMO antenna can generate in azimuth and elevation.	63

Figure 64: The TDD scheme used in simulations. The MaMIMO antenna radiates only in the downlink TTI. ...	63
Figure 65: 360 s Averaged Radiated Power.....	66
Figure 66: CDF of the 360s Averaged Radiated Power.....	67
Figure 67: Example of Users distribution in time.	67
Figure 68: 360 s Averaged Electric Field in the most exposed point for each cell. a) step average, b) rolling average	67
Figure 69: 1800 s Averaged Electric Field in the most exposed point for each cell. a) step average, b) rolling average	67
Figure 70: Time evolution of the exposure in the scenario. a) interval 1, b) interval 2, c) interval 3	68
Figure 71: a) 360 s Averaged Radiated Power; b) CDF of the 360s Averaged Radiated Power.....	68
Figure 72: 360 s Averaged Electric Field in the most exposed point for each cell. a) 360 s step average, b) 1800 s step average.....	69
Figure 73: a) 360 s Averaged Radiated Power; b) CDF of the 360s Averaged Radiated Power.....	69
Figure 74: 360 s Averaged Electric Field in the most exposed point for each cell. a) 360 s step average, b) 1800 s step average.....	69
Figure 75: a) 360 s Averaged Radiated Power; b) CDF of the 360s Averaged Radiated Power.....	70
Figure 76: 360 s Averaged Electric Field in the most exposed point for each cell. a) 360 s step average, b) 1800 s step average.....	70
Figure 77: a) 360 s Averaged Radiated Power; b) CDF of the 360s Averaged Radiated Power.....	71
Figure 78: 360 s Averaged Electric Field in the most exposed point for each cell. a) 360 s step average, b) 1800 s step average.....	71
Figure 79: a) 360 s Averaged Radiated Power; b) CDF of the 360s Averaged Radiated Power.....	72
Figure 80: 360 s Averaged Electric Field in the most exposed point for each cell. a) 360 s step average, b) 1800 s step average.....	72
Figure 81: a) 360 s Averaged Radiated Power; b) CDF of the 360s Averaged Radiated Power.....	73
Figure 82: 360 s Averaged Electric Field in the most exposed point for each cell. a) 360 s step average, b) 1800 s step average.....	73
Figure 83: a) 360 s Averaged Radiated Power; b) CDF of the 360s Averaged Radiated Power.....	73
Figure 84: 360 s Averaged Electric Field in the most exposed point for each cell. a) 360 s step average, b) 1800 s step average.....	73
Figure 85: a) 360 s Averaged Radiated Power; b) CDF of the 360s Averaged Radiated Power.....	74
Figure 86: 360 s Averaged Electric Field in the most exposed point for each cell. a) 360 s step average, b) 1800 s step average.....	74
Figure 87: Real town scenario and coverage.....	75
Figure 88: a) 360 s Averaged Radiated Power; b) CDF of the 360s Averaged Radiated Power.....	76
Figure 89: 360 s Averaged Electric Field in the most exposed point for each cell. a) 360 s step average, b) 1800 s step average.....	76
Figure 90: a) 360 s Averaged Radiated Power; b) CDF of the 360s Averaged Radiated Power.....	76
Figure 91: 360 s Averaged Electric Field in the most exposed point for each cell. a) 360 s step average, b) 1800 s step average.....	76
Figure 92: a) 360 s Averaged Radiated Power; b) CDF of the 360s Averaged Radiated Power.....	77
Figure 93: 360 s Averaged Electric Field in the most exposed point for each cell. a) 360 s step average, b) 1800 s step average.....	77
Figure 94: a) 360 s Averaged Radiated Power; b) CDF of the 360s Averaged Radiated Power.....	77

Figure 95: 360 s Averaged Electric Field in the most exposed point for each cell. a) 360 s step average, b) 1800 s step average.....	77
Figure 96: a) 360 s Averaged Radiated Power; b) CDF of the 360s Averaged Radiated Power.....	78
Figure 97: 360 s Averaged Electric Field in the most exposed point for each cell. a) 360 s step average, b) 1800 s step average.....	78
Figure 98: a) 360 s Averaged Radiated Power; b) CDF of the 360s Averaged Radiated Power.....	78
Figure 99: 360 s Averaged Electric Field in the most exposed point for each cell. a) 360 s step average, b) 1800 s step average.....	78
Figure 100: a) 360 s Averaged Radiated Power; b) CDF of the 360s Averaged Radiated Power.....	79
Figure 101: 360 s Averaged Electric Field in the most exposed point for each cell. a) 360 s step average, b) 1800 s step average.....	79
Figure 102: a) 360 s Averaged Radiated Power; b) CDF of the 360s Averaged Radiated Power.....	79
Figure 103: 360 s Averaged Electric Field in the most exposed point for each cell. a) 360 s step average, b) 1800 s step average.....	79
Figure 104: a) 360 s Averaged Radiated Power; b) CDF of the 360s Averaged Radiated Power.....	80
Figure 105: 360 s Averaged Electric Field in the most exposed point for each cell. a) 360 s step average, b) 1800 s step average.....	80
Figure 106: a) the 3D view of the scenario and b) and c) an example of coverage of the MaMIMO antenna.....	80
Figure 107: Arrangement of the antenna beams for the Indoor Hangar Industrial Scenario.....	81
Figure 108: a) 360 s Averaged Radiated Power; b) CDF of the 360s Averaged Radiated Power.....	82
Figure 109: Step Averaged Electric Field in PoCs. a) 360 s average, b) 1800 s average.....	83
Figure 110: a) 360 s Averaged Radiated Power; b) CDF of the 360s Averaged Radiated Power.....	83
Figure 111: Step Averaged Electric Field in PoCs. a) 360 s average, b) 1800 s average.....	83
Figure 112: The industrial hangar scenario and the positions of the radiating points.....	84
Figure 113: An example of coverage in the IHH scenario for one of the available beams on the cell.....	84
Figure 114: Arrangement of the antenna beams for the Indoor Hangar Industrial Scenario.....	84
Figure 115: a) 360 s Averaged Radiated Power; b) CDF of the 360s Averaged Radiated Power.....	87
Figure 116: 360 s Step Averaged Electric Field PoCs. a) PoC1, b) PoC2.....	87
Figure 117: 1800 s Averaged Electric Field in the PoCs. a) PoC1, b) PoC2.....	87
Figure 118: a) 360 s Averaged Radiated Power; b) CDF of the 360s Averaged Radiated Power.....	87
Figure 119: 360 s Step Averaged Electric Field PoCs. a) PoC1, b) PoC2.....	88
Figure 120: 1800 s Averaged Electric Field in the PoCs. a) PoC1, b) PoC2.....	88
Figure 121: The reduced MMGS scenario used for FR2 simulations. a) the position of antenna. b) 3D scenario and details on users' model.....	88
Figure 122: The main plaza with the presence of users.....	89
Figure 123: Schematic representation of the beams each MaMIMO antenna can generate in azimuth and elevation.....	89
Figure 124: field distribution in the scenario generated by 3 different beams. a) Test1, b) Test4.....	90

List of Tables

Table 1: Adherence to NextGEM's GA Tasks and Deliverables Descriptions.	13
Table 2: The structure of the polyline representing a building.	36
Table 3: A numerical example for the representation of buildings in the scenario.	36
Table 4: Parametrization of the material characteristics as defined in [7].	37
Table 5: Electromagnetic characteristics of the materials present in MMGS.	38
Table 6: FR1-FR2 frequency coding for 5G NR.	41
Table 7: Power associated with each BTS to be used in the computations.	42
Table 8: Estimate of the data traffic per month per smartphone (from [10]).	48
Table 9: Parameters for the FR1 Antenna	52
Table 10: Parameters for the FR2 antenna	54
Table 11: Parameters for the Indoor antenna.	55
Table 12: Simulation path for MMGS Scenario	64
Table 13: Cell Radiated Power	65
Table 14: Incident Energy Density for exposure time lower than 6 min in each Point of Control	65
Table 15: Cell Radiated Power	68
Table 16: Cell Radiated Power	69
Table 17: Cell Radiated Power	70
Table 18: Cell Radiated Power	71
Table 19: Cell Radiated Power	71
Table 20: Cell Radiated Power	72
Table 21: Cell Radiated Power	73
Table 22: Cell Radiated Power. StdDev = standard deviation.	74
Table 23: Service distribution per test	75
Table 24: Services considered in IO simulations and their characteristics.	81
Table 25: Description of the service load per hour of the day per user.	81
Table 26: Services considered in IIH simulations their characteristics	85
Table 27: Description of the service load per hour of the day per user.	85
Table 28: Maximum Electric field computed in PoC, the term F_{TDC} included in the field value.	90

Glossary of terms and abbreviations used

Abbreviation / Term	Description
5G NR	5G New Radio
5G gNB	5G g Node B
AAS	Active Antenna System
BTS	Base Transceiver Station
CENELEC	Comité européen de normalisation en électronique et en électrotechnique
EBB	Eigen Based Beamforming
FIA	Fast Indoor Analysis
EMF	Electromagnetic Field
FR1, FR2	Frequency Range 1, Frequency Range 2
GA	Grant Agreement
GoB	Grid of Beam
ICNIRP	International Commission on Non-Ionizing Radiation Protection
IEC	International Electrotechnical Commission
IEEE	Institute of Electrical and Electronics Engineers
MaMIMO	Massive Multiple Input Multiple Output
MGS	Madrid Grid Scenario
MMGS	Modified Madrid Grid Scenario
OOB	Out of Band
OFDM	Orthogonal Frequency Division Multiplexing
PBCH	Primary Broadcast Channel
PBCH-DMRS	Primary Broadcast Channel-DeModulation Reference Signal
PDCCH	Physical Downlink Control Channel
PDSCH	Physical Downlink Shared Channel
RE	Resource Element
SAR	Specific Absorption Rate

SINR	Signal to Interference plus Noise Ratio
SS	Synchronization Signal
SS-PBCH	Synchronization Signal – Primary Broadcast Channel
SSB	Synchronization Signal Block
UE	User Equipment
PE	Primary Element
RU	Radio Unit
U_{ab}	Absorbed Power Density
TDD	Time Division Duplex
TTI	Transmission Time Interval
TP3D	TIMPlan 3D
ZFB	Zero Forcing Beamforming

Executive Summary

This deliverable is relevant for the description and definitions of scenarios and parameters to be used in simulations to analyze the exposure distribution generated by Massive Multiple Input Multiple Output (MaMIMO) antennas as used in 5G New Radio (5G NR). All the aspects of the exposure evaluation are described:

- Scenarios: including a simplified model of a real town, an application scenario for mmWaves and an indoor scenario.
- MaMIMO antenna models: represented as a set of radiation patterns radiating in different directions.
- User's and network characterization.

The content of this deliverable, up to section 8, forms the basis for performing simulations planned in task T3.4 to characterize the whole-body EMF exposure generated by base station transmitters in as many realistic environments as possible, as allowed by the current technology and available computation tools and techniques.

From Section 9 onwards, the results of the simulation activities, based on the parametrizations described in this deliverable, are collected, subdivided by scenario. The time and space evolution of users is described as well as the load activity for each user, functional to the determination of the field level in each observation point.

As indicated in Section 2, exposure in wide area scenarios like the coverage area by a BTS is much different from local exposure. Such examples are the exposure generated by cellular phones or body worn devices. The two exposure contexts are not comparable; for this reason, international guidelines clearly distinguish the two exposure situations establishing exposure limits for localized exposure and whole-body exposure, even using different metrics and different limits, as well as dosimetry quantities that are simpler to measure with respect to localized exposure dosimetry quantities. This feature needs to be always considered when analysing the results generated in Task 3.4 and when relating these results with activities planned in other Tasks in NextGEM.

1 Introduction

The determination of the Electromagnetic Field (EMF) level in wide area scenarios, like a whole town or large rural areas, generated by base stations equipped with MaMIMO antennas requires the definition of a set of parameters such as:

- Definition of the geometrical and electromagnetic properties of the scenario,
- Definition of the properties and characteristics of the radiating systems,
- Definition of the load condition of the network,
- Definition of the users' time and space distribution and activity,
- Definition of the points where the exposure to EMF is observed,
- Definition of parameters for characterizing the exposure, as required by international guidelines and standards.

All these parameters contribute to the characterization of the simulation activities to compute the whole-body exposure in large scenarios, considering the time and space variability generated by MaMIMO antennas as used in 5GNR.

The aim of the first sections of this report is to provide the specification of common parameters, among the task T3.4 partners, that are involved in computations. By sharing and defining common parameters, like scenarios, radiated power, or MaMIMO radiation patterns will allow each partner to have a complete set of input data to evaluate the whole-body exposure to EMFs to perform simulations.

The development of the computational activities with a direct link to the requirement for evaluating the whole-body exposure, as required by international guidelines, allows a complete starting point for the evaluation of the local electromagnetic field in a complex and realistic environment.

The analysis within the activities planned in task T3.4, of the radiating characteristics of the MaMIMO antenna, by synthesizing the set of beams the antenna can generate to serve users dislocated in the scenario, allows to include the spatial statistics of the radiation in simulations. This is different from what was done for simulating fixed beam antennas used for technologies earlier than 5G NR.

The estimates of realistic network load condition, user activity, and throughput-Signal To Interference Noise Ratio (SINR) function, allow the characterization of the whole-body EMF exposure by considering all the aspects involved in a mobile network. This deliverable reports the results obtained in task T3.4, in conjunction with activities that will be developed in task T7.3. Deliverables D3.4 and D3.8 give a global and complete view of the exposure levels that can be found in deployment scenarios.

1.1 Mapping NextGEM Outputs

The purpose of this section is to map NextGEM's Grant Agreement (GA) commitments, both within the formal Task description and Deliverable, against the project's respective outputs and work performed.

Table 1: Adherence to NextGEM's GA Tasks and Deliverables Descriptions.

TASKS	
Task Number & Title	Respective extract from formal Task Description
Task 3.4 - 5G architecture modelling and mapping	One of the aspects to be considered when a new telecommunication technology is designed, is its impact on EMF exposure over the general population and on-field workers alike. Therefore, main aspects of the technology, such as architecture and radio access technologies used to distribute EMF over different scenarios, should be considered at the early stages of the new technology definition even for managing and radiation monitoring aspects. Thus, monitoring capabilities and radiated signal characteristics are considered by standardization bodies during early stages of a new technology. This task analyses aspects related to 5G NR technology by performing simulations and modelling in different scenarios to consider the effect of transmitter positioning and changes inside the scenario over the field distribution.

DELIVERABLES

Deliverable D3.8: Analysis of 5G architecture modelling and mapping – Final version (M31)

This deliverable will describe the 5G NR landscape after simulations in different scenarios considering the effect of transmitter positioning and changes inside the scenario over the field distribution.

1.2 Deliverable overview and report structure

The structure of deliverable D3.8 is as follows:

- Section 2 performs an overview of the international guidelines in force on exposure to EMF in the frequency range 100 kHz – 300 GHz; taken from International Commission on Non-Ionizing Radiation Protection (ICNIRP) 2020 guidelines [1] and includes an overview of the methodologies for the evaluation of the exposure, based on the standards by the international standardization bodies.
- Section 3 describes the design process to provide the best performances for exposure, coverage and users experiences. Each element must be considered simultaneously making the planning process a cyclical path in which each factor must match the design requirements. The section ends with a focus on MaMIMO Antennas and how the time dynamic coverage introduces the spatial diversity and related impacts on radio planning methodologies.
- Section 4 deals with MaMIMO antennas; being the most impacting innovation introduced by 5G NR that has required a revision of the approaches used for the evaluation of the exposure. MaMIMO antennas are able to generate dedicated radiation patterns for specific user requirements, generating a time-dependent radiation, and they can use two different types of radiation patterns: broadcast radiation patterns that define the coverage area where User Equipment (UE) can attach, and traffic radiation patterns provide data connection over the coverage area.
- Section 5 describes the activities to be carried out in task T3.4 and the expected results; determination of the time-space distribution of the exposure generated by MaMIMO antennas in scenarios considering time and spatial diversity based on user activity and distribution.
- Section 6 reports the requirements for simulations.
 - The environment scenarios: the Modified Madrid Grid Scenario (MMGS), and a real city as available to the task partners,
 - An mmWave scenario, including an open area like a plaza or park,
 - Indoor environment scenarios,
 - The characteristics of the base station, such as position and radiated power.
- Section 7 describes the computational tools used by each partner for the activity of the task.
- Section 8 explains the methodology of the analysis carried out for the evaluation of the exposure to EMF, starting from a previous pre-processing step, how to carry out the calculation, analysis requirements such as capacity assigned to each user and each Base Transceiver Station (BTS), users time and space distribution.

1.3 Updates from previous Deliverable D3.4 “Analysis of 5G architecture modelling and mapping - Initial version”

The following changes are included in this report compared to Deliverable D3.4:

- Updated Section 6.1.2.2, including the electromagnetic properties of the body
- Added Section 9 collecting all the simulation results performed by TIM/FIBER and UCAS
 - Radiation patterns for both FR1 and FR2, to be used for outdoor and indoor simulations.
 - Simulations in a simulated town in FR1
 - Simulations in a Real Town in FR1
 - Simulations in an office scenario in FR1
 - Simulations in an industrial scenario in FR1
 - Simulations in a simulated town in FR2
- Updated Reference sections with some more bibliographic references.

2 International Guidelines and Standards

ICNIRP 2020 Guidelines [1], from now on ICNIRP2020, were published in May 2020 as a revision of ICNIRP Guidelines published in 1998 [2]. ICNIRP2020 indicates the limits “for the protection of humans exposed to radiofrequency electromagnetic fields (EMFs) in the range 100 kHz to 300 GHz” and the main objective of ICNIRP2020 is “to establish guidelines for limiting exposure to EMFs that will provide a high level of protection for all people against substantiated adverse health effects from exposures to both short- and long-term, continuous and discontinuous radiofrequency EMFs”.

ICNIRP2020 defines exposure limits for both the general public and for occupational settings and differentiates between basic restrictions and reference levels.

Basic restrictions, reported in Figure 1, are frequency dependent and expressed in terms of Specific Absorption Rate (SAR) and Absorbed Power Density (S_{ab}).

Exposure scenario	Frequency range	Whole-body average SAR ($W\ kg^{-1}$)	Local Head/Torso SAR ($W\ kg^{-1}$)	Local Limb SAR ($W\ kg^{-1}$)	Local S_{ab} ($W\ m^{-2}$)
Occupational	100 kHz to 6 GHz	0.4	10	20	NA
	>6 to 300 GHz	0.4	NA	NA	100
General public	100 kHz to 6 GHz	0.08	2	4	NA
	>6 to 300 GHz	0.08	NA	NA	20

^aNote:

1. “NA” signifies “not applicable” and does not need to be taken into account when determining compliance.
2. Whole-body average SAR is to be averaged over 30 min.
3. Local SAR and S_{ab} exposures are to be averaged over 6 min.
4. Local SAR is to be averaged over a 10-g cubic mass.
5. Local S_{ab} is to be averaged over a square 4-cm² surface area of the body. Above 30 GHz, an additional constraint is imposed, such that exposure averaged over a square 1-cm² surface area of the body is restricted to two times that of the 4-cm² restriction.

Figure 1: Basic restrictions as defined in ICNIRP2020 for time intervals ≥ 6 min [1]

As can be noted in Figure 1, there is a reduction factor of 5 for exposure of the general public compared to occupational exposure, for all the considered quantities and for all the exposed parts of the body.

Basic restrictions for exposure durations shorter than 6 minutes are reported in Figure 2 and are expressed in terms of Specific energy Absorption (SA) and Absorbed energy density (U_{ab}).

Exposure scenario	Frequency range	Local Head/Torso SA ($kJ\ kg^{-1}$)	Local Limb SA ($kJ\ kg^{-1}$)	Local U_{ab} ($kJ\ m^{-2}$)
Occupational	100 kHz to 400 MHz	NA	NA	NA
	>400 MHz to 6 GHz	$3.6[0.05+0.95(t/360)^{0.5}]$	$7.2[0.025+0.975(t/360)^{0.5}]$	NA
	>6 to 300 GHz	NA	NA	$36[0.05+0.95(t/360)^{0.5}]$
General public	100 kHz to 400 MHz	NA	NA	NA
	>400 MHz to 6 GHz	$0.72[0.05+0.95(t/360)^{0.5}]$	$1.44[0.025+0.975(t/360)^{0.5}]$	NA
	>6 to 300 GHz	NA	NA	$7.2[0.05+0.95(t/360)^{0.5}]$

^aNote:

1. “NA” signifies “not applicable” and does not need to be taken into account when determining compliance.
2. t is time in seconds, and restrictions must be satisfied for all values of t between >0 and <360 s, regardless of the temporal characteristics of the exposure itself.
3. Local SA is to be averaged over a 10-g cubic mass.
4. Local U_{ab} is to be averaged over a square 4-cm² surface area of the body. Above 30 GHz, an additional constraint is imposed, such that exposure averaged over a square 1-cm² surface area of the body is restricted to $72[0.025+0.975(t/360)^{0.5}]$ for occupational and $14.4[0.025+0.975(t/360)^{0.5}]$ for general public exposure.
5. Exposure from any pulse, group of pulses, or subgroup of pulses in a train, as well as from the summation of exposures (including non-pulsed EMFs), delivered in t s, must not exceed these levels.

Figure 2 : Basic restrictions as defined in ICNIRP2020 integrated over < 6 min time interval [1]

As for basic restrictions for time average ≥ 6 min, there is a reduction factor of 5 for exposure of the general public with respect to the exposure of occupational for all the considered quantities and for all the exposed part of the body.

As stated in ICNIRP2020, “reference levels have been derived from a combination of computational and measurement studies to provide a means of demonstrating compliance using quantities that are more easily assessed than basic restrictions, but that provide an equivalent level of protection to the basic restrictions for worst-

case exposure scenarios”. Exposure limits reported in terms of reference level are evaluated on the basis of the whole body or portion of the body that is exposed and on the basis of the time averaging interval, see Figure 3, Figure 4 and Figure 5.

Exposure scenario	Frequency range	Incident E-field strength; E_{inc} ($V\ m^{-1}$)	Incident H-field strength; H_{inc} ($A\ m^{-1}$)	Incident power density; S_{inc} ($W\ m^{-2}$)
Occupational	0.1 – 30 MHz	$660/f_M^{0.7}$	$4.9/f_M$	NA
	>30 – 400 MHz	61	0.16	10
	>400 – 2000 MHz	$3f_M^{0.5}$	$0.008f_M^{0.5}$	$f_M/40$
	>2 – 300 GHz	NA	NA	50
General public	0.1 – 30 MHz	$300/f_M^{0.7}$	$2.2/f_M$	NA
	>30 – 400 MHz	27.7	0.073	2
	>400 – 2000 MHz	$1.375f_M^{0.5}$	$0.0037f_M^{0.5}$	$f_M/200$
	>2 – 300 GHz	NA	NA	10

^aNote:

1. “NA” signifies “not applicable” and does not need to be taken into account when determining compliance.
2. f_M is frequency in MHz.
3. S_{inc} , E_{inc} , and H_{inc} are to be averaged over 30 min, over the whole-body space. Temporal and spatial averaging of each of E_{inc} and H_{inc} must be conducted by averaging over the relevant square values (see eqn 8 in Appendix A for details).
4. For frequencies of 100 kHz to 30 MHz, regardless of the far-field/near-field zone distinctions, compliance is demonstrated if neither E_{inc} or H_{inc} exceeds the above reference level values.
5. For frequencies of >30 MHz to 2 GHz: (a) within the far-field zone: compliance is demonstrated if either S_{inc} , E_{inc} or H_{inc} , does not exceed the above reference level values (only one is required); S_{eq} may be substituted for S_{inc} ; (b) within the radiative near-field zone, compliance is demonstrated if either S_{inc} , or both E_{inc} and H_{inc} , does not exceed the above reference level values; and (c) within the reactive near-field zone: compliance is demonstrated if both E_{inc} and H_{inc} do not exceed the above reference level values; S_{inc} cannot be used to demonstrate compliance, and so basic restrictions must be assessed.
6. For frequencies of >2 GHz to 300 GHz: (a) within the far-field zone: compliance is demonstrated if S_{inc} does not exceed the above reference level values; S_{eq} may be substituted for S_{inc} ; (b) within the radiative near-field zone, compliance is demonstrated if S_{inc} does not exceed the above reference level values; and (c) within the reactive near-field zone, reference levels cannot be used to determine compliance, and so basic restrictions must be assessed.

Figure 3: Reference levels as defined in ICNIRP2020 per whole body exposure, averaged over a 30-minute time interval [1]

Exposure scenario	Frequency range	Incident E-field strength; E_{inc} ($V\ m^{-1}$)	Incident H-field strength; H_{inc} ($A\ m^{-1}$)	Incident power density; S_{inc} ($W\ m^{-2}$)
Occupational	0.1 – 30 MHz	$1504/f_M^{0.7}$	$10.8/f_M$	NA
	>30 – 400 MHz	139	0.36	50
	>400 – 2000 MHz	$10.58f_M^{0.43}$	$0.0274f_M^{0.43}$	$0.29f_M^{0.86}$
	>2 – 6 GHz	NA	NA	200
	>6 – <300 GHz	NA	NA	$275/f_G^{0.177}$
	300 GHz	NA	NA	100
General public	0.1 – 30 MHz	$671/f_M^{0.7}$	$4.9/f_M$	NA
	>30 – 400 MHz	62	0.163	10
	>400 – 2000 MHz	$4.72f_M^{0.43}$	$0.0123f_M^{0.43}$	$0.058f_M^{0.86}$
	>2 – 6 GHz	NA	NA	40
	>6 – 300 GHz	NA	NA	$55/f_G^{0.177}$
	300 GHz	NA	NA	20

^a Note:

1. “NA” signifies “not applicable” and does not need to be taken into account when determining compliance.
2. f_M is frequency in MHz; f_G is frequency in GHz.
3. S_{inc} , E_{inc} , and H_{inc} are to be averaged over 6 min, and where spatial averaging is specified in Notes 6–7, over the relevant projected body space. Temporal and spatial averaging of each of E_{inc} and H_{inc} must be conducted by averaging over the relevant square values (see eqn 8 in Appendix A for details).
4. For frequencies of 100 kHz to 30 MHz, regardless of the far-field/near-field zone distinctions, compliance is demonstrated if neither peak spatial E_{inc} or peak spatial H_{inc} , over the projected whole-body space, exceeds the above reference level values.
5. For frequencies of >30 MHz to 6 GHz: (a) within the far-field zone, compliance is demonstrated if one of peak spatial S_{inc} , E_{inc} or H_{inc} , over the projected whole-body space, does not exceed the above reference level values (only one is required); S_{eq} may be substituted for S_{inc} ; (b) within the radiative near-field zone, compliance is demonstrated if either peak spatial S_{inc} , or both peak spatial E_{inc} and H_{inc} , over the projected whole-body space, does not exceed the above reference level values; and (c) within the reactive near-field zone: compliance is demonstrated if both E_{inc} and H_{inc} do not exceed the above reference level values; S_{inc} cannot be used to demonstrate compliance; for frequencies >2 GHz, reference levels cannot be used to determine compliance, and so basic restrictions must be assessed.
6. For frequencies of >6 GHz to 300 GHz: (a) within the far-field zone, compliance is demonstrated if S_{inc} , averaged over a square 4-cm² projected body surface space, does not exceed the above reference level values; S_{eq} may be substituted for S_{inc} ; (b) within the radiative near-field zone, compliance is demonstrated if S_{inc} , averaged over a square 4-cm² projected body surface space, does not exceed the above reference level values; and (c) within the reactive near-field zone reference levels cannot be used to determine compliance, and so basic restrictions must be assessed.
7. For frequencies of >30 GHz to 300 GHz, exposure averaged over a square 1-cm² projected body surface space must not exceed twice that of the square 4-cm² restrictions.

Figure 4: Reference levels as defined in ICNIRP2020 per local exposure, averaged over a 6 minutes time interval [1]

Reference levels for local exposure, integrated over intervals of between >0 and <6 minutes, to electromagnetic fields from 100 kHz to 300 GHz (unperturbed rms values). ^a		
Exposure scenario	Frequency range	Incident energy density; U_{inc} (kJ m ⁻²)
Occupational	100 kHz – 400 MHz	NA
	>400 – 2000 MHz	$0.29f_M^{0.86} \times 0.36[0.05+0.95(t/360)^{0.5}]$
	>2 – 6 GHz	$200 \times 0.36[0.05+0.95(t/360)^{0.5}]$
	>6 – <300 GHz	$275f_G^{0.177} \times 0.36[0.05+0.95(t/360)^{0.5}]$
	300 GHz	$100 \times 0.36[0.05+0.95(t/360)^{0.5}]$
General public	100 kHz – 400 MHz	NA
	>400 – 2000 MHz	$0.058f_M^{0.86} \times 0.36[0.05+0.95(t/360)^{0.5}]$
	>2 – 6 GHz	$40 \times 0.36[0.05+0.95(t/360)^{0.5}]$
	>6 – <300 GHz	$55f_G^{0.177} \times 0.36[0.05+0.95(t/360)^{0.5}]$
	300 GHz	$20 \times 0.36[0.05+0.95(t/360)^{0.5}]$

^aNote:

1. "NA" signifies "not applicable" and does not need to be taken into account when determining compliance.
2. f_M is frequency in MHz; f_G is frequency in GHz; t is time interval in seconds, such that exposure from any pulse, group of pulses, or subgroup of pulses in a train, as well as from the summation of exposures (including non-pulsed EMFs), delivered in t seconds, must not exceed these reference level values.
3. U_{inc} is to be calculated over time t , and where spatial averaging is specified in Notes 5–7, over the relevant projected body space.
4. For frequencies of 100 kHz to 400 MHz, >0 to <6-min restrictions are not required and so reference levels have not been set.
5. For frequencies of >400 MHz to 6 GHz: (a) within the far-field zone: compliance is demonstrated if peak spatial U_{inc} , over the projected whole-body space, does not exceed the above reference level values; U_{eq} may be substituted for U_{inc} ; (b) within the radiative near-field zone, compliance is demonstrated if peak spatial U_{inc} , over the projected whole-body space, does not exceed the above reference level values; and (c) within the reactive near-field zone, reference levels cannot be used to determine compliance, and so basic restrictions must be assessed.
6. For frequencies of >6 GHz to 300 GHz: (a) within the far-field or radiative near-field zone, compliance is demonstrated if U_{inc} , averaged over a square 4-cm² projected body surface space, does not exceed the above reference level values; (b) within the reactive near-field zone, reference levels cannot be used to determine compliance, and so basic restrictions must be assessed.
7. For frequencies of >30 GHz to 300 GHz: exposure averaged over a square 1-cm² projected body surface space must not exceed $275/f_G^{0.177} \times 0.72[0.025+0.975(t/360)^{0.5}]$ kJ m⁻² for occupational and $55/f_G^{0.177} \times 0.72[0.025+0.975(t/360)^{0.5}]$ kJ m⁻² for general public exposure.

Figure 5: Reference levels as defined in ICNIRP2020 per local exposure, integrated over <6 minutes time interval [1]

2.1 Whole body vs localized exposure: different approaches

In general, exposure generated by base stations occurs in the far field region of the radiating system and involves the whole body; if this is the case, the exposure limits are those indicated in Figure 5 of ICNIRP2020. Exposure is evaluated in terms of incident power density, corresponding to 10 W/m² in the frequency range over 2.0 GHz for 5G NR technologies corresponding to 61.4 V/m in terms of electric field strength in the far field of the antenna.

Since exposure is evaluated in terms of incident power density, it can be associated with locations in the scenario. If all the accessible points (in the scenario) have an exposure below the limits, then any person standing or moving through the scenario will be exposed to an EMF level below the limits indicated in ICNIRP2020.

The situation is different for localized exposure, where only parts of the body are exposed to EMF. In this case, the exposure is expressed both in thresholds for the dosimetry quantities and in terms of geometrical surface where the exposure is evaluated, see notes in Figure 4.

As clearly indicated by ICNIRP2020 exposure limits expressed in terms of reference levels are relevant to the whole body and are expressed in terms of *incident* dosimetry quantities, meaning that they are evaluated in specific locations in the absence of the exposed body. Accordingly, exposure evaluated as a global quantity, such as the mean over large areas like a whole town has no meaning with respect to exposure limits.

MaMIMO antennas, that can be used in 5G NR, can generate a time variable radiation pattern to give service to specific locations where the user is, only for the required time. Once the service ends the antenna does not radiate anymore to the specific user. That means that the exposure time interval, specific for the user and for the serving antenna, could be very short. ICNIRP2020 introduced a new set of Reference Levels for brief exposure time intervals, shorter than 6 minutes, expressed in terms of incident energy density which thus could be relevant for exposure from MaMIMO antennas.

2.2 Status of standards

The methodologies for the evaluation of the exposure are described in technical standards, in Europe defined by Comité européen de normalisation en électronique et en électrotechnique (CENELEC) and at the international level by IEC (International Electrotechnical Commission) and IEEE (Institute of Electrical and Electronics Engineers). Standards, following the philosophy of the guidelines, are developed in two directions depending on the typology of devices and exposure. The current frame of normative documents is as follows:

- EN IEC 62232:2022 “Determination of RF field strength, power density and SAR in the vicinity of base stations for the purpose of evaluating human exposure”. This standard describes the computational and measurement methodologies to evaluate the exposure generated by base station systems, in terms of SAR, field and power density. It is identical to the IEC 62232 standard; technical works are developed within IEC TC106.
- IEC TR 62669:2019 “Case studies supporting IEC 62232. Determination of RF field strength, power density and SAR in the vicinity of radiocommunication base stations for the purpose of evaluating human exposure”. The technical report describes several case studies in which the exposure is evaluated by using the IEC 62232 standard; technical works are developed within IEC TC106.
- EN IEC/IEEE 62209-1528:2021 “Measurement procedure for the assessment of specific absorption rate of human exposure to radiofrequency fields from hand-held and body-mounted wireless communication devices Human models, instrumentation, and procedures (Frequency range of 4 MHz to 10 GHz)”. The standard describes measurement methodologies for the evaluation of SAR. It is equivalent to of the IEEE/IEC 62209-1528-2020; technical works are developed within IEC TC106.
- EN IEC 62209-3:2019 “Measurement procedure for the assessment of specific absorption rate of human exposure to radio frequency fields from hand-held and body-mounted wireless communication devices Vector measurement-based systems (Frequency range of 600 MHz to 6 GHz)”. The standard describes the methodologies for SAR measurement based on array of probes. It is equivalent to of the IEC 62209-3; technical works are developed within IEC TC106.
- IEEE/IEC 62704-1-2017 – “IEC/IEEE International Standard for Determining the Peak Spatial Average Specific Absorption Rate (SAR) in the Human Body from Wireless Communications Devices, 30 MHz - 6 GHz. Part 1: General Requirements for using the Finite Difference Time Domain (FDTD) Method for SAR Calculations”. The standard describes the methodologies for evaluating SAR by devices using the Finite Difference Time Domain (FDTD) technique; technical works are developed within IEC TC106.
- IEEE/IEC 62704-2-2017 – “IEEE/IEC International Standard -- Determining the peak spatial-average specific absorption rate (SAR) in the human body from wireless communications devices, 30 MHz to 6 GHz -- Part 2: Specific requirements for Finite Difference Time Domain (FDTD) modelling of exposure from vehicle mounted antennas”. The standard is developed within IEC TC106.
- IEEE/IEC 62704-3-2017 – “Determining the Peak Spatial-Average Specific Absorption Rate (SAR) in the Human Body from Wireless Communications Devices, 30 MHz - 6 GHz Part 3: Specific Requirements for Using the Finite Difference Time Domain (FDTD) Method for SAR Calculations of Mobile Phones”. The standard describes the methodologies for evaluating SAR generated by cellular phones using the Finite Difference Time Domain (FDTD) technique; technical works are developed within IEC TC106.
- IEEE/IEC 62704-4-2020 – “IEC/IEEE International Standard - Determining the peak spatial-average specific absorption rate (SAR) in the human body from wireless communication devices, 30 MHz to 6 GHz – Part 4: General requirements for using the finite element method for SAR calculations”. The standard describes the methodologies for evaluating SAR by devices using the Finite Element Method (FEM); technical works are developed within IEC TC106.

It should be noted that many of those standards issued by CENELEC, IEC and IEEE are the same.

3 Mobile network planning: exposure to EMF, coverage, and performances requirements need to be matched at the same time.

The network planning process requires to satisfy, at the same time, three conditions:

1. A sufficient level of signal at the UE position to be in connection with the base station to establish the communication.
2. A sufficiently clean (evaluated by using metrics fixed by the communication standard) signal at the UE position which can be correctly interpreted to resume information and to reach the best possible performances depending on the service required¹
3. Compliance with the limits for human exposure to EMF everywhere in the locations accessible to people.

The first and second points are technology-dependent, meaning that each technology is designed almost standalone with the aim of managing the interference for those technologies sharing the same band². However, the third point must be satisfied globally, considering the whole EMF environment. The EMF exposure generated by all deployed technologies from all the BTSs and from all the mobile operators, including contributions coming from other stakeholders (as an example broadcasters) must be below the limits established by authorities. The latter makes the design process difficult and requires matching all the design requirements in a complex and diversified scenario from both the electromagnetic and geographical points of view.

For clarification, it is possible to outline the mobile network design as a cyclic process, see Figure 6, in which the requirements are tuned step by step to get the best possible deployment allowed by requirements, coverage and performance, and boundary conditions, i.e., exposure to EMF.

In the general case, the first step is the determination of the coverage area, since there are constraints due to the positioning of the base station and height and orientation of the antenna(s) in reference to the existing installations in the same location or in neighbouring locations. A tentative power feeding the antenna is assumed to generate a first rough indication of the coverage area and SINR distribution, the second step in the deployment context.

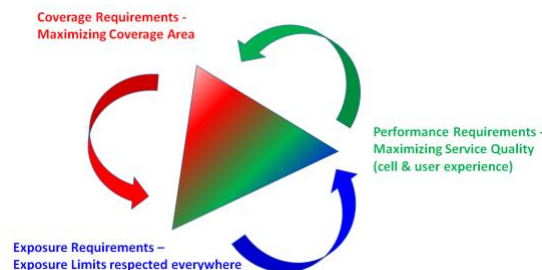


Figure 6: The design process of a mobile telecommunication network.

The third step consists of the evaluation of the exposure level in the scenario, considering the EMF environment in the surroundings. The exposure is evaluated as power density in the far field region of the radiator at:

- Specific points or planar surfaces at a defined height from the walking surfaces
- Surfaces, a balcony, or an accessible location for buildings.
- Iso-surfaces, namely the compliance boundary, at a fixed exposure level applied to the phase-centre of the antenna.

Any time it is verified that specific points, surfaces, or the compliance boundary over the limits intersect regions where people can be exposed, it is required to restart the whole design process from the beginning, acting on one or all the design parameters to match requirements. It could be even possible that requirements could not be

¹ For the scope of task T3.4 only downlink is of interest for determining the exposure in the scenario. A good coverage and a low level of SINR guarantee the lower possible level of emissions in uplink from the UE side due to the internal mechanisms of power management.

² Sharing the same band means working exactly on the same frequency band. As an example, 5GNR works in the band N78 hosting the service for all operators. A proper sub-band is assigned to each operator, different from the sub-band assigned to any other operator. In these conditions, the noise generated at a location comes from neighbouring base stations from the same operator and by out-of-band emissions from other sources.

matched and then a different location for the transmitter must be chosen, which may happen in overloaded towers shared with other operators in over-crowded locations, like downtown areas.

For the evaluation of the exposure, depending on national spectrum management rules, it can be possible that the whole electromagnetic environment is not known to each operator. As an example, the power feeding the antenna, the antenna radiation pattern, and the orientation for each transmitter could not be known since these are industrial confidential information specific to each operator. In this case, the design process is much more complicated, requiring extra information coming from, e.g., in-situ measurements and the need to check the compliance of the design with national authorities.

The process previously described can be defined as “traditional”, accounting for antennas generating time-fixed beams, like passive antennas. In this case, the coverage area can be considered as statically determined, the time-varying power is applied to a static radiation pattern, and the coverage is static and limited by the maximum power feeding the antenna ³.

One of the main innovations introduced by 5G NR is MaMIMO antennas, able to generate time/space variable narrow beams, by which the radiation is focused only in the direction where there is the need to hold up the links to active users. This is a change of paradigm in the mobile telecommunications industry that has required a different approach in the network design and requires new approaches in the modalities to evaluate the exposure to EMF. It is the first time in the mobile communication era that there is the opportunity to optimize and manage the time-spatial distribution of the radiation and the exposure accordingly. The benefits introduced by the MaMIMO technology, regarding exposure to EMF, are listed below:

- the power is no longer spread over the entire coverage area but only in the direction of the active users. The power dedicated to a user is applied to a narrow beam instead to wide beams preventing radiation in directions where there is no need to deliver energy, strongly impacting coverage, SINR and exposure.
- narrow beams mean higher radiation pattern gain, allowing to reach a user’s location with a lower (transmit) power with respect to the case with wider radiation patterns with lower gain or, to get a better SINR at the location.
- narrow beams mean lower SINR requirements corresponding to a cleaner communication scenario allowing to use higher modulation schemes with associated higher data throughput, reducing the transmission time for the same quantity of payload and, therefore, lowering the exposure time.

On the other hand, the introduction of MaMIMO antennas has required changing the network design methodologies; since radiation follows the active users’ distribution in the scenario, the exposure to EMF is no longer deterministic but statistically related to that of the user’s spatial distribution, see Figure 7.

All the previous aspects will be analyzed in the following section and the design of the activities planned in task T3.4 are devoted to highlight the time-space statistics of the radiation and determining parameters in view of the exposure to EMF.

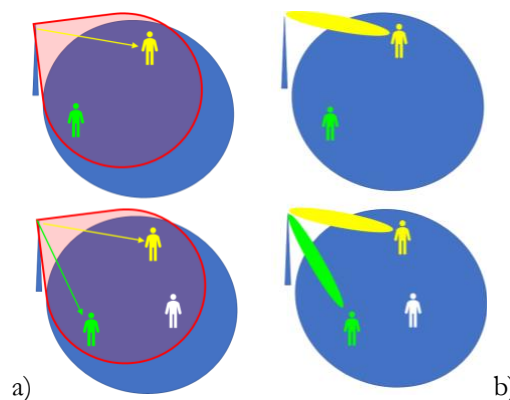


Figure 7: a) Passive antennas radiation pattern coverage. b) MaMIMO antennas coverage.

³ In the context of the static radiation pattern antenna, static means that the radiation pattern does not change over the time; the coverage area is evaluated with the maximum configured power on the radiating system, even if the coverage can change due to the time variations of the power feeding the antenna and managed by the power management control system. Once the power is applied to the antenna, it is spread over the whole coverage area that depends on the radiation pattern characteristics, without any distinction on directions.

4 MaMIMO antennas require a new approach for evaluating exposure to EMF

4.1 MaMIMO Antennas in 5G NR

For the scope of activities planned in task T3.4, the most impacting innovation introduced by 5G NR⁴ are the MaMIMO antennas (also known as Active Antennas System (AAS)) generating time dependent radiation patterns differently from traditional passive antennas generating time static radiation patterns.

A MaMIMO antenna can change its own radiative characteristics over time, according to the service requested by the users distributed over the coverage area, generating specific beams⁵ directed to each user; such a prerogative makes the coverage temporally dynamic and introducing the spatial diversity and, as an additional degree of freedom, the possibility to manage interference, see Figure 8 in which each user is reached by a narrow beam not covering neighbouring users.

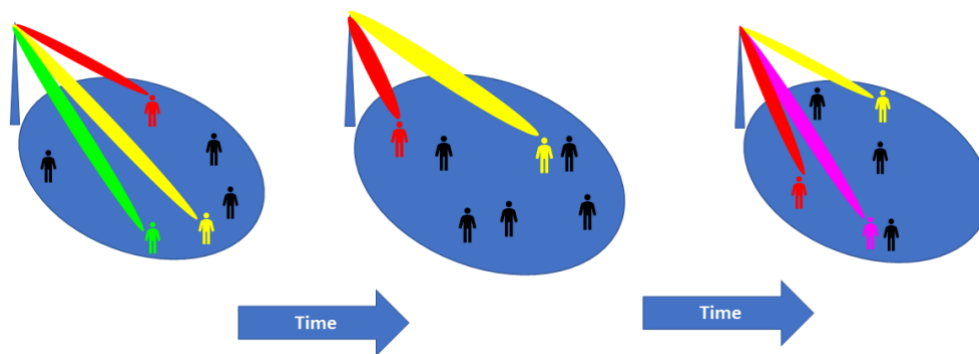


Figure 8: The time dependent beam arrangement to serve users located in the scenario.

In contrast to previous technologies, 5G NR using MaMIMO antennas decouple the signalling (or control) plane⁶ from the traffic (or user) plane⁷ by using two different (logically or physically) radiation patterns. Attach procedures to connect the UE to the network and signalling required to maintain the communication travel on different (logical or physical) beams with respect to the beams used to transport the payload once the communication has been established. Specifically, there are two different (logical or physical) radiation pattern sets:

- broadcast radiation pattern(s), used for defining the coverage area in which the UEs can attach and control operations. The broadcast radiation patterns belong to the broadcast beamset, which can contain one to several beams depending on the used approach, namely static or sweeping scanning of the coverage region.
- traffic radiation pattern(s), used to provide data connection over the coverage area once the UEs have completed the attachment procedure on the broadcast beam(s). The traffic beam(s) belong to the traffic beamset; it can contain a one-time variable beam or many depending on the used approach, namely the Eigen-Based Beamforming (EBB) or zero-forcing beamforming (ZFB), or the grid of beam (GoB) approach, which will be described later on.

Prior to the description of MaMIMO antenna's usage of beams from the view of the exposure to EMF, an analysis is done of the consequences of separating the signalling plane from the traffic plane in 5G NR. The independence of the broadcast beamset from the traffic beamset avoids distributing the power everywhere in the coverage area, reserving energy only for the specific link(s) delivered only when and where required, see Figure 8

The broadcast beamset is a set containing several beams that the MaMIMO antenna has available to define the coverage area; the beamset is populated with a minimum of one beam or a few or tens of beams, depending on

⁴ In this section will be given the information about MaMIMO antennas only required for the exposure to EMF purposes. A more detailed description of the of the concept described here can be found in specialistic publications, books or standards.

⁵ Beam is a term used as synonym for radiation pattern.

⁶ With signaling or control plane, simplifying, is intended the set information exchanged between the base station and the device for establishing, and controlling a communication. Signaling happens before, during and after the service required by a device in parallel with the activity for which the service has been required.

⁷ With traffic plane is intended, simplifying, the activity performed by the device and base station for accomplishing the task for which the service has been required; the service is delivered under control of the signaling plane.

the service to be delivered and the operating frequency band. The coverage area assumes different shapes depending on the shape of the radiation pattern(s) populating the beamset for the specific coverage in the specific scenario. This means the coverage area can be adapted to the specific type of service to be delivered in the specific deployment scenario (a lot of flexibility). As an example, the shape of the broadcast beam(s) can be selected differently, if the service required is coverage of an urban horizontal scenario compared to coverage of an urban vertical scenario. The shape of the coverage the MaMIMO antenna can generate by selecting a specific broadcast beam(s) is named configuration; the MaMIMO antennas may provide several configurations specialized for specific deployments or service scenarios.

Once the configuration has been selected, see Figure 9, the coverage area can be determined with two different methodologies:

- Fixed broadcast beam: the coverage area is defined by just one time-static beam, exactly as done for previous technologies using traditional passive antennas, see Figure 10a. In this case, the beam has a wide aperture (as an example 120 degrees on the azimuth plane) with a medium to low radiation pattern gain value. The position of the user is estimated by means of Angle of Arrival methodologies.
- Sweeping broadcast beam: the coverage area is divided into sub-areas as defined by the configuration, both in the elevation plane as well as in the azimuth plane, each one covered by a specific beam in the configuration. The beam set is periodically swept to scan the whole attached area; see Figure 10b. The UE probes the broadcast beamset and, on the base of the received signal level, reports to the MaMIMO antenna which of the beams in the configuration is best received, hence determining the electromagnetic link direction.

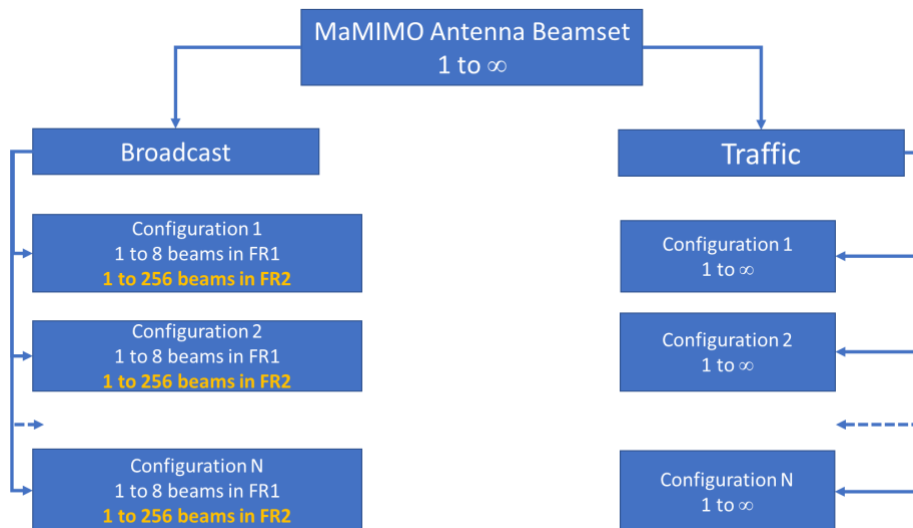


Figure 9: The configuration structure for a generic MaMIMO antenna.

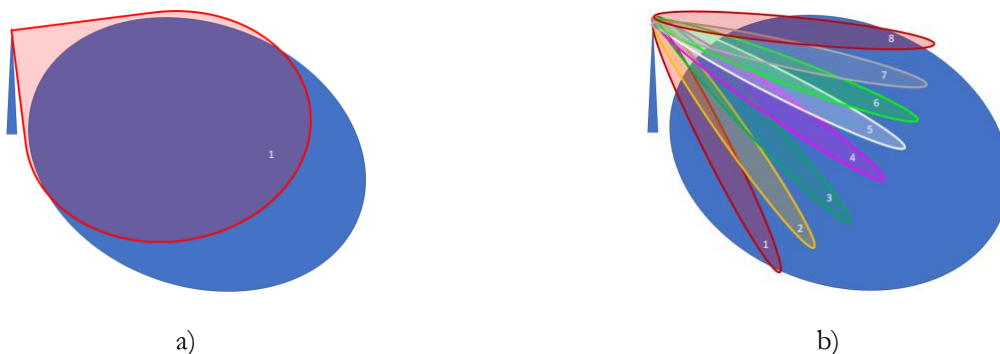


Figure 10: Broadcast fixed beam coverage (a) and sweeping beam (b) coverage area definition.

When a user requires the service (e.g., internet services or data download), after performing the attach procedures by using the broadcast beamset, the MaMIMO antenna generates one or more traffic beams, from the traffic beamset, in the electromagnetic direction where the user(s) is (are) located, to download the payload.

MaMIMO antennas can be categorized into two classes:

- GoB or codebook antennas: the antenna has a pre-determined set of beams (weights⁸) available. Once the procedures activated during the attach phase or management of the link have been established, the antenna selects the best beam(s) in the set available for serving or maintaining the service to user(s). The beamset can be populated with many beams, with different shapes, to best serve the traffic conditions and user distribution over the scenario, see Figure 11a and Figure 12a.
- EBB: the antenna generates the set of weight in real time to generate just one radiation pattern with lobes in the electromagnetic direction of users and nulls in direction where it is required to manage the interference, depending on the user distribution and load condition in the specific. The antenna provides, theoretically, an infinite number of weights whose shape, and direction cannot be defined until the traffic environment is defined, see Figure 11b and Figure 12b. Similar to EBB antennas, the ZFB antennas generate a radiation pattern null in the direction of interference.

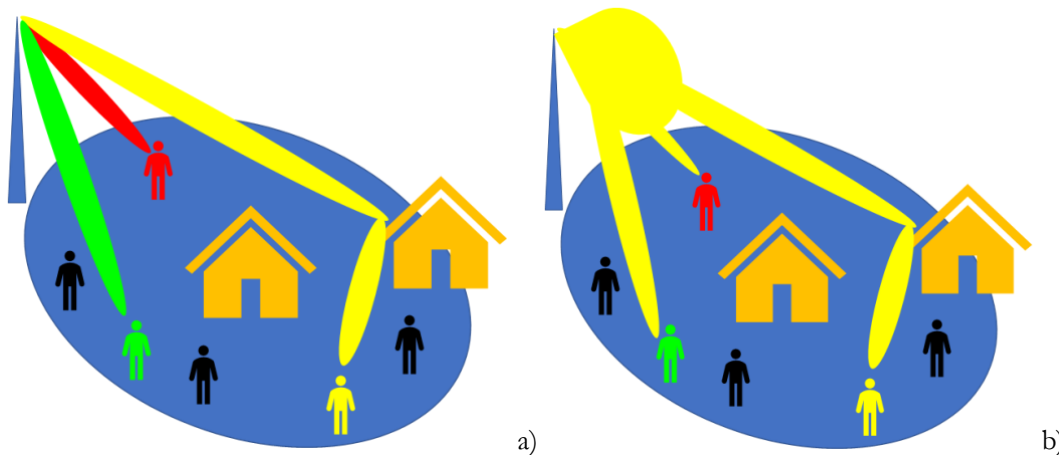


Figure 11: Traffic beams of a GoB MaMIMO antenna (a) and Traffic beam for an EBB MaMIMO antenna (b).

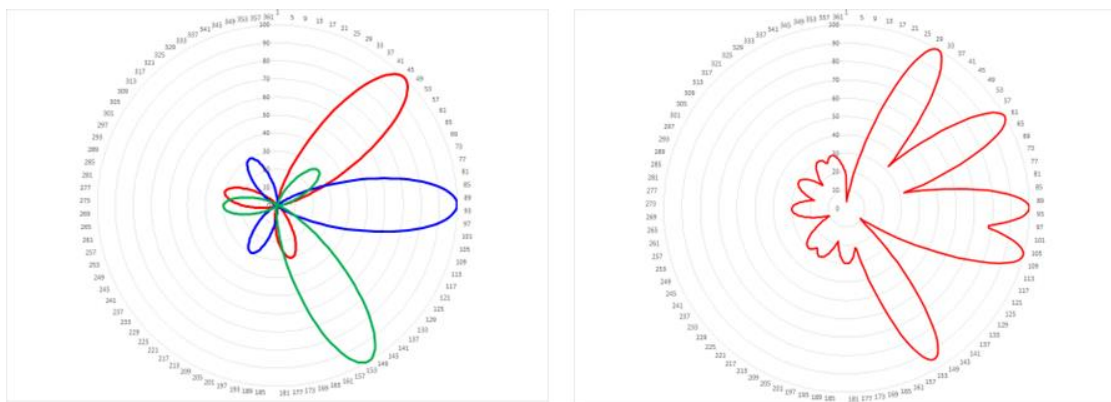


Figure 12: Time Traffic Radiation Pattern of a GoB MaMIMO antenna (a) and Time Traffic Radiation Pattern for an EBB MaMIMO antenna (b).

From the information about the operation of a MaMIMO antenna, it is possible to make the following observations:

1. It is not possible to a-priori define the radiation pattern; it depends on the users' distribution, specific scenario, and interference context.
2. The radiation is directed to where there is a service request and only for the time required to complete the task.
3. The exposure, on an observation point, changes over time due to the temporal changes of power and direction of the radiation. It could happen that in some time intervals, the radiation in the observation point is not present since the antenna is pointing the radiation pattern in a different direction.

⁸ Each beam the antenna can generate corresponds to a set of “weights” represented by complex numbers for managing the current (in strength and phase) feeding each radiating element of the array constituting the MaMIMO antenna.

4. The same considerations hold for SINR. Since the field level in each point over the scenario depends on how power is distributed by the MaMIMO antenna, SINR changes over time depending on other users' distribution and activity with respect to the served user.
5. Traffic coverage exists only where the service is required and, on the base of what is stated in bullet 1, some changes in the network design process need to be adopted.

4.1.1 The envelope radiation pattern

The spatial indeterminacy of coverage, a feature introduced by 5G technology with MaMIMO antennas, requires the need to redesign and review the network coverage project methods. A new approach in the modalities to plan radio coverage and to evaluate the exposure to EMF is the introduction of the antenna envelope radiation pattern.

An envelope radiation pattern is a radiation pattern that provides, for each specific direction in azimuth and elevation, the maximum gain that the antenna can generate between all synthesizable beams, for each specific configuration. The envelope radiation pattern is non-physical because it does not respond to energy conservation: the integral over the whole sphere of the envelope radiation pattern does not preserve the energy [3], Figure 13.

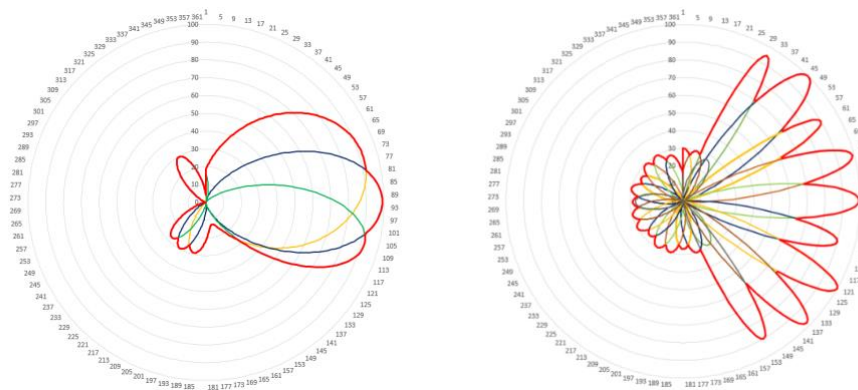


Figure 13: Example of Envelope Elevation Radiation Pattern: the red curve identifies the maximum gain in each direction.

The use of the envelope radiation pattern involves a change of perspective also when evaluating the exposure to electromagnetic fields. It resolves the randomness of the direction of the radiation within the coverage area, since the maximum gain that can be synthesized by the antenna is considered in each direction, and the use of the maximum performance that the antenna can provide in each direction of space involves an overestimation of exposure to electromagnetic fields. The envelope radiation pattern concept is valid for both broadcast and traffic diagrams:

- The Broadcast Envelope Radiation Pattern: this is the envelope pattern for each Broadcast Beam Configuration. An AAS can use different broadcast configurations for specific coverage requirements, so the number of Broadcast envelope radiation patterns is equal to the number of configurations implemented by the AAS.
- Traffic Envelope Radiation Pattern: this is the envelope pattern of the traffic beams associated with a Broadcast Configuration.
- An AAS can have several broadcast envelope radiation patterns, and a traffic envelope radiation pattern⁹. correspondsto each of them.

4.1.2 Power associated with Broadcast and power associated with Traffic beams: the 5G NR frame

The 5G NR frame has a sophisticated structure, conceived to serve UE terminals having a wide range of different characteristics in terms of bandwidth, latency time, and request of reliability, with high attention toward energy efficiency.

A thorough description of the signalling structure of the 5G frame can be found in D2.2. In the following, some characteristics relevant to the power associated with the different beams used in the 5G NR gNB are briefly recalled.

⁹ A MaMIMO antenna can have just one traffic envelope radiation pattern for all configurations; in this case traffic beams radiating in directions where the broadcast configuration does not give coverage, are not used.

In particular, 5G NR limits the “always on” signals as much as possible, packing all the fundamental information necessary for accessing the network in a signal structure highly concentrated in frequency, time, and possibly space, called Synchronization Signal – Primary Broadcast Channel (SS-PBCH), or “Synchronization Signal Block” (SSB), that includes the Synchronization Signals (SS), the Primary Broadcast Channel (PBCH) and the Primary Broadcast Channel-DeModulation Reference Signal (PBCH-DMRS). The structure of the SSB is very compact. SSB is mapped into 4 OFDM symbols in the time domain and 240 contiguous subcarriers in the frequency domain. Accordingly, SS-PBCH occupies only a fraction of the entire 5G NR frame. It is important to stress again that SS-PBCH is the only “always on” signal in 5G NR. Accordingly, in the absence of users, the 5G NR frame is almost empty apart from the Resource Elements (REs) associated with the SS-PBCH, and some control signals. An example of a 5G NR frame in the absence of users is shown in Figure 14. The power of the REs of the frame are plotted in false colours, from red (highest power) to blue (lowest power). We can note 6 SSBs, with different colours, i.e., different received powers in the position where the frame has been measured. Each SSB is associated with a different beam of the set of the gNB Broadcast Beams.

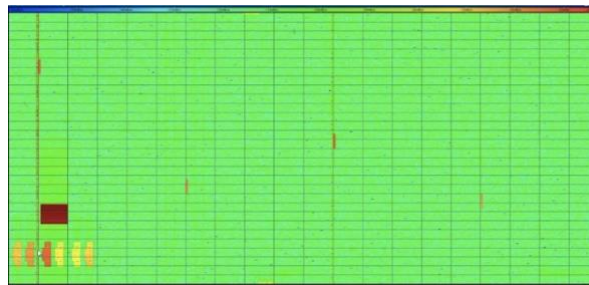


Figure 14: 5G frame in the absence of users; on the left bottom 6 SSBs are visible; apart the SSB and some control signals, the frame is void.



Figure 15: Full-loaded 5G frame; on the left bottom 6 SSBs are visible; the void area in the centre and at the end of the frame are the sections of the frame reserved for uplink data, almost all the remaining area is filled by PDSCH REs (users data).

With reference to downlink transmission, there are many other physical channels (Physical Downlink Shared Channel (PDSCH), Physical Downlink Control Channel (PDCCH), PBCH, Physical Broadcast Channel) with their own Demodulation Reference Signal (DMRS) for channel estimation and equalization. In particular, PDSCH is responsible for delivering user-specific downlink data from the gNB to the connected user equipment, including voice, video, and other types of data. PDSCH resources are allocated dynamically to UEs based on the varying communication requirements, employ adaptive modulation and coding to optimize data transfer, and maintain reliable communication in diverse radio environments.

In Figure 15 the downlink frame in case of full allocations of the resources is shown. The most part of the REs of the frame is filled by PDSCH data. The void area in the centre and at the end of the frame are the sections of the frame reserved for uplink data. In the lower (left) bottom part, it is possible to see the SSBs.

It is interesting to note that the power of the PDSCH REs is higher than the power of the SSBs. This is due to the use of traffic beams to transmit PDSCH data with respect to SSBs, that use broadcast beams (Figure 16). Since traffic beams have higher Gain compared to broadcast beams, even if the REs of the SSBs and PDSCH are transmitted at the same power, they are received at different power.

The analysis of the frames gives two important observations.

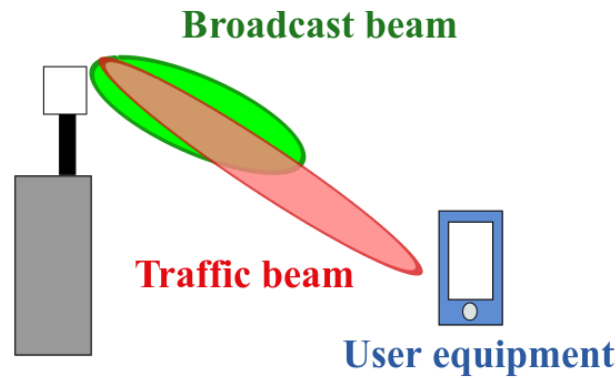


Figure 16: The higher received power of the PDSCH REs compared to the SSB REs is due to the different beams used, broadcast beams for SSBs and traffic beams for PDSCH; traffic beams (used to send payload data to the UE) have a greater directivity than the broadcast.

Firstly, almost all the received power is associated with the PDSCH RE, i.e., user data, while the SSBs make an almost negligible contribution to the received power. As a result, the power associated with broadcast channels is a small fraction of the power associated with traffic and can be neglected when defining exposure.

Secondly, Figure 15 represents an extreme and, in practice, unrealistic condition. This condition gives an upper bound of the field strength in any operative conditions of the gNB and is the value obtained using Maximum Extrapolation Techniques estimations. In real scenarios, the frame is only partially filled, according to the traffic user level, and the field strength is between the one given by the unloaded condition (Figure 14) and the fully loaded condition (Figure 15).

4.2 A change of paradigm in radiation: from a deterministic to a statistical approach

Before the introduction of the Actual Max Approach in [4][5] and MaMIMO antennas the conformance boundary¹⁰ associated to a transmitter was determined by using the EIRP considering the configured power¹¹ on the transmitter applied to the radiation:

$$EIRP(\vartheta, \varphi) = P_{configured} A_{Line} G(\vartheta, \varphi) \quad (1)$$

where

- EIRP is the Equivalent Isotropic Radiate Power in W
- $P_{configured}$ is the power the transmitter is allowed to deliver to the antenna in W
- A_{line} is the total transmission line attenuation and/or amplification between the transmitter and the antenna connector.
- G is the antenna gain
- ϑ is the elevation coordinate.
- φ is the azimuth coordinate.

When designing the exposure generated at a location, the precautionary approach is applied by considering that the transmitter constantly radiates the configured power. This approach does not consider the power control mechanisms, if any, implemented in the transmitter resulting in an overestimation of the exposure everywhere and for the whole averaging time¹² in the serving area, see Figure 17. While the methodology is useful for determining the size and shape of the coverage and SINR areas, indicating the maximum performance the system can generate

¹⁰ The conformance boundary is a surface centered on the phase center of the antenna outside that the exposure is always and everywhere below a limit

¹¹ The configured power is the maximum power that the transmitter is allowed to deliver to the antenna, apart from the line losses; it is lower or equal to the maximum power the transmitter can generate.

¹² Exposure is averaged over a time interval as defined by international or national laws or guidelines, see [1].

in terms of service, it is not practical for EMF exposure assessment, especially in regions where many systems are deployed.

In this case the coverage, SINR areas, and EMF conformance boundary are frozen in shape and levels, without considering any users' location. For the aims of the exposure to EMF it appears as the power would be spread all over the scenario for the whole averaging time.

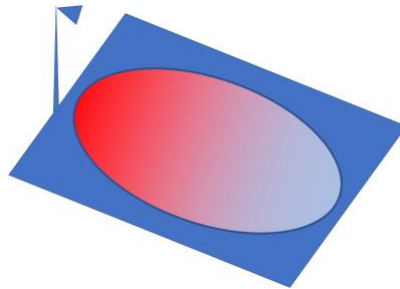


Figure 17: Scenario coverage without any power control or beamsteering.

As was shown in the previous sections, this does not correspond to the normal operations of transmitters. Hence, the following two cases can be described:

- Transmitters (technologies) implementing power control mechanisms (only for some technologies): the transmitter changes the power very fast in the time (depending on the frame structure implemented by the technology) to adapt to the channel conditions and to maintain the service quality at UE position. If the power is applied to a passive antenna, having a fixed radiation pattern, it appears as the coverage changes in the time (breathing effect), reducing and increasing the coverage area, with an upper limit corresponding to the covered area when applying the configured power, see Figure 18.
- MaMIMO Antennas: the power may change in the time with a mechanism like the one described in the previous bullet but also the direction of the radiation may change, see Figure 19.

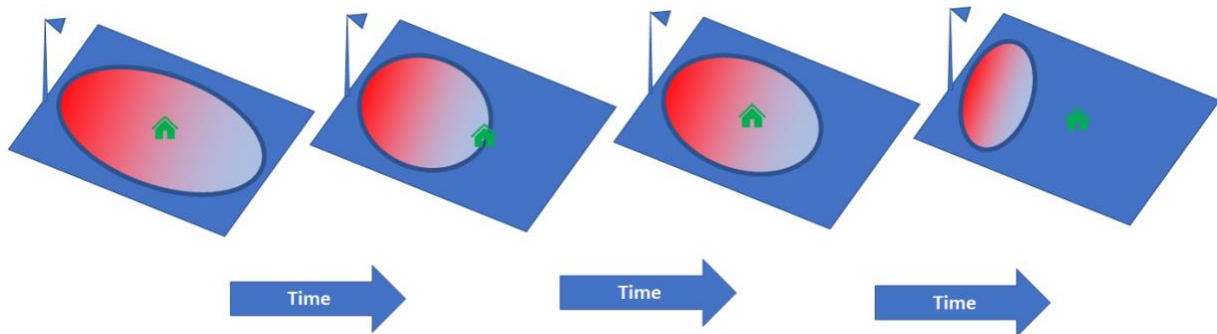


Figure 18: Scenario coverage with a technology implementing power control applied to a passive antenna.

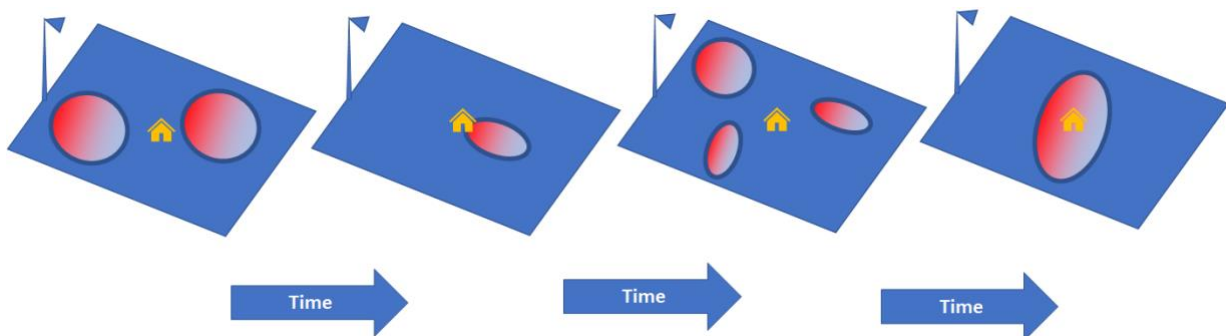


Figure 19: Scenario coverage with a technology implementing power control applied to a MaMIMO antenna.

The situation shown in Figure 18 can be formalized as

$$EIRP(\vartheta, \varphi, t) = P(t)_{\leq P_{\text{configured}}} A_{\text{Line}} G(\vartheta, \varphi) \quad (2)$$

where $P(t)$ is the radiated power at time t by the antenna. As can be noted the shape of the EIRP does not change in the space but assumes higher or lower values depending on the time value of the power. The situation depicted in Figure 19 can be described as

$$EIRP(\vartheta, \varphi, t, t') = P(t)_{\leq P_{configured}} A_{Line} G(\vartheta, \varphi, t') \quad (3)$$

in which there is a double dependence of the EIRP from the time, accounting for possible variations of the radiated power over time, and over different directions in the time.

In general, the exposure evaluated at the location can be expressed as

$$L(\mathbf{r}, \vartheta, \varphi, t) = L(\mathbf{r}, t) = \mathfrak{F}(EIRP(\vartheta, \varphi, t) PL(\mathbf{r}, \vartheta, \varphi, t)) \quad (4)$$

$$L(\mathbf{r}, \vartheta, \varphi, t, t') = L(\mathbf{r}, t, t') = \mathfrak{F}(EIRP(\vartheta, \varphi, t, t') PL(\mathbf{r}, \vartheta, \varphi, t, t')) \quad (5)$$

Where L is the exposure level in time at the position of the observation point, PL is the path loss between the source points and the observation point, and \mathfrak{F} is the functional parameter linking the EIRP to the exposure quantities (E field, H field or power density).

The determination of the coverage area for a MaMIMO antenna, corresponding to the maximum area where the base station should deliver the service, can be still reconstructed to the classical approach as used for passive antennas by substituting in equation (4) and (5) the envelope radiation pattern and the configured power. In this case the area is the larger area where the antenna can deliver the service for a single user¹³. With this approach one of the network design requirements can be obtained, as shown in Figure 17.

The same is not applicable for the determination of the exposure and SINR since it depends:

- on the location of users with respect to the observation point for the exposure;
- the location of the specific user, in relation to the other users for SINR.

4.2.1 Exposure at location

Each position in the scenario has associated a time variable exposure, independent of whether there is a user requiring service in that position there is. The total exposure at the position is determined by all the contributions from all transmitters in the surrounding, independent of the technology or service. By using the formulation adopted in [4][5], a contribution is significant if the exposure ratio ER ¹⁴ is greater than 5% with respect to the limit, so transmitters generating an ER lower than 5% of the limit are not considered.

In general, and for the goal of this task, the exposure at a location is given by:

$$L(\mathbf{r}, \vartheta, \varphi, t) = \sum_{k=1}^{K_{Passive\ Antennas}} L_k(\mathbf{r}, \vartheta, \varphi, t)|_{ER>0.05} + \sum_{k=1}^{K_{MaMIMO\ Antenna}} L_k(\mathbf{r}, \vartheta, \varphi, t, t')|_{ER>0.05} \quad (6)$$

where,

- L is the exposure at location (E or H field or Power density S)
- $K_{Passive\ Antennas}$ is the number of transmitters radiating on time static beams of passive antennas
- $K_{MaMIMO\ Antennas}$ is the number of transmitters radiating on MaMIMO antennas

For the aims of this project the analysis will be focussed only on the exposure generated by MaMIMO antennas in 5GNR. Hence, the exposure of such type of devices can be expressed as:

¹³ In this context single user does not correspond to the situation where there is just one user in the cell, but the situation in which at the specific time, the antenna is serving just one user.

¹⁴ The Exposure Ratio ER is the ratio between the quantity representing the exposure to the exposure limit; for E and H field the quantity and the limit are squared to convert to power density.

$$L_k(r, \vartheta, \varphi, t, t')|_{ER>0.05} = \sum_{n=1}^{N_k} \mathcal{U}_n(t) \mathfrak{S}[EIRP_n(\vartheta, \varphi, t, t') PL_n(r, \vartheta, \varphi, t, t')] \quad (7)$$

for GoB MaMIMO antennas, see Figure 20, in which

- N_k is the number of beams in the antenna beamset of the specific configuration for the k-th MaMIMO antenna,
- PL_n is the Path Loss to the observation point associated to the n-th beam in the scenario
- \mathcal{U} is a unitary function that assumes a value of 1 when the beam is active, otherwise 0, for the specific time interval.

$$L_k(r, \vartheta, \varphi, t, t')|_{ER>0.05} = \mathfrak{S}(EIRP_k(\vartheta, \varphi, t, t') PL_k(r, \vartheta, \varphi, t, t')) \quad (8)$$

for the k-th EBB MaMIMO antenna.

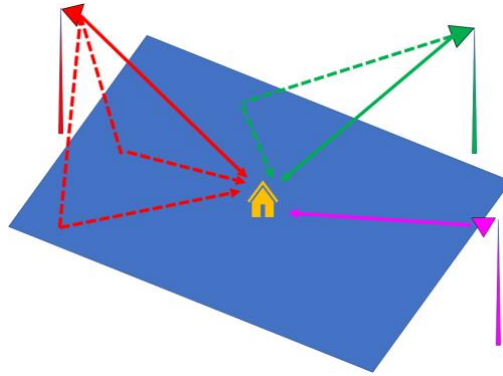


Figure 20: Exposure contributions to an observation point.

4.2.2 SINR at location

Each position in the scenario has associated a SINR depending only on the specific frequency band assigned to the serving BTS with potential contributions coming from Out of Band (OOB) emissions by other operators in the same band allocated for the service (as an example band N78 for 5G NR). For the scopes of this task, the OOB emissions coming from adjacent channels are neglected, without any loss of generality and effects on the results.

In the case of 5G NR, in each position, SINR exists only if in the position there is an active UE.

$$SINR(p, t, t') = \frac{P_{useful}(p, t, t')}{P_{sameMaMIMOAntenna}(p, t, t') + P_{otherMaMIMOantennas}(p, t, t') + ThermalNoise(B)} \quad (9)$$

where,

- P_{useful} is the received power at the location, generated by the MaMIMO antenna for delivering service with the specific beam at location
- $P_{sameMaMIMO antenna}$ is the received power at the location generated by the same MaMIMO antenna delivering service to other users with other beams of the same beamset.
- $P_{otherMaMIMO antennas}$ is the received power at the location generated by other MaMIMO antennas delivering service to other users.
- $ThermalNoise(B)$ is the thermal noise over the channel at temperature T , determined as $N = KTB$ where K is the Boltzman constant, T is the temperature in Kelvin and B the bandwidth in Hz.

SINR can be determined once the power associated to each beam and activity of beams is known and is strongly time, position and user activity dependent.

5 Activities planned in Task 3.4

5.1 Background

The deployment of MaMIMO antenna technology in a mobile communication network has highlighted the statistical connotation of the radiation. It was only in 2019 that the international standards introduced a concept of statistics in exposure to EMF from BTS with a technical report [4], but it was only in 2023 that standards implemented some statistics by the Actual Max Approach [2][5]. Before the Actual Max Approach was introduced, the evaluation of the exposure was considered static once the antenna's radiation pattern and configured power were defined.

When looking at the exposure to EMF from BTS, some basic concepts need to be considered:

- The field level or power density level generated in a spatial point determines the exposure that depends on antenna characteristics, the time evolution of the power, the position of the point in the scenario EM environment, and, in the case of MaMIMO antennas, on the position of users in the scenario. On the other hand, the concept of exposure has no meaning if the position of the evaluation point is not specified. It is required to pay attention to concepts like “average value of the exposure on large areas or whole town” or “the exposure in a point is XX% lower than the limit” if the position of the points with respect to the EM context is not specified.
- A MaMIMO antenna optimizes the energy distribution, radiating only where it is needed and for the level and time it is needed; the radiation generated in a mobile communication network is managed on a user basis. That is a change of paradigm: from observing the exposure to designing the exposure.
- Currently, the statistic of the communication is considered with the time statistics of the power while the statistics of the spatial distribution of the radiation need to be improved and considered in the design stages for the deployment of a base station.
- It is required to better understand the mechanisms, the statistics, and which statistical parameter better characterizes the space-time radiation distribution. This is hard to obtain by the real base station in operational conditions. Simulations can be of great help in understanding the phenomenon.
- It would be important to translate information acquired on the time-space distribution of the radiation to operational methodologies to design the exposure.

Accordingly, the exchange of experiences shared by the different stakeholders involved in the project can give, and enrich all the phases of the analysis with different views, different needs, and different design methodologies for an effective description of the problem.

The activities planned in the task are mainly devoted to the time-space analysis of the radiation generated by MaMIMO antennas, to extract information, and to define methodologies to characterize the exposure.

In this project, there are some tasks, such as T7.3, dealing with measurements of 5G NR signals in real scenarios. The exposure evaluation, at the design stages, requires the use of statistical concepts; these concepts can be translated into measurement procedures to experimentally evaluate the exposure in real operational conditions. Now, in [5], the methodology adopted for measurements does not consider the space and time distribution of the radiation, leading to an overestimation of the exposure. Analysis and results obtained in task T3.4 could be helpful in designing measurement activities and giving answers to the open questions regarding the experimental evaluation of the exposure.

5.2 Structure and Expected Results

The planned activity can be summarized as the determination of the time-space distribution of the exposure generated by MaMIMO antennas in scenarios considering time and spatial diversity based on user activity and distribution, expressed in terms of electromagnetic field or power density in locations of a scenario, as summarized in Figure 21.

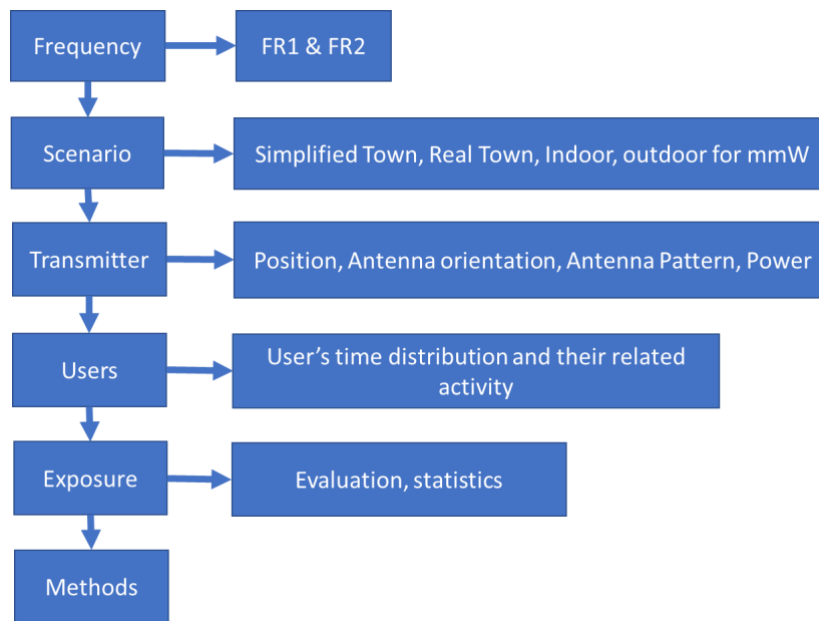


Figure 21: The simulation scheme adopted in task T3.4.

The analysis is planned to be performed both in FR1 and in FR2, analysing frequencies used for 5G NR Time Division Duplex (TDD)

Three types of scenarios are planned to be considered:

- The modified Madrid grid scenario (MMGS): it consists of a simplified town scenario, the same for all partners performing computations. The scenario is composed of a basic tile, including buildings, streets, and green areas. The basic tile is repeated to form an array so that the complex of a town is obtained. Each tile is considered flat, so changes in the height of the terrain are not considered, while changes in the building height are taken into account. A detailed description of the MMGS can be found in section 6.1.2.
- The real town scenario: depending on the availability of town models by each partner working in task T3.4, a portion of a real town scenario is considered. The scenario consists of the digitized model of a real town, considering the shape of buildings and details of the terrain. For industrial property reasons, the name of the town could not be declared, as well as the file containing the scenario could not be made available in the project. A description of the real-town scenario can be found in section 6.1.3.
- Indoor scenario: the scenario represents the internal of a building including room, door, windows, corridors, ceiling, and furniture. The presence of a simplified human's model could be included too. For the indoor scenario, the priority is the analysis in FR2. A description of the scenario can be found in section 6.1.4.

Each base station is made of a number of radiating systems equipped with MaMIMO antennas. Each MaMIMO antenna is represented with a set of traffic beams for covering the serving area. For the scope of the project, only traffic beams will be considered, meaning that the antenna is equipped with just one broadcast beam for defining the attached area. Each radiating system has associated a configured power, see 6.2.3.

As indicated previously, the MaMIMO antenna activity depends on the user's distribution and activity. Accordingly, a distribution of users will be generated and distributed in the scenario as well, and the activity of each user will be defined, which generates the random activity of the antenna and, consequently, the exposure, see 8.1. Each user will be assigned an amount of data to be downloaded in the activity session, defining the download time and, consequently the activity of the antenna, section 8.1.1.

The exposure is evaluated on observation points. For the scope of the activities of the task, it is not strictly required that the observation points correspond to points where exposure limits can be exceeded since the attention is to the time behavior of the exposure. From there, a statistical analysis will be performed to extract the characteristics of the exposure.

Activities planned during the task at the design stage can be modified on the basis of the results found.

6 Requirements for Simulations

The scheme for the simulation activities to be performed in task T3.4 is shown in Figure 22. After the parametrization of each single part of the entire activity, some of these are developed in this section, while some will be decided along the way depending on the specific needs of the activity. Initially, it is planned to start with the analysis of a simplified scenario, like the MMGS, to check and to make experiences on the proposed approaches, as indicated in sections 4 and 5. In the second part the proposed approaches are applied to the real scenarios, indoor and outdoor, to collect data for drawing conclusions and to have some suggestions for the activities planned in task T7.3.

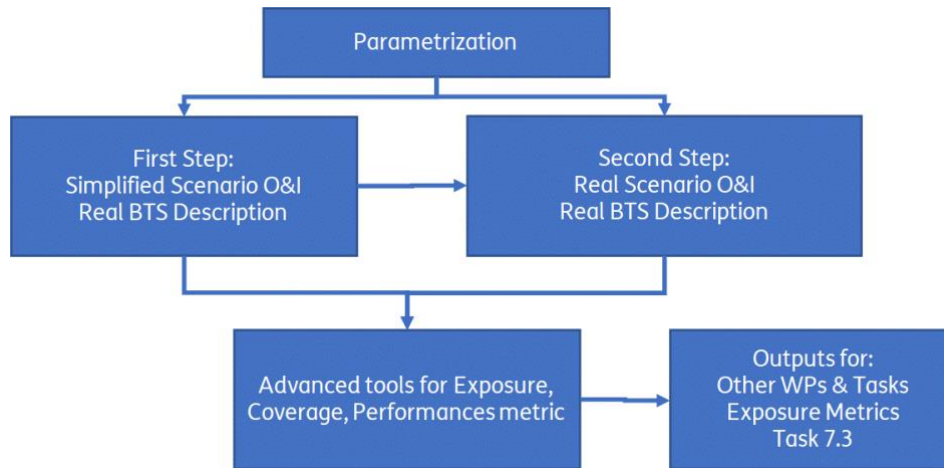


Figure 22: A schematic view of the simulation activities in task T3.4.

Each element of the problem is analyzed in the following so as to let each partner implement the activity on a common basis.

6.1 The Scenario

6.1.1 General

Outdoor simulations are planned to be carried out in three types of scenarios:

- a simplified scenario, based on the Madrid Grid Scenario (MGS) [6] with some changes, as specified later to adapt to the scope of this task.
- a real town scenario
- a reduced-size scenario for simulations in FR2.

Indoor simulations are planned to be carried out in two types of scenarios:

- a professional environment with offices and corridors,
- an industrial scenario, including simulating machinery.

Activities planned for MaMIMO antennas modelling and mapping are planned to investigate exposure to EMF in the surrounding of the BTS related to coverage over large areas considering users' distribution.

Simulations performed on common scenarios allow partners to have a common basis for comparing computation results.

6.1.2 The Modified Madrid Grid Scenario

The MMGS consists of an ordered and regular distribution of buildings and open areas, separated by regularly distributed streets. The whole scenario is constructed by placing the basic element, the tile (containing buildings, open areas, and streets), close to each other. When connected to each other, tiles generate continuity for the roads on an ordered chessboard.

Each tile is defined as follows:

- The tile consists of a 387 m by 552 m area, including sidewalks, parking lanes, and roads, as shown in Figure 23. Two shapes of buildings are considered, the square base building and the rectangular base building,

- The square base buildings are sized 120 m x 120 m,
- The rectangular base buildings are sized 120 m x 30 m,
- Building height does not follow the MGS rules and is described in section 6.1.2.1,
- The open areas are sized 120 m x 120 m,
- Sidewalks surround each building and are 3 m wide. Pedestrians are allowed to move on sidewalks and overlaying elements like bus stops, building entrances, and metro entrances. In the MMGS there are two special types of sidewalks:
 - Gran Via sidewalk: 6 m wide
 - Calle Preciados: South-north oriented sidewalk of 21 m between rectangle-shaped buildings
- The roads are 3 m wide and there is always one lane in one direction, accompanied by parking lanes. A special type of road is Gran Via, where there are no parking lanes on any side and there are three road lanes in each direction,
- Building's entrances are sized 3m x 3m and placed as follows in the scenario, see Figure 24,
- Square-based buildings have six symmetrical entrances with two possible configurations:
 - Horizontal. Each building wall with an east-west orientation has two entrances, with the center positioned 40.5 m from the closest building corner while building walls with a south-north orientation have only one entrance with the center in the middle of the wall,
 - Vertical. Each building wall with a south-north orientation has two entrances, with the centre positioned 40.5 m from the closest building corner; instead, building walls with an east-west orientation have only one entrance with the centre in the middle of the wall.
- Rectangle-based buildings have 4 entrances, two on each side of the building positioned 40.5 m from the closest building corner,
- There are 8 metro stations sized 3m x 3m, adjacent to the buildings, overlaying the sidewalk, positioned 4.5m away from the closest buildings corners; their position is shown in Figure 25,
- There are 8 Bus stops size 3m x 18m, adjacent to the buildings and overlaying the sidewalk, positioned 15 m from the closest building corner. The position of each bus stop is shown in Figure 25,
- There are Crossing lanes at the intersection with each building. Crossing lights are 3 m wide and there are no traffic lights at Calle Preciados, see Figure 26,
- Each tile consists of:
 - 7 square building,
 - 8 rectangular buildings,
 - 1 open area.

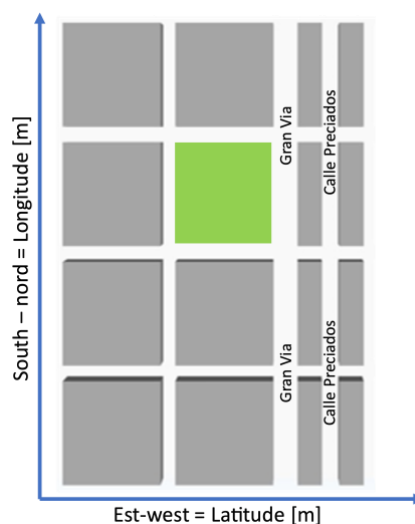


Figure 23: The basic tile of the MMGS.

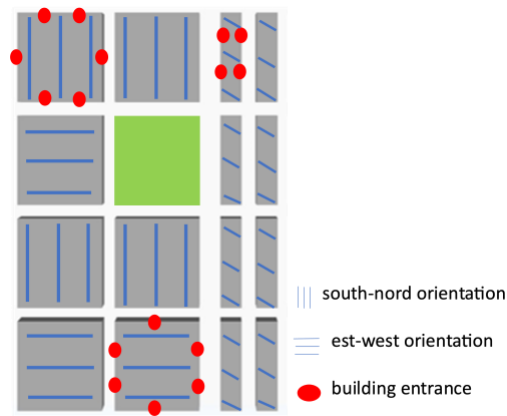


Figure 24: The basic tile of the MMGS with building entrance. Building marked in the same way have building entrances in the same location.

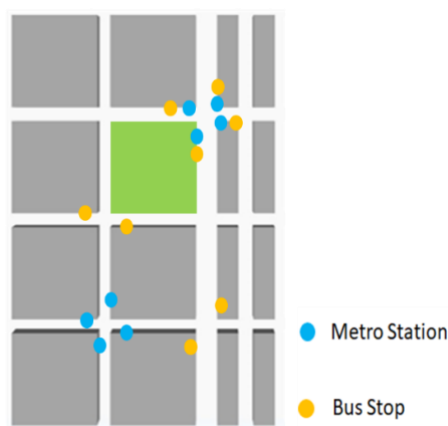


Figure 25: The basic tile of the MMGS with metro entrance and bus stop.

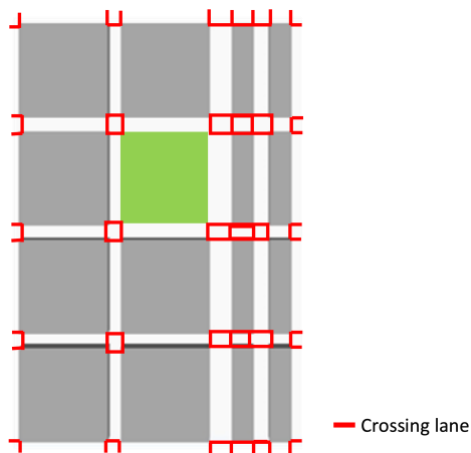


Figure 26: The basic tile of the MMGS with crossing lanes.

The adopted coordinate system is Cartesian and the orientation of the MMGS base tile is oriented as shown in Figure 27.



Figure 27: The basic tile of the MMGS with adopted cartesian coordinates.

In the data file representing the MMGS, each element (building and green areas) is represented as a polyline defined by vertices. There is no need to represent roads since they are obtained by the building's position in the basic tile. Building entrances, bus stops, and metro stations are not represented in the data file since they do not contribute to the computation of the EMF field level. File structure for the representation of the scenario

The polyline describing a building is a collection of vertices; a pair of coordinates represent each vertex; vertices are counter-clockwise ordered, see Figure 28, and the last vertex must be equal to the first one. Each element is described by a block of information constituted by:

- The header row:
 - An integer label representing the material of the element. To label the electromagnetic properties of each material, permittivity and conductivity can be associated,
 - Two integer labels valued at zero,
 - A float indicating the height of the building, in meters,
 - Each number is separated by the space character.
- As many vertex rows as the number of vertices, each one representing:
 - The X coordinate (Latitude) in meters of the vertex,
 - The Y coordinate (Longitude) in meters of the vertex,
 - Each number is separated by the space character.
- A closing vertex having the same coordinates as the first vertex
 - The closing block keyword “END”,
 - The closing file keyword “END”.

The description file is shown in Table 2, while a numerical example is shown in Table 3

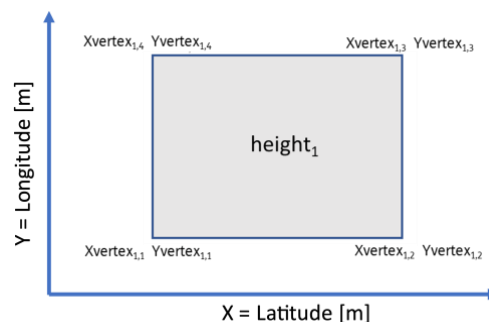


Figure 28: Example of the building represented by MMGS data file.

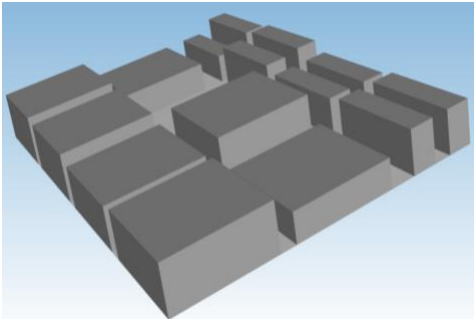
Table 2: The structure of the polyline representing a building.

List of Polyline vertices	Description	Comment
Material label₁ 0 0 height₁	Header row	Building 1
Xvertex_{1,1} Yvertex_{1,1}	Vertex row	
Xvertex_{1,2} Yvertex_{1,2}	Vertex row	
...	...	
Xvertex_{1,M} Yvertex_{1,M}	Vertex row	
Xvertex_{1,1} Yvertex_{1,1}	Closing vertex	
END	Closing block	
...
Material label_N 0 0 height_N	Header row	Building N
Xvertex_{N,1} Yvertex_{N,1}	Vertex row	
Xvertex_{N,2} Yvertex_{N,2}	Vertex row	
...	...	
Xvertex_{N,M} Yvertex_{N,M}	Vertex row	
Xvertex_{N,1} Yvertex_{N,1}	Closing vertex	
END	Closing block	
END	Closing file	

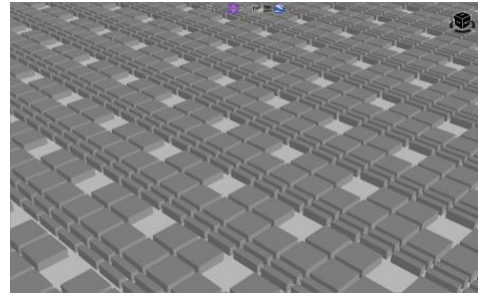
Table 3: A numerical example for the representation of buildings in the scenario.

1 0 0 55.0	First Building: The element material is coded with the label 1 and is 55.0 m height
0.0 0.0	The first vertex is at X = 0.0 m, Y = 0.0 m
100.0 0.0	The second vertex is at X = 100.0 m, Y = 0.0 m
100.0 100.0	The third vertex is at X = 100.0 m, Y = 100.0 m
0.0 100.0	The fourth vertex is at X = 0.0 m, Y = 100.0 m
0.0 0.0	The closing building vertex has the same coordinate as the first vertex
END	The closing building Label
2 0 0 0.25	Second Building: The element material is coded with the label 2 and is 25.0 cm height
0.0 0.0	The first vertex is at X=0.0 m, Y= 0.0m
100.0 0.0	The second vertex is at X = 100.0 m, Y = 0.0 m
125.0 50.0	The third vertex is at X = 125.0 m, Y = 50.0 m
100.0 100.0	The fourth vertex is at X= 100.0 m, Y=100.0m
0.0 100.0	The fifth vertex is at X= 0.0 m, Y=100.0 m
0.0 0.0	The closing building vertex has the same coordinates as the first vertex
END	The closing building Label
END	The closing file Label

Figure 29 a) shows the basic MMGS tile while Figure 29 b) represents the MMGS by approaching tiles each other to form an array.



a)



b)

Figure 29: a) the basic MMGS tile in 3D representation, b) the representation of a town.

6.1.2.1 Building heights

The original MGS defines the height of each building according to the number of floors; each floor is 3.5 m high. Differently by MGS, in the MMGS, the height of each building was changed and defined as:

$$h_{building} = h_{floor} * N_{floor}$$

$$h_{floor} = 3.5 \text{ m}$$

$$N_{floor} \in [5; 15] \text{ uniformly random distributed} \quad (10)$$

6.1.2.2 Materials

Each element of the scenario is associated with the electromagnetic properties of the different materials. Within the MMGS there are two distinguished elements, namely buildings and green areas, and the roads made of elements' separation. The electromagnetic properties of the materials for each element have been obtained by the following equations where f is the frequency in GHz and σ is conductivity in S/m (see [7]).

$$\varepsilon' = a * f^b$$

$$\sigma = c * f^d$$

$$\varepsilon'' = 17.98 * \frac{\sigma}{f} \quad (11)$$

Parameters a, b, c, d in equation (11) are reported in Table 4.

Table 4: Parametrization of the material characteristics as defined in [7].

Material class	Real part of relative permittivity		Conductivity S/m		Frequency range
	a	b	c	d	GHz
Vacuum (\approx air)	1	0	0	0	0.001-100
Concrete	5.24	0	0.0462	0.7822	1-100
Brick	3.91	0	0.0238	0.16	1-40
Plasterboard	2.73	0	0.0085	0.9395	1-100
Wood	1.99	0	0.0047	1.0718	0.001-100
Glass	6.31	0	0.0036	1.3394	0.1-100
Glass	5.79	0	0.0004	1.658	220-450
Ceiling board	1.48	0	0.0011	1.0750	1-100
Ceiling board	1.52	0	0.0029	1.029	220-450
Chipboard	2.58	0	0.0217	0.7800	1-100
Plywood	2.71	0	0.33	0	1-40
Marble	7.074	0	0.0055	0.9262	1-60
Floorboard	3.66	0	0.0044	1.3515	50-100
Metal	1	0	10^7	0	1-100
Very dry ground	3	0	0.00015	2.52	1-10 only
Medium dry ground	15	-0.1	0.035	1.63	1-10 only
Wet ground	30	-0.4	0.15	1.30	1-10 only

In the MMGS:

- roads have been modeled as concrete,
- green areas have been modeled as wood,
- buildings have been modeled as brick.

Values are taken from [7] and [15].

Table 5: Electromagnetic characteristics of the materials present in MMGS.

Material	Relative Permittivity	Conductivity [S/m]
Frequency 3.6 GHz		
Concrete	5.24	0.12
Wood	1.99	0.02
Brick	3.91	0.03
Frequency 26.0 GHz		
Concrete	5.24	0.59
Wood	1.99	0.15
Brick	3.91	0.04
Human Body	17.7	24.4

6.1.3 The Real Town Scenario

The real town scenario involves an exposure study in a more complex scenario than the MMGS, due to the greater complexity of the propagation environment.

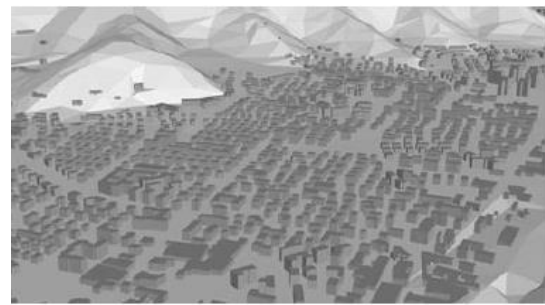
A real town often has a non-regular and non-orderly conformation of the streets, a non-orderly layout of the buildings and parks, green areas, and rivers are in the urban environment; the randomness of the real environment and geographical characteristics are fundamental for determining the field distribution and to investigate exposure to EMF.

The reconstructed and digitized model of a real town shows, with high precision, all the characteristic elements of the city, the details of all the buildings, the orography, and the surrounding environment, including, for example, the green areas, the mountain reliefs, the river, etc. Each element of the mathematical model of the entire city, being distinct, can be characterized by its specificity. In fact, each building or any other element present in the town is represented through a specific object and is uniquely characterized, assigning it the correct characteristics, such as the shape, dimensions, and electromagnetic characteristics at the working frequencies.

The orography is represented using specific objects and there is the possibility of evaluating its impact on EMF exposure, associated with the differentiation of the territory based on orographic characteristics; there may be extensive portions of mountainous territory, perfectly flat and regular portions of territory and other portions in which the conformation of the ground is not perfectly flat, see Figure 30, Figure 31.



a)



b)

Figure 30: a) Portion of real town. b) reconstructed model.



Figure 31: a) Portion of real town. b) reconstructed model.

The reconstructed mathematical model of the city is provided as an input parameter for the process of determining the radio coverage and subsequent calculation of the EMF exposure.

For the reproduction of a real city, one of the methodologies used is stereoscopic aero photogrammetry, in which aerial shots taken from multiple angles are processed using stereoscopes; they are instruments that allow the reproduction of a three-dimensional view starting from two-dimensional images. The stereoscopic reconstruction process allows the fusion of two or more different images into a single three-dimensional vision and is based on the physiological principle of the perception of three-dimensionality in human vision.

6.1.4 The Indoor Scenario

The aim of the indoor exposure analysis is to focus on radio propagation in a simulation scenario inside buildings.

The scenarios considered will be models of real environments. In some of these environments, measurement campaigns can be planned depending on the development of the indoor technology, especially in FR2. The level of detail of the models will include building plan (planimetric) info like walls, windows, etc. (as an example see Figure 32)



Figure 32 Example of a real environment model with planimetric info.

The wall materials considered will be the one related to the environment where measurements will be carried out and will be characterized according to the ITU_R_P.2040 [7] report. Typically, such a list will contain concrete walls, brick walls, plasterboard walls, glass with metallic frame. Wall thickness will range from 10 to 30 cm, (external walls being thicker), real values will be used when available.

Two examples have been modelled and proposed to partners: an example of a small office environment (see Figure 33) and an example of an industrial hangar with machinery (see Figure 34).

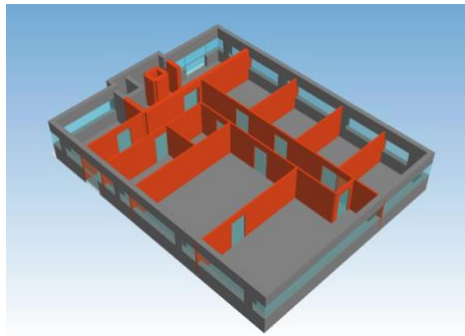


Figure 33: Example of an office indoor modelling proposed to partners.

The office building is 17 x 14 meters wide and 3 meters high. External walls are made of concrete and glass, 30 cm thick. Internal walls are 10 cm thick brick walls except for the elevator shaft and stairways in concrete and bricks, which are 30 cm thick; doors are made of glass 10 cm thick. The example is derived from a real environment in one of TIM’s premises.

The industrial hangar is 160 meters wide and 56 meters across with a height of seven meters. External walls and columns are made of 30 cm thick concrete; machineries are made of 30 cm thick metal with different height of 6,5,3 and 2 meters, respectively. This example is a prototype environment.

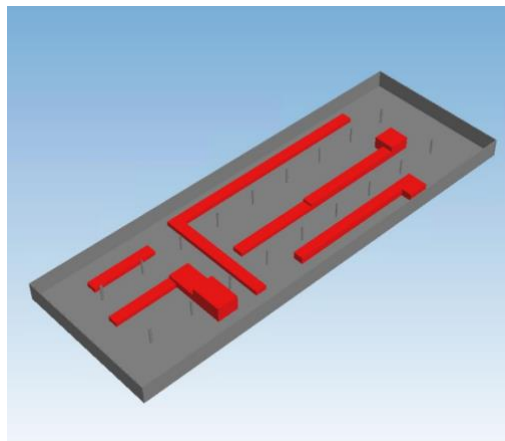


Figure 34: Example of an industrial hangar modelling proposed to partners.

6.1.5 The Scenario in FR2

For the scope of the activities planned in Task T3.4, the working group has decided to analyse a scenario made up of 3 basic tiles of MMGS. The description is in section 6.1.2. The representation of the environment model to use in FR2 is in Figure 35.



Figure 35: Scenario adopted in FR2.

6.2 Transmitter

6.2.1 Position and height

6.2.1.1 BTS in FR1

The BTS are deployed randomly in the scenario with the following constraints:

- All BTS are deployed not closer than a minimum distance of 300 m to guarantee the coverage,
- The BTS are installed on the top of buildings on corners, on borders or any position of the roof surface,
- Each BTS is at a fixed height from the roof of the building at 4 m from the walking surface. Note that as the buildings have variable height, the BTS have a variable height.

Each BTS consists of:

- Up to 3 sectors per layer; each sector is equipped with a MaMIMO antenna or a passive antenna depending on the frequency layer,
- Each sector is 120 degrees apart from the others, and the rotation of sectors is random with respect to the origin; different orientations of the antennas for each sector are allowed for coverage purposes,
- the direction of the radiation pattern, even if it is an envelope, is the same as the direction of the sector,
- Up to 3 degrees of downtilt is considered for each layer; uptilt is not considered.

Figure 36 shows an example of 5 BTS and 7 transmitters deployment

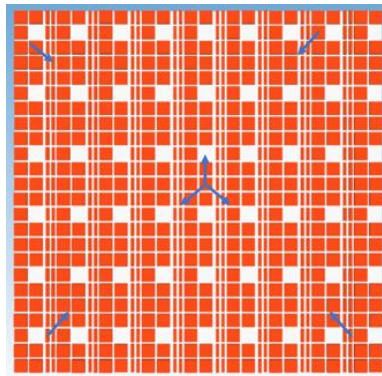


Figure 36: example of installed BTS in the MMGS.

6.2.2 Frequencies

Frequencies used for mobile services are subdivided in two ranges, namely FR1 and FR2, see Table 6 [8] where:

- FR1 includes frequencies below 6 GHz,
- FR2 includes frequencies that range beyond 6 GHz.

Table 6: FR1-FR2 frequency coding for 5G NR.

Band Name	Duplex Mode	Band	Simulation Frequency: the mid of band n78
		[MHz]	[MHz]
n78	TDD	3300.0 – 3800.0	3600.0
n257	TDD	26500.0 – 29500.0	28000.0
n258	TDD	24250.0 – 27500.0	28000.0

For the aims of the activities planned in the task, the channel bandwidth is not considered, all the power associated to a transmitter will be considered as concentrated in the centre frequency of the channel; so, simulations will be performed by considering a tone at the frequency carrying all the power. This assumption has no impact on the conclusions that will be drawn on coverage and exposure to EMF.

Depending on the implementations of the solvers used to perform computations, each frequency for each transmitter can be considered as a frequency layer, so coverage and exposure to electromagnetic field evaluations can be managed separately in postprocessing.

6.2.3 Power

It was agreed to define a fixed power for each operating frequency for each transmitter. Starting from this arbitrarily chosen value, the simulations will be carried out using power values, assigned to each transmitter for each used frequency, which could be fixed or vary randomly in a defined interval, as preferred by each partner, for example, 20% from the value reported in Table 7. Please note that transmission power has been established; EIRP is consequently obtained through antenna gain.

Table 7: Power associated with each BTS to be used in the computations.

Band	Power	Allowed Range
	[W]	[W]
N78	200.0	160.0 to 240.0
N258	1.0	0.8 to 1.2

6.2.4 Radiation pattern

Differently from previous generation communications systems, the MaMIMO antenna allows for generating several patterns, particularly a large number of narrow radiation patterns, that allow for performing advanced multi-user communication. Including these particular antenna patterns in the simulations is of paramount importance for effectively understanding the achievable performance level, as well as the realization of the desired coverage and the satisfaction of the exposure limits for the safety of people. Knowing the antenna pattern can also greatly help to understand and interpret the results of measurements.

Unfortunately, there are few definite guidelines for the generation of antenna patterns of this kind. Manufacturers have a stringent policy on the description of the radiating and structure characteristics of their antennas. In general, the antenna is described as a black box, with very little information on the radiating characteristics, often limited only to main parameters like beamwidth or the side lobe level, without a complete description of the pattern, for which only the main azimuthal and elevation cuts are provided. On the other hand, as noted above, for the correct simulation of the field level it is necessary to know the set of 3D patterns. The pattern description should include the level and directions of the sidelobes and possibly back-radiation. The problem of estimating 3D patterns from scarce information about the pattern represents an extremely challenging problem.

From a mathematical point of view, the problem of pattern identification starting from a few data points (gain, frequency, envelope of beams) is an ill-posed problem, which presents a non-unique solution. To identify the solution in this set it is necessary to introduce additional a priori information of the problem that narrows the search set.

Following a study on the possible a priori information generally available, a choice was made based on the geometric and construction constraints of the radiating structure. The first constraint is represented by the electrical dimension (i.e. the dimension normalized to the operating wavelength of the antenna). The physical dimensions of the antennas actually limit the range of fields that can be irradiated. Another characteristic generally available or obtainable from an analysis of the antenna geometry is represented by the specific sub-array structure implemented in the antenna under test. The radiating systems used in 5G are based on sub-array architectures which allow a reduction in the number of control points of the array. This structure further limits the set of electromagnetic field configurations (beams) that can be irradiated. The approach followed leads to a modeling of the array in subarrays which includes the presence of the ground plane. An example of a model is shown in Figure 37.

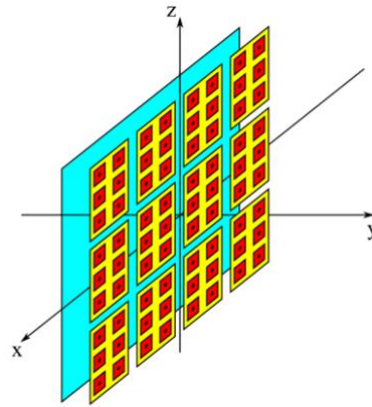


Figure 37: Scheme of the regular array (red elements) organized into subarrays (yellow rectangles) with a ground plane (cyan).

To obtain pattern estimation this model must be complemented with some pattern information, which is typically made available by vendors like: central frequency, horizontal and vertical beamwidth, gain, horizontal and vertical steering, presence of electrical/mechanical tilting, and if available, one or more cuts of the radiation patterns or of the envelope pattern.

To provide all the partners with a clear and non-ambiguous representation of the pattern, the data will be provided by means of the BASTA 2.0 .3drp standard [9]. An example of this file is provided in Figure 38.

```

Reference BASTA White Paper Version:2.0
Antenna Model:ExamplePattern
Reference Date:2024-01-01
  PatterName:Pencil
  BeamID:B101
Pattern Type:Generic
Frequency:3700MHz
  EIRP:<void>dBm
Configured Output Power:<void>dBm
  AAS Gain:17.8008dBi
Nominal Polarization:+45
  <Data>
Theta(deg)  Phi(deg)  MagAttenuation(dB)
  -90        -180      29.44
  -90        -179      29.44
  ...

```

Figure 38: example of BASTA 2.0 .3drp standard

For each pattern a different plain text file has to be provided. The file is essentially divided into two parts. In the first (marked in red in the example) some information on the file structure and the pattern characteristics (like frequency, maximum gain, polarization) are given. In the second (marked in blue in the example), the radiation pattern is provided with 1° step accuracy in a spherical coordinate system centred on the antenna. The provided values “MagAttenuation (dB)” represent the reduction of the gain in the prescribed direction with respect to the maximum (“AAS Gain”).

UCAS has provided the partners with the pattern files generated according to requirements discussed with the partners, and for each pattern, a summary figure containing some pattern plots and information has also been provided. Finally, the envelope of all the calculated patterns has been provided in a separate .3drp file.

7 Description of the Computational Tools

Ray tracing is a Deterministic Propagation Model based on the approximation of the electromagnetic wave as a ray, namely the vector normal to the surface wavefront, and uses the basic concepts of geometrical optics. Through the concept of ray, the main electromagnetic propagation mechanisms can be easily identified; when the interaction occurs between a ray and an element present in the propagation scenario, one or more electromagnetic interactions, such as reflection, refraction, and diffraction, can occur.

The use of ray tracing requires a 3D representation of each object inside the scenario and it's very reliable in terms of accuracy of the result at the cost of increasing computational resources as a function of the scenario's size.

7.1 UNICAS simulation tool

The simulation tool realized by UCAS unit is “Ray Launching Cassino” (RLC); it is a tool specifically designed for the estimation of the channel matrix that is established between a base station antenna and one or more terminals that are in the external areas of a city landscape (i.e. Madrid grid or real city models). To perform this task, it employs a ray-tracing approach, specifically a ray launching (or pincushion) method. Within the activity planned in NextGEM, RLC is used to generate computational results.

The tool requires the definition of:

- The scenario, of arbitrary size, developed on a planar ground; the buildings in the scenario are represented as rectangular cuboids that can be arbitrarily stacked and oriented; for each item (terrain or cuboids) the user can select the complex permittivity relative to vacuum,
- An antenna model for the base station; the antenna model can be provided in terms of radiation patterns or an antenna geometry (layout and basic element type); in the latter case, the antenna pattern will be calculated taking into account the polarization of the radiated field by the software,
- A set of measurement points representing the coordinates of the receiving antenna(s); for the receiver's elementary radiators are employed,
- The ensemble of parameters for the simulations, like frequency, number of rays to launch, and maximum number of reflections.

The tool, developed using MATLAB, generates a sphere of beams departing from the base station antenna; these beams can be reflected by the environment's buildings or the terrain, and multiple successive reflections for each ray can be calculated. For each reflection the reflection coefficient is calculated, considering the TE/TM components of the field so that the information on the polarization of the field is preserved.

Once the rays have been calculated, the rays that contribute to the calculation of the field in the desired measurement points are selected; the field is then calculated using the information on the radiation of the base station in the specific direction of these rays and considering the free-space attenuation as well as the variation in amplitude/polarization due to the considered reflections. It is worth noting that once the BS-users channel matrix has been calculated, different communication schemes, like grid-of-beam or various beamforming approaches, can be considered, and their influence on the system performance can be readily evaluated.

The main advantage of RLC compared to other tools is represented by its capability to evaluate the parameters of the channel matrix that is created between the BS antenna and the users. Knowledge of the communication channel matrix allows the optimal synthesis of the beam radiated by the antenna, efficiently exploiting the propagation environment.

The ability to calculate the channel matrix will be exploited using a deterministic approach to study the impact of this beamforming technology, which is expected to be widely used in future generation communication systems, on the power radiated by base station antennas into the environment.

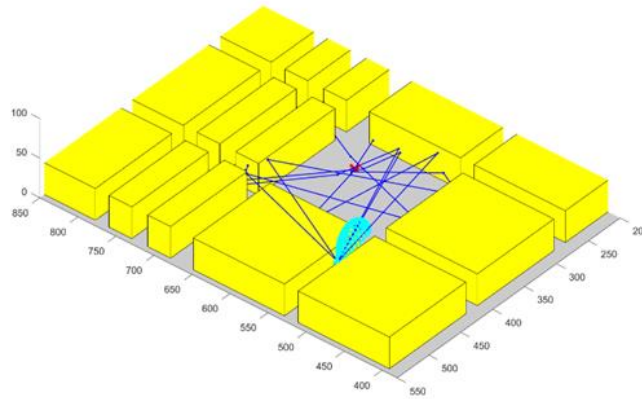


Figure 39: Example of the calculated rays (Blue) for the connection to a user (red) and the pattern used by the base station for the connection (cyan).

7.2 TIM - FiberCop simulation tool (T3D e FIA)

7.2.1 General

TIMPlan 3D (TP3D) is a tool for radio coverage and channel estimation in macro/micro/indoor environments developed by TIM. It responds to the need to have one propagation simulator for all cell configurations, suitable to simulate active and passive antennas, in simulated and real scenarios at any frequency, by considering the electromagnetic characteristics of materials.

TP3D is suitable for designing mobile networks in Outdoor and Indoor Environments by using the following two approaches:

- Intelligent Ray Tracer,
- Fast Indoor Analysis (FIA).

Within the activity planned in NextGEM, TP3D generates computational results. However, the TP3D tool is not shared with or made available to NextGEM.

7.2.2 Intelligent Ray Tracer

The Intelligent Ray Tracer technique is based on optimized Ray Tracing methodologies that strongly reduce calculation times and allow reasonable execution time even in large scenarios.

The methodology can be schematically described with the following steps:

- Creation of the environment model

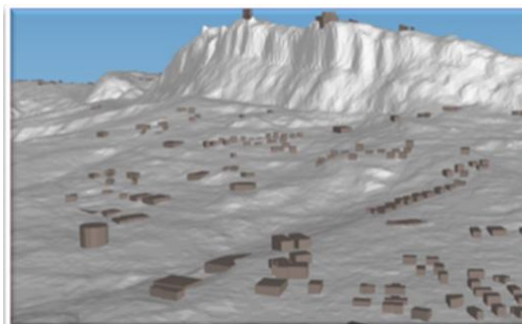


Figure 40: example of 3D scenario in TP3D.

- Research of relationship between elements of the scenario

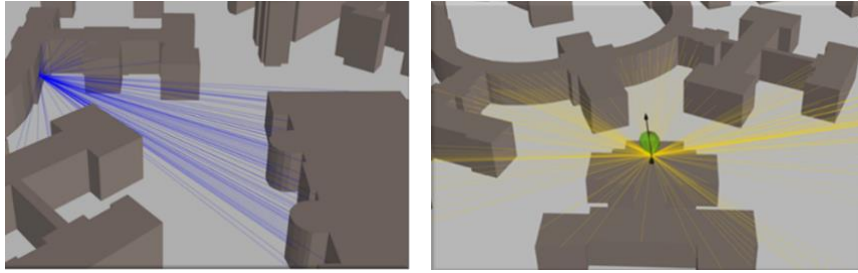


Figure 41: example of connection between element of the scenario.

- Field calculation

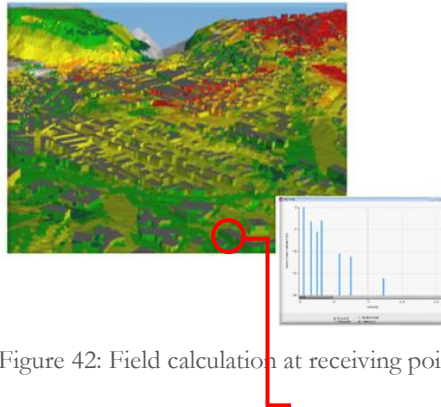


Figure 42: Field calculation at receiving point.

7.2.3 Fast Indoor Analysis

The Fast Indoor Analysis (FIA), suited for projects requiring a fast design response, uses simple 3D modelling starting from planimetric information and the propagation model COST231 multi-wall. As the module is integrated within TIMplan 3D, 3D Models of buildings can also be analyzed with the Intelligent Ray Tracing approach and included in a wider Urban environment to create an integrated simulated scenario.

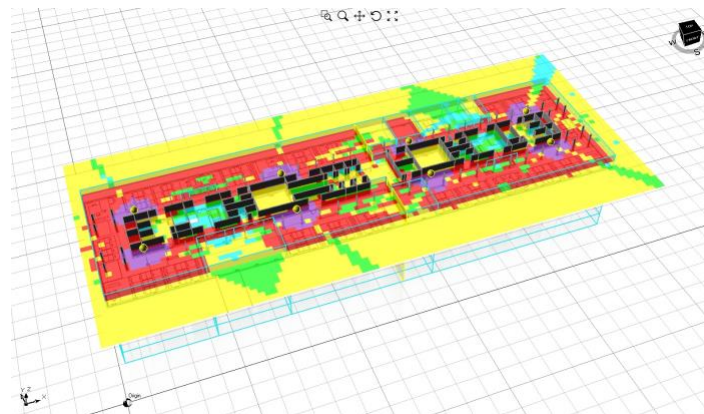


Figure 43: Example of a FIA simulation.

8 Evaluation of the exposure to EMF

The field strength level, and eventually the exposure, in each observation point, depends on the following factors:

- The power radiated on the specific radiation pattern (beam) at the specific time frame,
- The characteristics of the radiation pattern,
- The distribution of the users,
- The scenario, including the EM characteristics of each object,

On the basis of previous sections, the following holds:

- The exposure in each observation point is given by the survey of all the contributions generated by all the active beams at the specific time from all the antennas present in the scenario. Some contributions coming from far away base stations or from NLOS base stations could be negligible,
- Each user is active for the time required to download the amount of data required, then the user ends its activity and does not stimulate the antenna to radiate in its direction anymore,
- The amount of data that can be downloaded in each time frame depends on the interference scenario and the total antenna activity, so the power to be used to get the required SINR level can be determined.

The previous statements allow to separate the specific coverage by each beam from the computation of the exposure level. That means a reference coverage for each beam with a reference power can be computed a priori and then, in post-processing, the exposure can be evaluated on the basis of the specific users and traffic distribution.

Let us start by discretizing the time in steps, as an example every 5G NR Transmission Time Interval (TTI) (1 ms). For each time step, the following actions can be assumed, see Figure 44:

- Management of the active set of users:
 - Update of data amount to be downloaded,
 - Management of the active set:
 - Removal of the users that have downloaded the amount of assigned data from the active set,
 - Generation of new active users to be included in the active set and definition of the amount of data to be assigned (downloaded) by each user.
- Determination of SINR¹⁵ at the user's position,
- Determination of the amount of data to be downloaded,
- Determination of the field level at position.

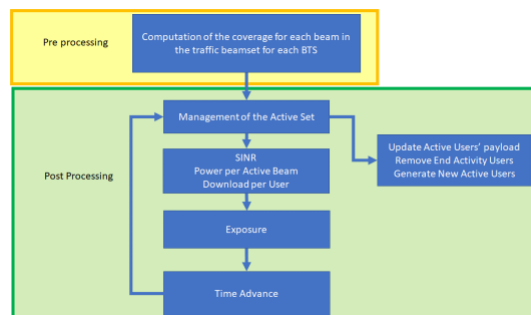


Figure 44: A schematic view of the computation process.

The exposure level in a specific point¹⁶ and at a specific time as a function of the active users requiring downloading an amount of data can be defined as:

¹⁵ SINR is assumed to be evaluated in the specific time step; this is an acceptable approximation within the time step

¹⁶ The position of the observation point in general is not the same as the position of the user.

$$E^2(p, t) = \sum_{k=1}^{K_{BTS}} \sum_{n=1}^{N_{kbeams}} E_{k,n}^2(p, t) U_{k,n}(t) \quad (12)$$

where,

- $E^2(p, t)$ is the squared total electric field (or magnetic field or power density) at the specific point and at the specific time,
- K_{BTS} is the number of BTS contributing to the exposure,
- N_{kbeams} is the number of beams for each BTS,
- $E_{k,n}^2(p, t)$ is the squared total electric field (or magnetic field or power density) at the specific point and at the specific time generated by the specific beam of the specific BTS,
- $U_{k,n}(t)$ is a unitary function that assumes value 1 if the beam is active at the specific time step, otherwise is 0.

The electric field (or magnetic field or power density) in a specific point and at a specific time is given by the addition of all contributions coming from all the active beams serving each user generated by all the BTS in the scenario. Each field contribution depends on:

- the position of the evaluation point in the scenario,
- the serving beam,
- the power assigned to the beam,
- the position of the users in the scenario.

While time advances in steps, the exposure, in points and/or all over the scenario, can be determined and thus obtaining the time evolution of the exposure in the observation point that depends on activity over the simulated scenario.

8.1 Users Distribution manages the exposure

8.1.1 Amount of data assigned to each user

In a recent publication, [10], the forecast for the next years of the amount of data traffic per smartphone per month and per geographical area is reported. That could be the basis for the determination of the amount of data expected per month that could be used as the basis for bordering the activity of each user in the scenario. From [10] for some countries, the amount of data per month per smartphone is shown in Table 8, in the same table there is an extrapolation to the amount of data downloaded per day, by simply spreading the monthly traffic over a day. Those figures could be used as input for the simulations to define users' activity per day.

Table 8: Estimate of the data traffic per month per smartphone (from [10]).

Country	Estimate 2023 traffic		Estimate 2026 traffic		Estimate 2029 traffic	
	Monthly	Daily	Monthly	Daily	Monthly	Daily
Western Europe	27.00	0.90	43.00	1.43	64.00	2.13
Central and Eastern Europe	19.00	0.63	30.00	1.00	43.00	1.43

Once the amount of data per day is defined, the amount of data per session of activity per each smartphone can be estimated. If it is supposed that each smartphone periodically attaches to the network for downloading data, that could be used as a basis to establish the amount of data per session. As an example, if each smartphone performs an activity every 15 minutes, then the amount of data that can be downloaded in 2023 per session is 9.4 MB in Western Europe.

Two further refinements can be assumed:

- By type of activity: as an example, it can be assumed to distinguish the downloaded data per activity type, as an example voice call, normal download activity, and huge activity (intended as heavy download session, as an example streaming), each one having a different amount of downloaded data,
- By randomizing the amount of downloaded data per activity.

All the previous assumptions contribute to defining the time each smartphone remains active on the network, contributing to defining the exposure in an observation point.

Of course, the previous numbers are assumptions, other assumptions can be adopted by the partners performing computations.

8.1.2 Capacity of each 5G NR BTS equipped with MaMIMO antenna

What is described in section 8.1.1 indicates the downloaded data per smartphone per session; the time required to download the assigned amount of data to each smartphone depends on the capacity of the MaMIMO antenna to deliver data, by the number of active users per unit of time, and the interference environment in the specific time-space point.

Since, at the moment of writing of this report, the load of 5G NR BTS is not so high, to establish the day capacity of traffic download per BTS, the following approach has been used:

- 13 Italian towns have been selected (big town to medium town),
- 13 heavy loaded cells 4G, 1 each per town, have been selected,
- Each cell has been observed for 7 days,
- The counter monitoring the throughput reported over 15 minutes, or each cell has been considered,
- Each cell throughput has been scaled to 5G NR band (100 MHz),
- A function linking the amount of data downloaded every 15 minutes has been generated as the average over the observation period and over all the cells of the time throughput.

The function allows to define the global activity of the equivalent 5G NR cell during the day in terms of number of bits downloaded per quarter of hour. If considering the amount of data assigned to each smartphone per activity session, as described in 8.1.1, that allows to determine how many users are active in that specific time interval. Figure 45 shows the time to load function of the BTS, in which the origin corresponds to midnight.

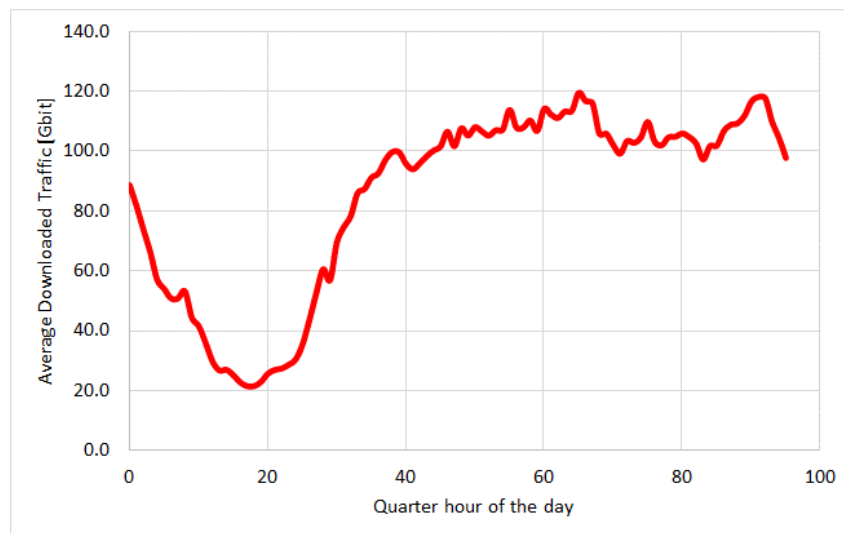


Figure 45: Downloaded data per quarter of hour by the cell.

8.1.3 SINR to Throughput

In publication [11] it is reported the downlink level throughput on the basis of the characteristics of the 5G NR technology (Figure 48); for the purposes of task T3.4, the top yellow line reports a max throughput of 1.752 Gbps. This figure can be used to establish the amount of data that can be delivered to the specific user in the time interval used in simulations. Once the SINR at the specific location where the users are is determined, the amount of delivered data is known and then removed from the payload until depletion. After that, the user is removed from the active set.

Figure 1: Results of SUT Model – Downlink (for a DL/UL ratio of 3:1)

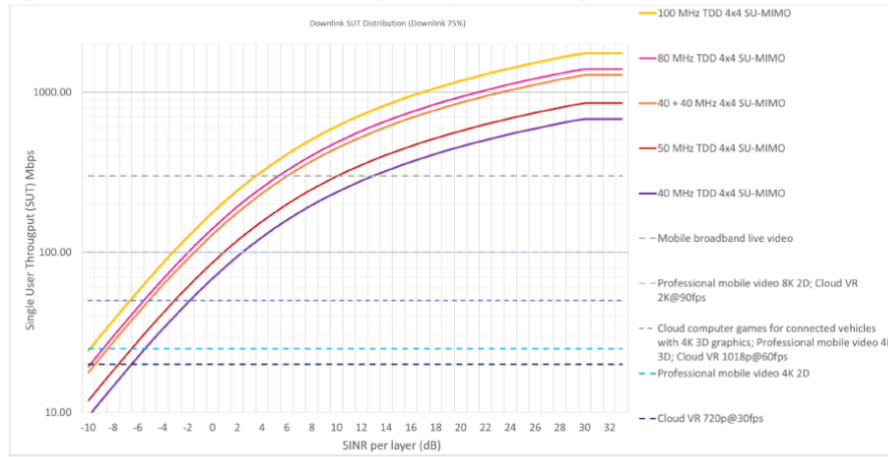


Figure 46: Downlink link level throughput.

By expanding equation (9), SINR at user location can be determined on the base of the active beams from the same base station and from other base stations in the surrounding in the specific frame:

$$SINR = \frac{P_u(m, p, t)}{KTB + \sum_{n=1}^N P_{Same\ BTS}(n; n \neq m, p, t) + \sum_{k=1}^K \sum_{n=1}^N P_{Other\ BTS}(n, k, p, t)} \quad (13)$$

where,

- $P_u(m, p, t)$ is the received power by the user at a location in the specific time interval generated by the serving beam m ,
- KTB is the thermal noise power,
- $P_{Same\ BTS}(n; n \neq m, p, t)$ is the received power coming from the active beams of the same BTS at the user location in the specific time interval different by the serving beam,
- N is the number of active beams of the same BTS serving the user,
- $P_{Other\ BTS}(n, k, p, t)$ is the received power coming from the active beams of other BTS at the user location in the specific time interval,
- K is the number of surrounding BTS,
- (p, t) is the space-time position of the user.

8.1.4 Users time and Space distribution

Sections 8.1.1 to 8.1.3 allow the establishment of the amount of data each user can download and the time the user stays active on the network, resulting in the MaMIMO antenna generating a beam toward the location of the user for the time required. It remains to define where the user is located in the time and the space in the scenario. For the scope of the task T3.4:

- the time position has been selected randomly in the specific quarter of hour,
- the space position is selected randomly in the coverage area of each BTS with two approaches:
 - only in the streets of the scenario,
 - everywhere, streets and building roofs.

Other users' distributions can be adopted by partners.

8.1.5 Power level assigned to each beam

For the aims of task T3.4, the power assigned to each beam has been determined in the following way:

- The configured power is subdivided among all the active beams of the MaMIMO antenna,
- A maximum number of simultaneous users can be served at the same time, which is done in order to avoid a reduction of the traffic coverage area of the cell,
- There is not a power control mechanism that reduces or increases the power on the base of SINR at user position.

9 Simulations and Results

9.1 UNICAS Simulations and Results

9.1.1 Antenna model

With reference to Figure 47, the numerical model we propose for the pattern is relative to a planar array in the (x, z) plane. This array is built by a regular $N_x \times N_z$ grid of subarrays, with a horizontal spacing between the centres of the subarrays of d_x and a vertical spacing between the centers of the subarrays of d_z . Each subarrays has $M_x \times M_z$ elements, with spacings p_x and p_z , in x and z directions respectively.

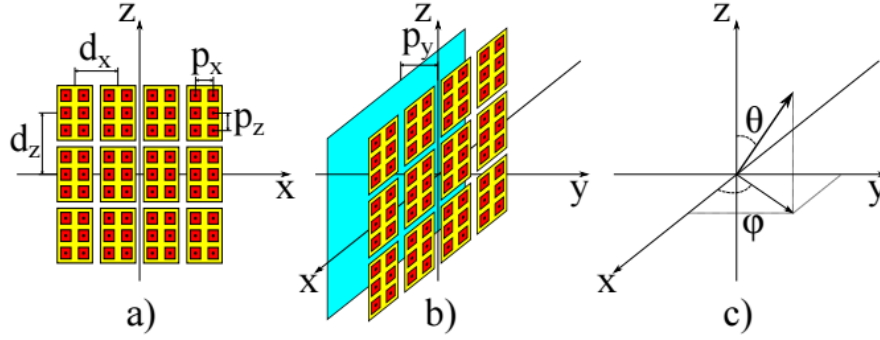


Figure 47 Array scheme: a) (x, z) view; b) perspective view; c) spherical coordinate system employed.

We will consider the possibility of exciting the radiators with the same amplitude but with a controllable linearly increasing phase shift on the array level (on the N_x columns and the N_z rows), and a fixed linearly-increasing phase shift on the subarray rows (i.e., allowing a vertical tilting of the beam on a subarray level).

Using a standard spherical coordinate system (as in Figure 47c), neglecting an inessential multiplicative constant, the amplitude of the electrical field radiated by this system at the specific wavelength $\lambda = c_0/f_0$, can be written as:

$$E(\theta, \phi) = F_1(\theta, \phi)F_2(\theta, \phi)F_3(\theta, \phi)F_4(\theta, \phi)F_E(\theta, \phi) \quad (14)$$

where $F_E(\theta, \phi)$ is the element factor and:

$$F_1(\theta, \phi) = D_{N_x}(\beta d_x(\sin \theta \cos \phi - u_0)) \quad (15)$$

$$F_2(\theta, \phi) = D_{N_z}(\beta d_z(\cos \theta - v_0)) \quad (16)$$

$$F_3(\theta, \phi) = D_{M_x}(\beta p_x \sin \theta \cos \phi) \quad (17)$$

$$F_4(\theta, \phi) = D_{M_z}(\beta p_z(\cos \theta - v_T)) \quad (18)$$

with $\beta = 2\pi/\lambda$, $u_0 = \sin \theta_0 \cos \phi_0$ and $v_0 = \cos \theta_0$ are obtained according to the wanted pointing direction (θ_0, ϕ_0) and $v_T = \cos \theta_T$ defines the vertical electrical tilting for the subarray elements. The function $D_P(\alpha)$ is the Dirichlet function, or periodic sinc function, defined as:

$$D_P(\alpha) = \begin{cases} \frac{\sin(P\alpha/2)}{P \sin(\alpha/2)} & \text{for } \alpha \neq 2n\pi \text{ and } n \in \mathcal{Z} \\ (-1)^{n(P-1)} & \text{for } \alpha = 2n\pi \text{ and } n \in \mathcal{Z} \end{cases} \quad (19)$$

Several choices are possible for the element factor $F_E(\theta, \phi)$. Focusing on elementary sources, we have:

- Vertical Dipoles: $F_E(\theta, \phi) = \sin \theta$
- Horizontal Dipoles: $F_E(\theta, \phi) = \sqrt{1 - (\sin \theta \cos \phi)^2}$
- Diagonal $\pm 45^\circ$ (deg) Dipoles: $F_E(\theta, \phi) = \sqrt{1 - (\sin \theta \cos \phi \pm \cos \theta)^2/2}$

- Circularly Polarized Dipoles: $F_E(\theta, \phi) = \sqrt{1 - (\sin \theta \cos \phi + \cos \theta)^2/4 - (\sin \theta \cos \phi - \cos \theta)^2/4}$

To take into account the presence of a reflective ground plane (the cyan square in Figure 47b), we can modify the mentioned element factor in the following way:

$$F'_E(\theta, \phi) = F_E(\theta, \phi)(1 - c_y e^{-j2\beta p_y \sin \theta \sin \phi}) \quad (20)$$

where p_y is the distance of the source from the ground plane, and c_y is a complex factor that could be used to approximate the effect of a non-ideal non-infinite ground plane ($c_y = 1$ in the case of an infinite PEC ground plane).

According to the results published in [12], the model shows good agreement with the pattern of commercially available antennas, and it is worth underlining that once the physical model parameters have been retrieved, patterns for different frequencies/pointing directions can be easily generated.

9.1.2 Generated pattern for FR1

In this Section we will describe the antenna pattern generated at the University of Cassino and Southern Lazio for the reference antenna “REF02”. The synthesized antenna has been designed according to some specifications discussed with the partners in order to obtain an antenna that behaves similarly to the antennas currently sold by manufacturers for FR1 5G applications while being independent of specific manufacturer choices. The specifications are listed in Table 12.

Table 9: Parameters for the FR1 Antenna

	Horizontal				Vertical		
	Frequency	HPBW	Range	Step	HPBW	Range	Step
	[MHz]	[°]	[°]	[°]	[°]	[°]	[°]
FR1	3600	10	-60;60	5	6	-4;12	1

- The synthesized antenna is constituted by 12x12 radiators, organized in vertical subarrays of 2 elements. The elements of the subarray are excited with equal amplitude signals, with a phase shift that electronically tilts the beam of 4° vertically (to better cover the requested vertical range).
- The radiators are ±45° elementary dipoles, built on a non-ideal reflecting screen in order to achieve a small backfire radiation.

We have calculated 425 possible patterns organized in a regular grid (25 horizontal and 17 vertical directions). The highest directivity beam has a directivity of about 27.2dBi, and is pointed in $\theta=4^\circ$ and $\varphi=0^\circ$, and shows an horizontal beamwidth of about 10° and a vertical beamwidth of about 6°. The directivity of the other beams, as well as their beamwidth, slightly changes with the scanning of the beam.

The pattern data is provided in separate files; for each pattern 2 files are given, a text-based .3drp BASTA 2.0 data file, and a summary figure containing some pattern plots and information.

As an example, in the file name “UNICAS_REF02_3600_B1309_-45_Pencil_Generic_draft.3drp”

- **UNICAS_REF02** identifies the antenna
- **3600** provides the frequency in MHz
- **B1309** identifies the 13th horizontal direction - 9th vertical direction (in this case $\theta=4^\circ$ and $\varphi=0^\circ$)
- **-45** specifies the radiating element polarization employed.

In the image file, the left side contains a cartesian plot and a polar plot of the vertical cut of the pattern relative to the specific φ direction (blue curves); the right side contains a cartesian plot and a polar plot of the horizontal cut of the pattern, relative to the specific θ direction (black curves); in the central section, we have a zoom of the vertical and horizontal pattern relative to the main beam, and a 3D view/imagemap of the overall pattern. The name of the pattern, its calculated horizontal/vertical beamwidth as well as the directivity are also provided in the figure. An example pattern is provided in Figure 48.

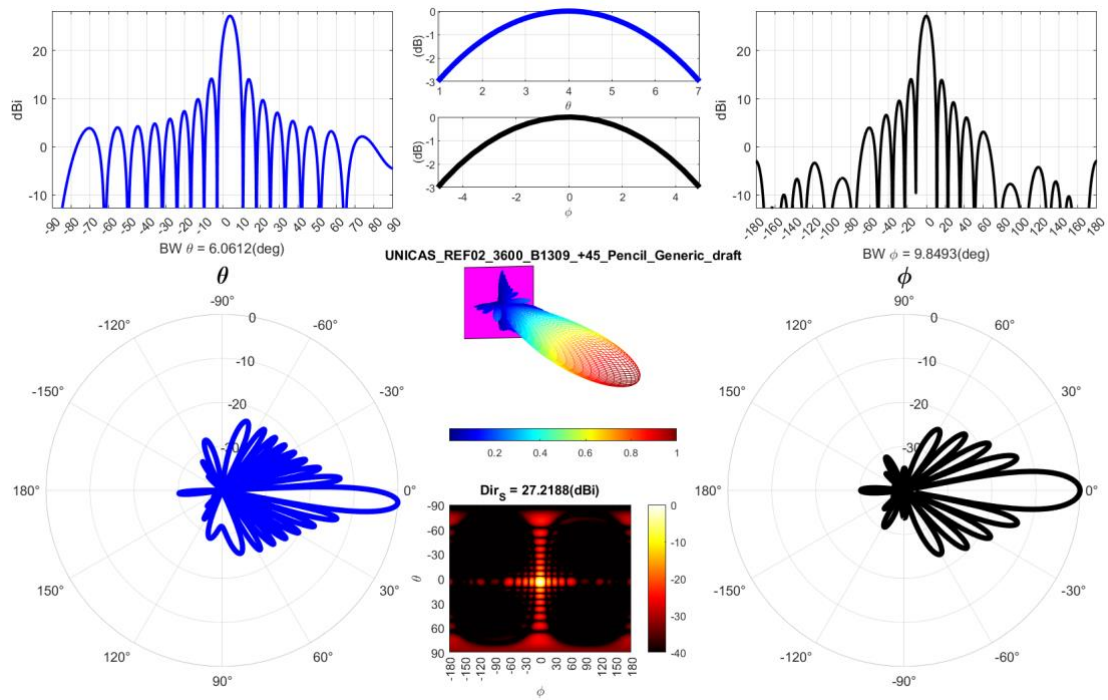


Figure 48 Example pattern for the FR1 antenna synthesized, relative to the file UNICAS_REF02_3600_B1309_+45_Pencil_Generic_draft.3drp

The envelope of all the calculated patterns is provided in a separate file. The name of this file is “UNICAS_REF02_3600_E425_+45_Envelope_Generic_draft”, where “E425_+45” stands for “Envelope of 425 overall patterns with $\pm 45^\circ$ polarization”. The envelope pattern plot is provided in Figure 49.

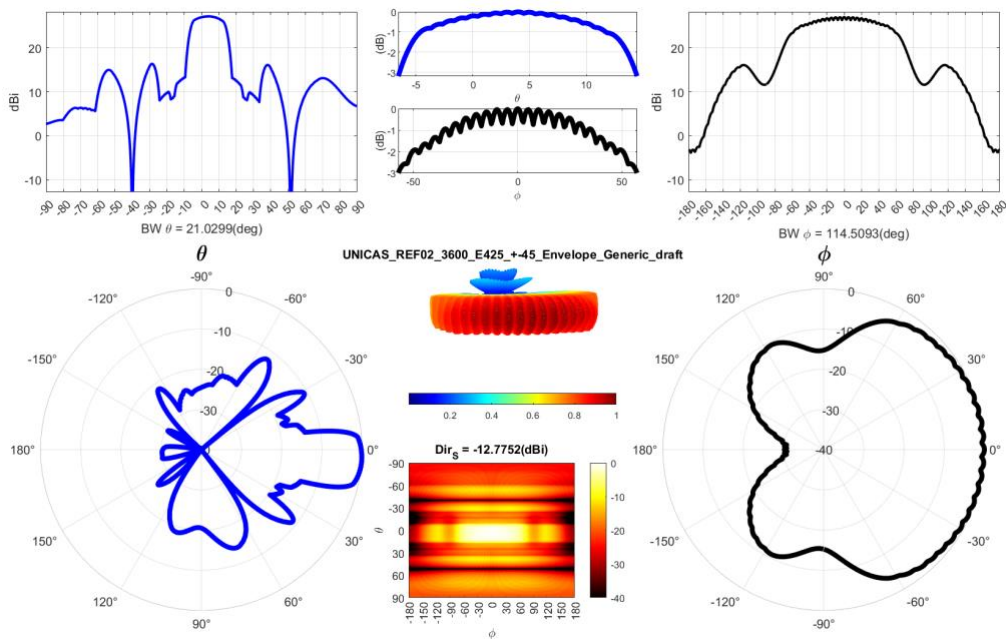


Figure 49 envelope Patten for the FR1 antenna synthesized, relative to the file UNICAS_REF02_3600_E425_+45_Envelope_Generic_draft

9.1.3 Generated pattern for FR2

In this section we will describe the antenna pattern generated at the University of Cassino and Southern Lazio for the reference antenna “REF03”. The synthesized antenna has been designed according to some specifications discussed with the partners, in order to obtain an antenna that behaves similarly to the antennas currently sold by manufacturers for FR2 5G applications while being independent from specific manufacturer choices. The specifications are listed in the following table:

Table 10: Parameters for the FR2 antenna

	Horizontal				Vertical		
	Frequency	HPBW	Range	Step	HPBW	Range	Step
	[MHz]	[°]	[°]	[°]	[°]	[°]	[°]
FR2	26000	5	-60;60	3	5.5	-12;12	2

- The synthesized antenna is constituted of 20x20 radiators organized in vertical subarrays of 2 elements. The elements of the subarray are excited with equal amplitude signals without a phase shift.
- The radiators are $\pm 45^\circ$ elementary dipoles, built on a non-ideal reflecting screen in order to achieve a small backfire radiation.

We have calculated 533 possible patterns organized in a regular grid (41 horizontal and 13 vertical directions). The highest directivity beam has a directivity of about 30.7dBi, and is pointed in $\theta=0^\circ$ and $\varphi=0^\circ$, and shows an horizontal beamwidth of about 5° and a vertical beamwidth of about 5.5° . The directivity of the other beams, as well their beamwidth, slightly changes with the scanning of the beam.

The pattern data is provided in separate files; for each pattern 2 files are given, a text-based .3drp BASTA 2.0 data file, and a summary figure containing some pattern plots and information.

As an example, in the file name “UNICAS_REF03_26000_B2107_-45_Pencil_Generic_draft.3drp”

- **UNICAS_REF03** identifies the antenna
- **26000** provides the frequency in MHz
- **B2107** identifies the 21th horizontal direction - 7th vertical direction (in this case $\theta=0^\circ$ and $\varphi=0^\circ$)
- **-45** specifies the radiating element polarization employed.

In the image file, the left side contains a cartesian plot and a polar plot of the vertical cut of the pattern relative to the specific φ direction (blue curves); the right side contains a cartesian plot and a polar plot of the horizontal cut of the pattern, relative to the specific θ direction (black curves); in the central section, we have a zoom of the vertical and horizontal pattern relative to the main beam, and a 3D view/imagemap of the overall pattern. The name of the pattern, its calculated horizontal/vertical beamwidth as well as the directivity are also provided in the figure. An example pattern is provided in Figure 50.

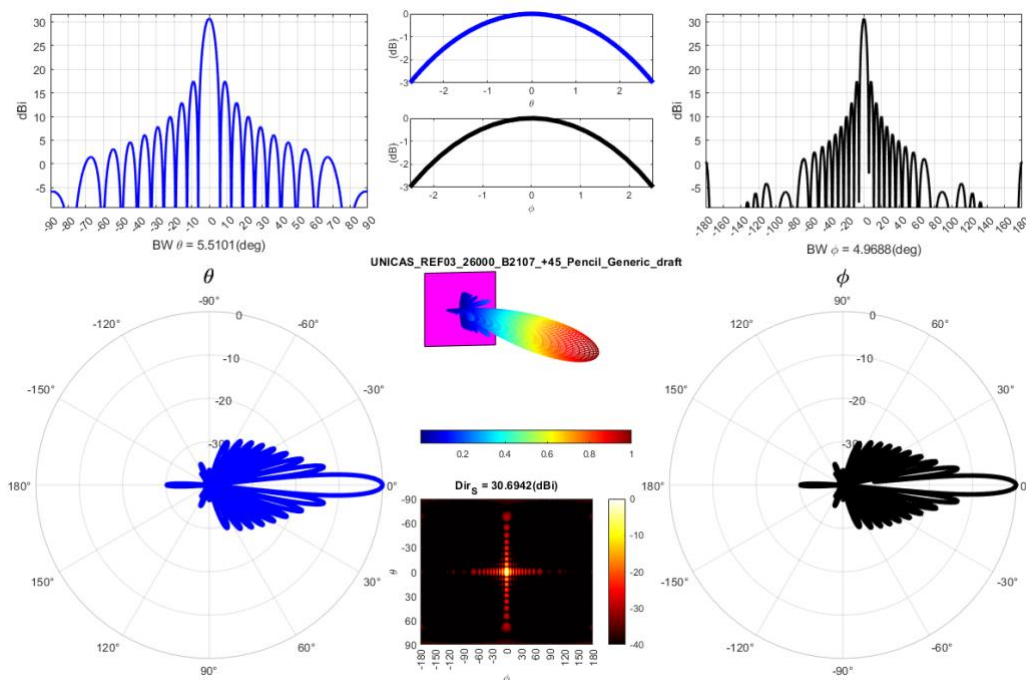


Figure 50 Example pattern for the FR2 antenna synthesized, relative to the file UNICAS_REF03_26000_B2107_+45_Pencil_Generic_draft

The envelope of all the calculated patterns is provided in a separate file. The name of this file is “UNICAS_REF03_26000_E533_+45_Envelope_Generic_draft”, where “E533_+45” stands for “Envelope of 533 overall patterns with $\pm 45^\circ$ polarization”. The envelope pattern plot is provided in Figure 51.

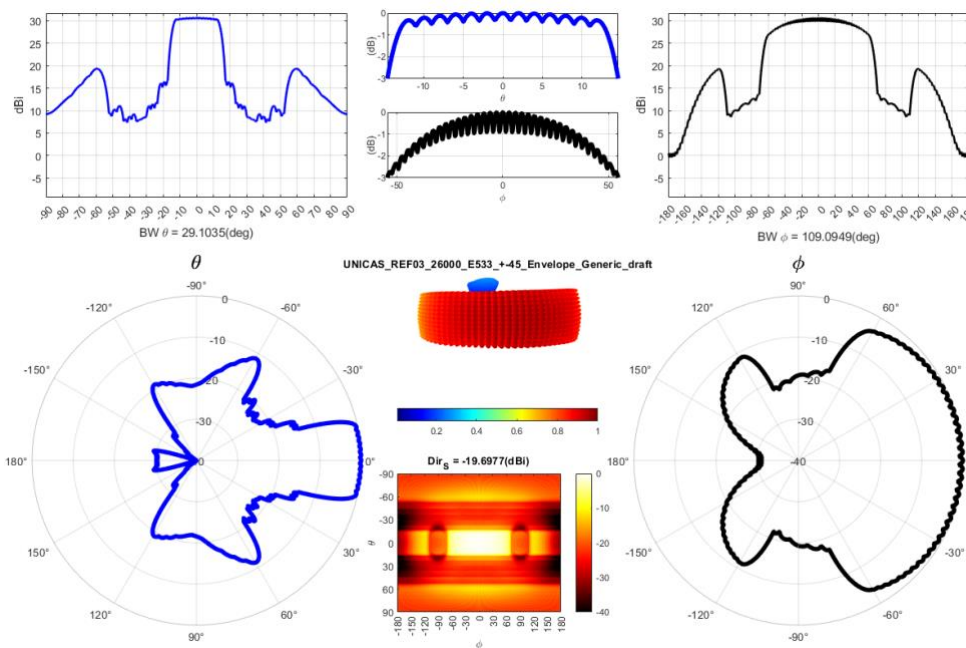


Figure 51 envelope Patten for the FR2 antenna synthesized, relative to the file UNICAS_REF03_26000_E533_+45_Envelope_Generic_draft

9.1.4 Generated pattern for INDOOR

In this section, we will describe the antenna pattern generated at the University of Cassino and Southern Lazio for the reference antenna “REF04”. The synthesized antenna has been designed according to some specifications discussed with the partners, in order to obtain an antenna that behaves similarly to the antennas currently sold by manufacturers for Indoor 5G applications while being independent from specific manufacturer choices. The specifications are listed in the Table 11:

Table 11: Parameters for the Indoor antenna

	Horizontal				Vertical		
	Frequenc	HPBW	Range	Step	HPBW	Range	Step
	[MHz]	[°]	[°]	[°]	[°]	[°]	[°]
FR1 INDOOR	3700	15	-45; +45	8	10	0	1

- The synthesized antenna is constituted by 8x8 radiators, organized in vertical subarrays of 8 elements. The elements of the subarray are excited with equal amplitude signals without a phase shift.
- The radiators are $\pm 45^\circ$ elementary dipoles, built on a non-ideal reflecting screen in order to achieve a small backfire radiation.

We have calculated 8 possible patterns (8 horizontal pointing directions). The highest directivity beam has a directivity of about 23.2dBi, and is pointed in $\theta=0^\circ$ and $\phi=5.8^\circ$, and shows a horizontal beamwidth of about 14.8° and a vertical beamwidth of about 10.1° . The directivity of the other beams, as well as their beamwidth, slightly changes with the scanning of the beam.

The pattern data is provided in separate files; for each pattern 2 files are given, a text-based .3drp BASTA 2.0 data file, and a summary figure containing some pattern plots and information.

As an example, in the file name “UNICAS_REF04_3700_B401_-45_Pencil_Generic_draft.3drp”

- **UNICAS_REF04** identifies the antenna
- **3700** provides the frequency in MHz
- **B401** identifies the 4th horizontal direction - single vertical direction (in this case $\theta=0^\circ$ and $\varphi=5.8^\circ$)
- **-45** specifies the radiating element polarization employed.

In the image file, the left side contains a cartesian plot and a polar plot of the vertical cut of the pattern relative to the specific φ direction (blue curves); the right side contains a cartesian plot and a polar plot of the horizontal cut of the pattern, relative to the specific θ direction (black curves); in the central section, we have a zoom of the vertical and horizontal pattern relative to the main beam, and a 3D view/imagemap of the overall pattern. The name of the pattern, its calculated horizontal/vertical beamwidth, and the directivity are also provided in the figure. An example pattern is provided in Figure 52.

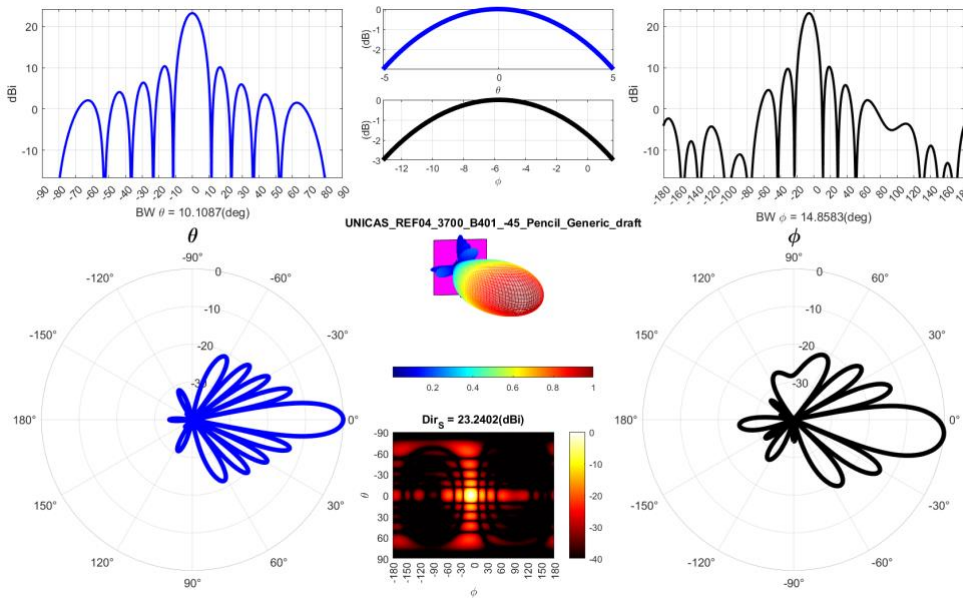


Figure 52 Example pattern for the INDOOR antenna synthesized, relative to the file UNICAS_REF04_3700_B401_-45_Pencil_Generic_draft

The envelope of all the calculated pattern is provided in a separate file. The name of this file is “UNICAS_REF04_3700_E8_+45_Envelope_Generic_draft”, where “E8_+45” stands for “Envelope of 8 overall patterns with +45° polarization”. The envelope pattern plot is provided in Figure 53.

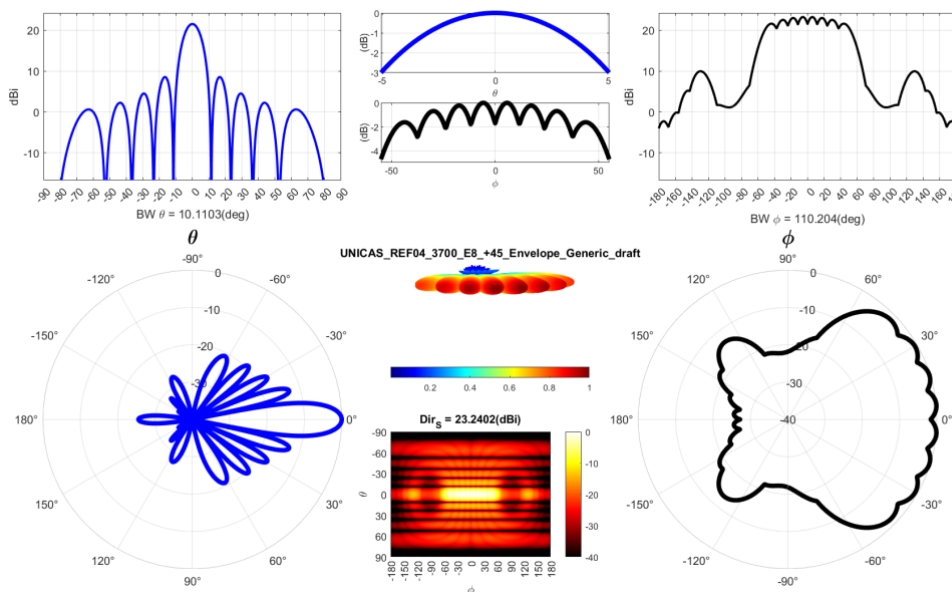


Figure 53 envelope Patten for the INDOOR antenna synthesized, relative to the file UNICAS_REF04_3700_E8_+45_Envelope_Generic_draft

9.1.5 Simulations in MMGS

Current generation 5G systems mostly adopt a grid-of-beam approach to provide coverage in the areas of interest. In the future, a further increase in performance is expected thanks to the use of more sophisticated beamforming schemes that exploit eigen-beams to improve system throughput and guarantee more effective multiplexing schemes.

In this section, we will try to perform a preliminary assessment on the relevant question of how much the use of advanced beamforming schemes affects the field levels to be expected. The general analysis of this problem is not straightforward, and it would be beyond the scope of the NextGEM project, so we have focused on a specific problem, the variation of radiated power by the Base station antenna when it employs different beamforming schemes.

More specifically, we have selected the following simulation parameters:

- Modified Madrid Grid Scenario as communication environment.
- Use of the antenna REF02, working in FR1 band and described in Section 9.1.2 as a base-station antenna.
- $P=1000$ randomly positioned user terminals located in one of the square areas of the MMGS in order to elaborate coherent sets of data (with similar angular spreading of the signals and a non-significant variation of the distance to the base station).
- Use of the Ray Launching Software developed in Cassino to identify the amplitude and phase of each path that is followed by the signal in travelling from the transmitting BS to the user, as depicted in Figure 54.

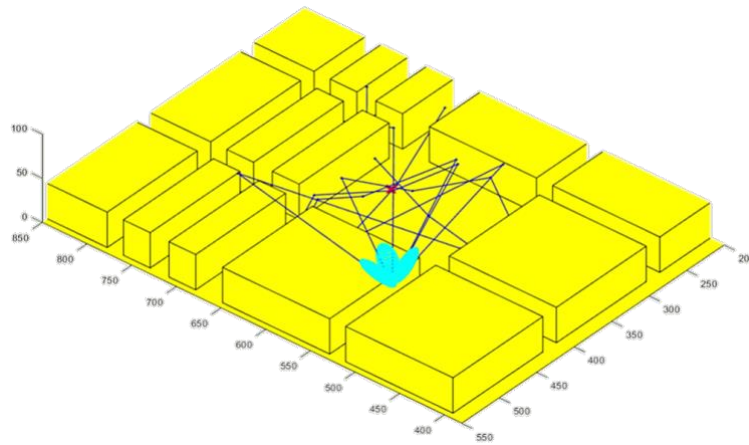


Figure 54 Examples of the paths calculated with the Ray Launching Software

The analysis has been performed following these steps for each one of the randomly positioned users:

1. Evaluation of the power level received by the user employing each one of the 425 beams synthesized for the REF02 antenna using a reference transmitted power of 1W.
2. Identification of the beam that allows the highest received power level P_G evaluated in dB.
3. Calculation of the base station radiating element excitation according to the conjugate matching rule [13] to evaluate the characteristics of the resulting eigen-beam pattern.
4. Evaluation of the power level P_E evaluated in dB received by the randomly positioned user using the calculated eigen-beam pattern with a reference transmitted power of 1W.
5. Evaluation of the difference between the powers $\Delta_P = P_E - P_G$; this difference is always a non-negative number since the eigen-beam is, by definition, always able to perform better than any other pattern.

The value of Δ_P may have two different interpretations: we can see it as the power increase at the receiver that can be achieved by employing the more sophisticated communication eigen-beamforming, or it can be seen as the possible reduction in radiated power that can be obtained by using the eigen-beamforming guaranteeing the same performance level for the user served by the grid-of-beam system.

In the following figures, from Figure 55 to Figure 58, we analyze four different squares (“A” to “D”) in the MMGS. In each figure, we can see five subplots: in subplot d), we have a plot of the scenario with emphasized the square (blue) and the position of the BS antenna; in subplot a), we have the absolute power level received with the grid-of-beam approach; in subplot b), we have the power level difference; in subplot c), we have a scattering plot in which for each user we have the relationship between the received power level with the GoB approach, and the

variation in power level; in subplot e), we have the cumulative density function for the distribution of the variation of power level.

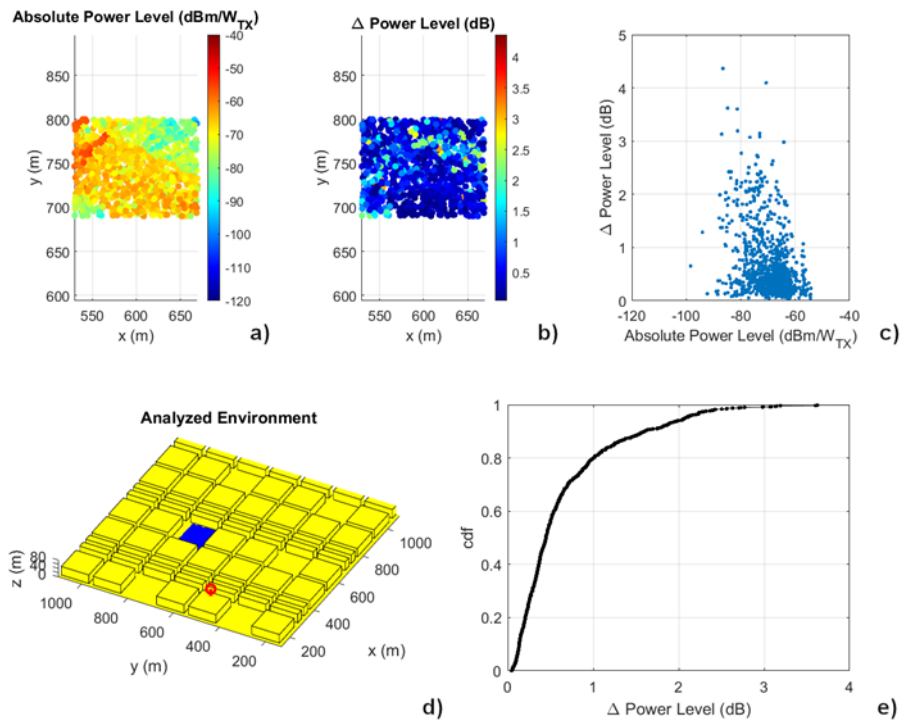


Figure 55 Analysis of square A

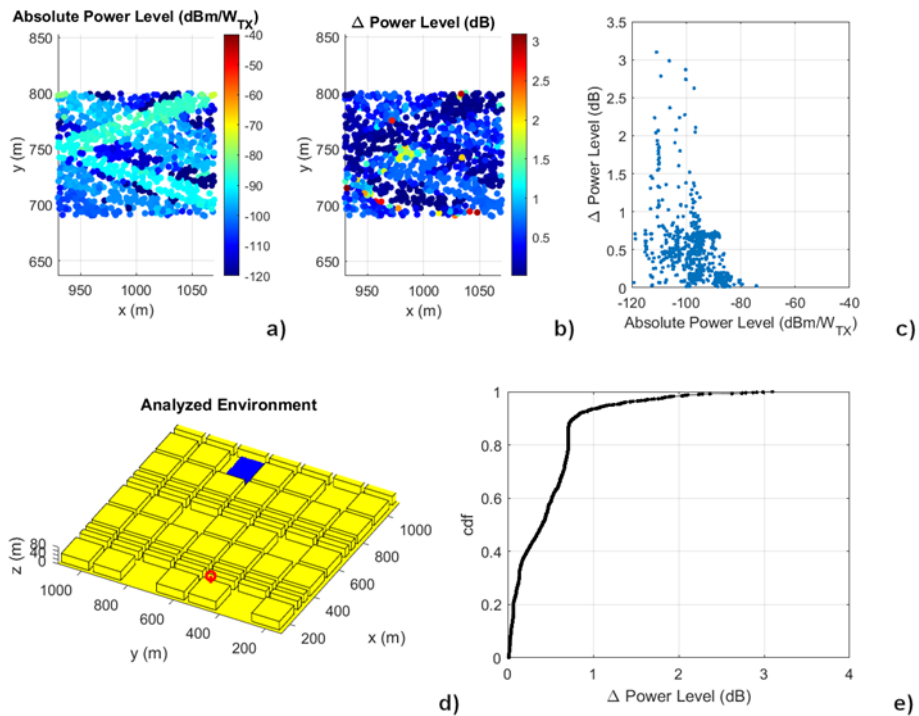


Figure 56 Analysis of Square B

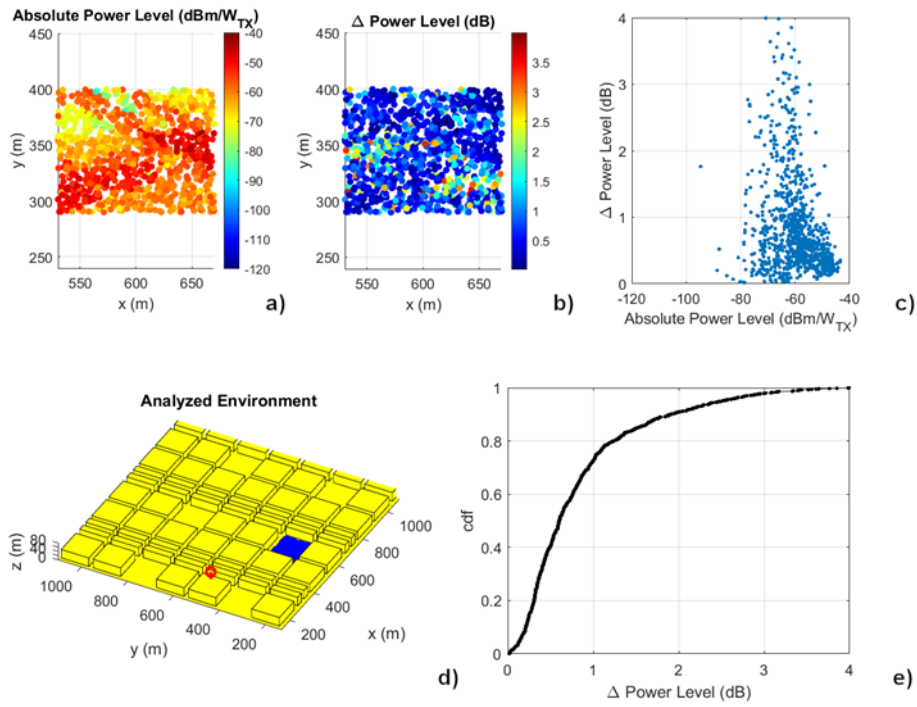


Figure 57 Analysis of Square C

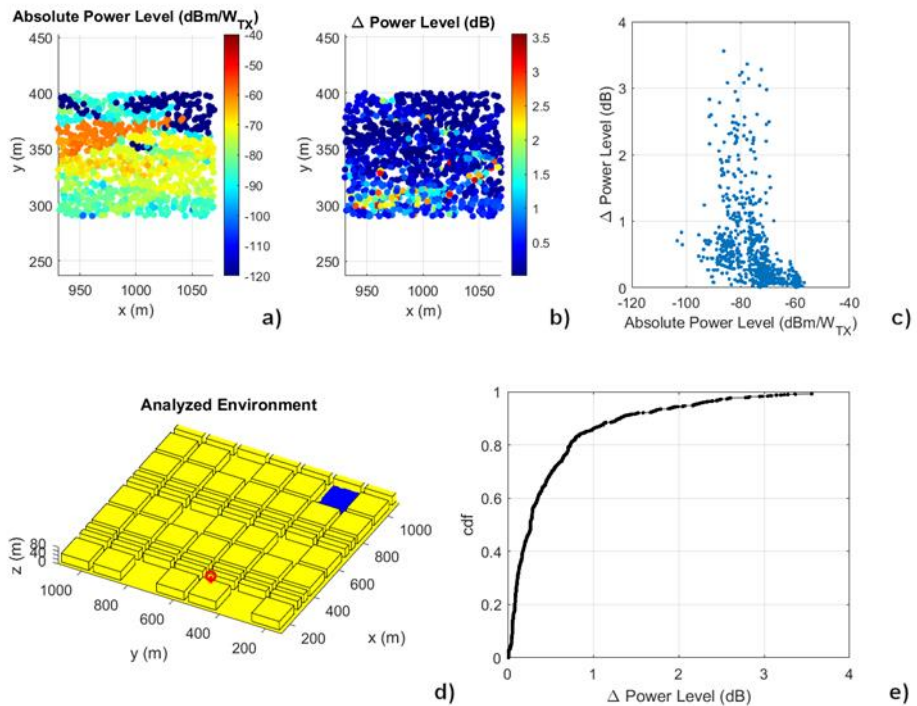


Figure 58 Analysis of square D

The analysis of the results seems to show similar trends in the four squares; in particular, it seems that the power variation is usually limited, below 1dB, and the scattering plot relating the variation in power level and the absolute receive power with GoB seems to show a bell-like shape: the improvement using eigen-beamforming is very limited when the received power is already very high, because of the presence of a strong Line-of-Sight component, and when the received power is very low (when all the paths connecting the BS with the user show a strong attenuation) since the eigen-beamforming can only better exploit paths that are already present in the environment. To achieve a better insight on the difference in power levels, in Figure 59b we have collected the cumulative density function

related to the four different squares shown in Figure 59a. In particular, the two squares, A and C, that are closer to the BS, show a value that is greater than 1dB in 26% and 20% of the cases, while for the farthest squares, B and D, this percentage drops to 13 and 7%.

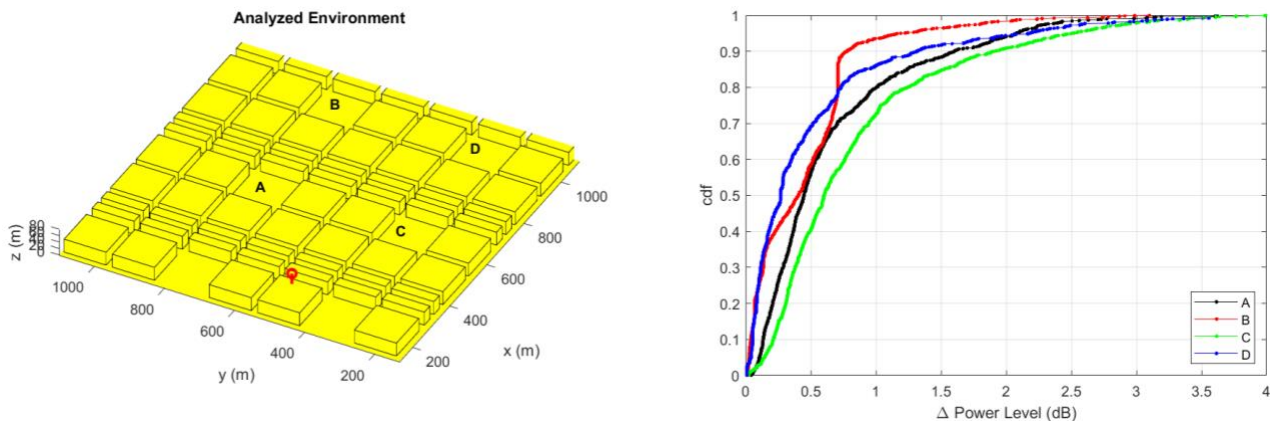


Figure 59 Summary of the difference in power level achieved in the four squares

These results are also confirmed by other simulations on different squares and streets, employing a different positioning of the transmitting antenna that have been performed but are not presented in this report for the sake of conciseness.

Two considerations can be inferred from the shown results.

The first regards the use of grid-of-beam for the realization of simulations regarding the EMF power levels evaluated for security issues: the grid-of-beam could provide an overestimation of the real field levels, but the achieved bounds are more than reasonable.

The second regards the effective advantage of using eigen-beamforming in 5G communication systems: the improvement in terms of power level is mostly limited, and the increase of the coverage or the increase in performance that could have been expected is limited. The use of eigen-beamforming schemes seems to be much more appealing for the increase of multiplexing capability of systems, i.e., the ability for the base station antenna to activate quality contemporary connection with multiple users at the time. However, some published results in the literature suggest that also, in this case, the bounds calculated with grid-of-beam approach should be sufficient to achieve a trustable assessment of the EMF levels in covered areas.

A final notice on this point is required. The use of GoB is reliable if the position of the user is within the coverage area of the grid, otherwise the obtained results may be inconsistent. In Figure 60: and Figure 61 we perform the same analysis that has been conducted on the squares on two streets.

The first, street E depicted in Figure 60: it is orthogonal with respect to the pointing direction of the BS antenna, and the results are very similar to what has been achieved for the squares: apart from a larger spreading of the absolute power levels of the user signals, due to the fact that the street represents a more “various” environment with respect to a square, a difference in power level greater than 1dB is rarely seen, and in no case we have more than 4dB difference.

The second, street F depicted in Figure 61d, is instead parallel to the pointing direction of the antenna, and we can see that there is a non-negligible probability of finding a value of Δ_P greater than 10dB. The analysis of the top center subplot allows us to identify that the points for which this phenomenon occurs are the ones closer to the antenna. More precisely, these points are located at the starting points of the street, very close to the BS, but not in positions that are directly served by the main beams of the Grid-of-Beam; when using GoB, those points are served by the sidelobes of the pattern, but the overall received power is very high because of the proximity of these points to the antenna. The eigen-beamforming is, instead, not limited to specific directions and can focus a beam in any direction. Consequently, the significant difference in field levels observed close to the antenna is due to the fact that these points are not covered by the Grid-of-Beams (GoB) but are covered by the eigen-beamforming. This leads to a misleading estimation of the effects of using eigen-beamforming technology instead of Grid-of-Beams (GoB) technology when this effect is analyzed at these points.

Summing up, as far as the GoB system is designed to effectively cover the range of points that must be analyzed, the achieved results allow an efficient assessment of the overall power levels.

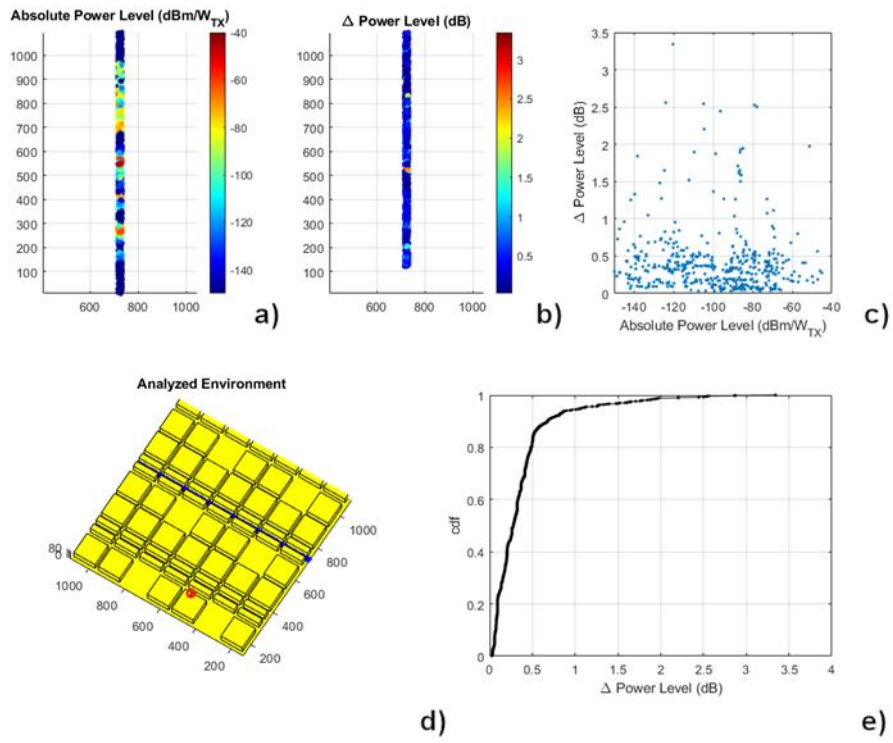


Figure 60: Analysis of street E

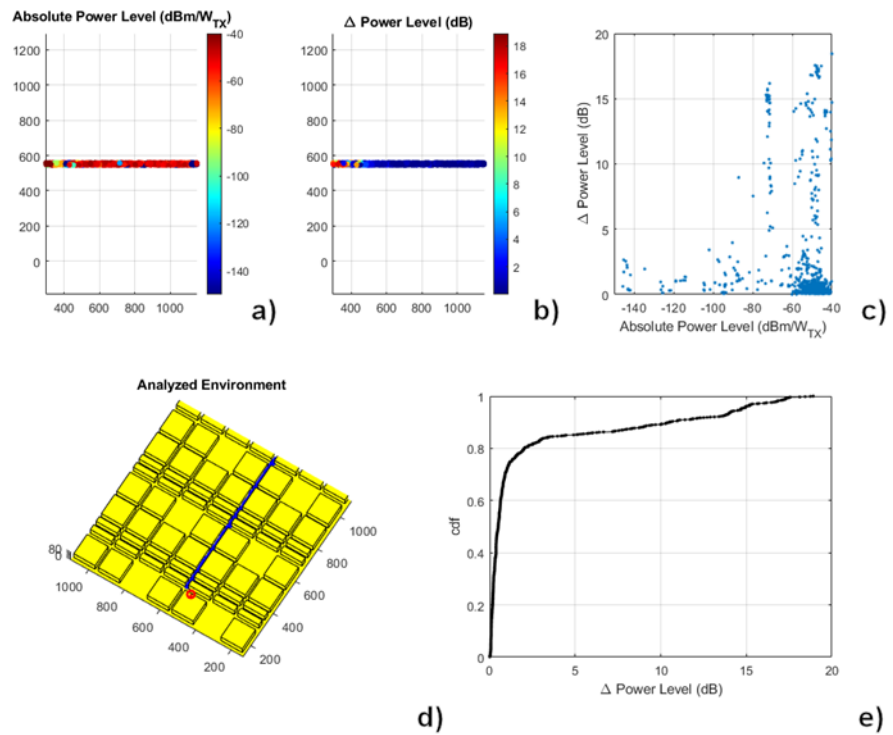


Figure 61 Analysis of street F

9.2 TIM - FiberCop Simulations

9.2.1 Simulations in MMGS Scenario

The following approach has been used for simulations in the MMGS scenario:

- MMGS scenario consists of an area 3x3 km² wide, see Section 6.1.2;
- 7 MaMIMO antennas have been considered, 1 antenna for each corner, 3 antennas in the centre of the scenario for which each antenna is 120 degs from the other:
 - Antenna 1: position x=457m, y=3110m, z=60m, pan 135 degs, mechanical tilt 0 degs
 - Antenna 2: position x=2777m, y=3106m, z=60m, pan 225 degs, mechanical tilt 0 degs
 - Antenna 3: position x=3072m, y=344m, z=60m, pan 315 degs, mechanical tilt 0 degs
 - Antenna 4: position x=363m, y=341m, z=60m, pan 45 degs, mechanical tilt 0 degs
 - Antenna 5: position x=1754m, y=1726m, z=60m, pan 0 degs, mechanical tilt 0 degs
 - Antenna 6: position x=1754m, y=1726m, z=60m, pan 120 degs, mechanical tilt 0 degs
 - Antenna 7: position x=1754m, y=1726m, z=60m, pan 240 degs, mechanical tilt 0 degs.

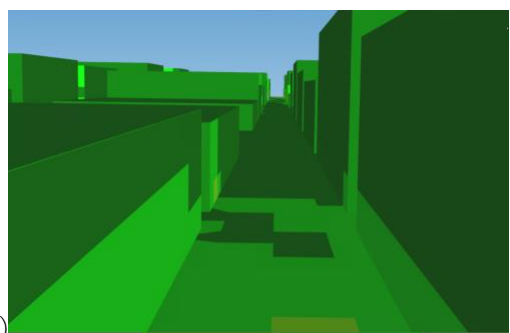
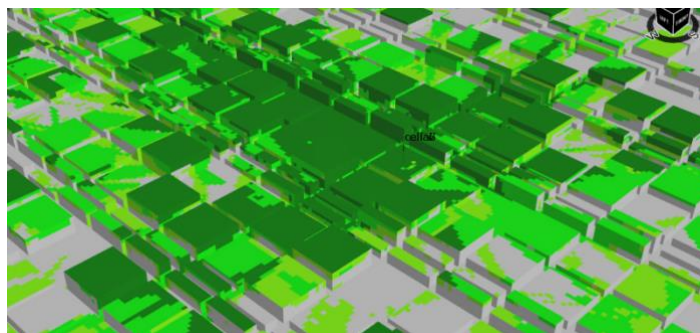
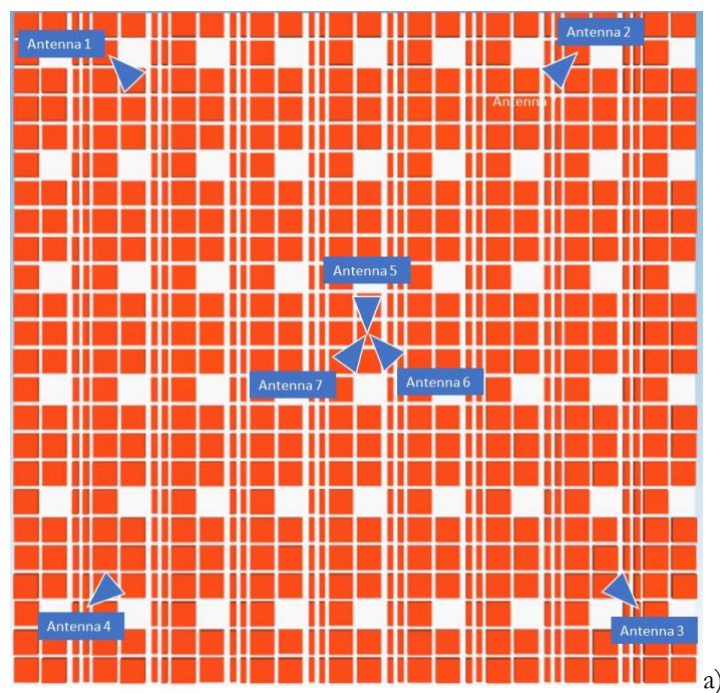


Figure 62: a) a scheme representing the positions of the cells in the MMGS and b) a 3D portion of the MMGS scenario radiated by 1 beam; c) exposure along a street surrounded by buildings.

- Each antenna is equipped with a set of 117 beams, distributed over 3 layers
 - Layer 1, made of 39 beams, is -2 degs beamforming tilted.
 - Layer 2, made of 39 beams, is 4 degs beamforming tilted.
 - Layer 3, made of 39 beams, is 10 degs beamforming tilted.
 - Each layer covers 120 degs in azimuth.

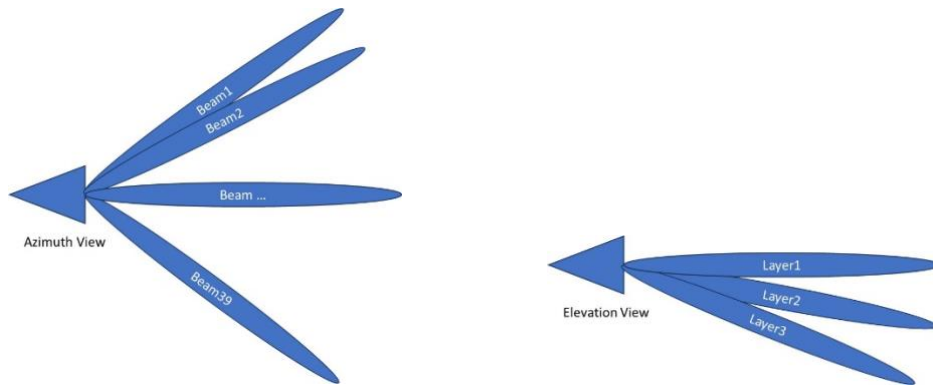


Figure 63: Schematic representation of the beams each MaMIMO antenna can generate in azimuth and elevation.

- Each antenna has 200 W configured power.
- An 8-2 TDD pattern has been adopted, DDDDDDDDUU, as shown in Figure 64. Each TTI is 1 ms.

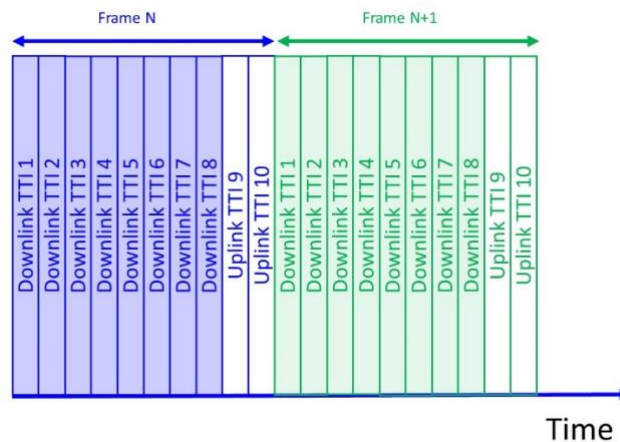


Figure 64: The TDD scheme used in simulations. The MaMIMO antenna radiates only in the downlink TTI.

- The observation period is a whole day, discretized in steps of 1 ms, consisting of 86.4 million iterations.
- Cell Load has been obtained with the procedure indicated in Section 8.1.2.
- For each user:
 - The payload has been estimated in [10], see Section 8.1.1, with the following assumptions:
 - The monthly payload has been equally subdivided per each day of the month and per each quarter of an hour of the day.
 - Three types of services have been supposed:
 - “Download”: maximum payload per service is defined as the monthly payload [10], equally divided by 30 days in a month, by supposing each user requires 1 service per quarter of hour, see Section 8.1.1, resulting in a payload of 9.4 MB per session. This service represents a data connection for, as an example, web navigation. Payload size is randomized with uniformly distributed function.
 - “Phone call”: maximum payload per service is 0.94 MB, representing 10% of “Download” payload service.
 - “Huge Download”: maximum payload per service is 50 MB, representing about 5 times the payload of “Download” service.
 - A mix of the three services, based on percentages, is adopted during the day (ex: 20 % “Phone calls”, 70 “Download”, 10% “Huge Download”).
 - For each TTI, the SINR at user locations has been evaluated; see Section 4.2.2.
 - Throughput is based on the Ofcom link curve, see Section 8.1.3.
 - Service Time duration is taken from the payload divided by the throughput; since the payload has been randomized for each service, then the service time duration for each user is variable.
 - User position in time is uniformly random distributed. User position in space is uniformly distributed over the serving region of the cell, positioned everywhere in the town area (outside buildings) or only on the streets.

- From the amount of data per each user and cell capacity, the number of simultaneous users requiring services is determined.
- Simulations have been performed with a different number of active users served simultaneously, from 1 to 5 to prevent service coverage issues.
- Power has been equally divided among all served users per each TTI.
- After completing the service, the user is removed from the list of users to be served.
- Observation points are the most exposed point for each cell or randomly distributed over the scenario.
- Results have been generated in terms of:
 - Time distribution of time-averaged cell power for each cell:
 - 360 and 1800 s time average has been considered as indicated in [1] and [2];
 - Step average and rolling average have been considered.
 - CDF and PDF of the averaged power.
 - Time distribution of the averaged electric field for the observation points:
 - 360 and 1800 s time average has been considered as indicated in [1] and [2];
 - Step average and rolling average have been considered.
 - CDF and PDF of the averaged electric field have been calculated.
 - Short time exposure, less than 360 s, as required by [1], evaluated in terms of incident energy.
- General parameters
 - 5G NR Band: 100 MHz
 - External Temperature: 25.0 Celsius
 - TTI Duration: 1 ms
 - Receiver Gain: 0 dBi
 - Receiver Noise Figure: 3.0 dB
 - Frequency: 3600.0 MHz

Simulations have been performed by following the pattern reported in Table 12.

Table 12: Simulation path for MMGS Scenario

Test Name	User Position	Max Simultaneous Served Users	Payload per User Per Month (*) [GB]	Service Distribution
Test1	Streets	5	27	20% Voice, 70% Web Surfing, 10% Huge Download
Test2	Streets & Buildings	5	27	20% Voice, 70% Web Surfing, 10% Huge Download
Test 3	Streets	3	27	20% Voice, 70% Web Surfing, 10% Huge Download
Test4	Streets	10	27	20% Voice, 70% Web Surfing, 10% Huge Download
Test5	Streets	5	43	20% Voice, 70% Web Surfing, 10% Huge Download
Test6	Streets	5	64	20% Voice, 70% Web Surfing, 10% Huge Download
Test7	Streets	5	27	100% Voice
Test8	Streets	5	27	100% Web Surfing
Test9	Streets	5	27	100% Huge Download

Note: data from Ericsson Mobility Report November 2023

9.2.1.1 MMGS Scenario Test 1: Reference

Table 13 reports the statistics of the power radiated by each cell for the specific example. Since the same load to each cell has been assigned, see Section 8.1.2, averages and standard deviations do not differ among cells. It can be noted that, for the parametrization used, the maximum of the average radiated power is about 10 % of the total configured power.

Table 13: Cell Radiated Power

			Cell1	Cell2	Cell3	Cell4	Cell5	Cell6	Cell7
Step Average 360s	Min	[W]	2.6	2.2	2.4	2.5	2.6	2.7	2.7
	Max	[W]	16.4	16.2	16.6	16.4	16.5	16.6	16.3
	Mean	[W]	11.1	11.1	11.1	11.1	11.1	11.1	11.1
	StdDev	[W]	4.1	4.1	4.1	4.1	4.1	4.1	4.1
Rolling Average 360s	Min	[W]	2.5	2.1	2.3	2.3	2.4	2.4	2.5
	Max	[W]	16.9	17	17.1	17.4	16.7	17.1	17
	Mean	[W]	11.1	11.1	11.1	11.1	11.1	11.1	11.1
	StdDev	[W]	4.1	4.1	4.1	4.1	4.1	4.1	4.1
Step Average 1800s	Min	[W]	3	3	3	3	3	3	3
	Max	[W]	15.4	15.4	15.4	15.4	15.4	15.4	15.4
	Mean	[W]	11.1	11.1	11.1	11.1	11.1	11.1	11.1
	StdDev	[W]	4.1	4.1	4.1	4.1	4.1	4.1	4.1
Rolling Average 1800s	Min	[W]	2.8	2.8	2.8	2.9	2.9	2.8	2.9
	Max	[W]	15.6	15.7	15.7	15.9	15.7	15.6	15.7
	Mean	[W]	11.1	11.1	11.1	11.1	11.1	11.1	11.1
	StdDev	[W]	4.1	4.1	4.1	4.1	4.1	4.1	4.1

Table 14 shows the highest value of the Incident Energy Density computed in the most radiated Point of Control for each cell when considering contiguous active TTI, see ICNIRP2020.

Table 14: Incident Energy Density for exposure time lower than 6 min in each Point of Control¹⁷

		Cell1	Cell2	Cell3	Cell4	Cell5	Cell6	Cell7
Maximum Number of Contiguous Active TTI		8	8	8	8	8	8	8
Incident Energy Density	[m]/m ²	2.7	4.0	8.8	13.0	3.2	2.1	3.3
ICNIRP2020 Limit	[J]/m ²	784.5	784.5	784.5	784.5	784.5	784.5	784.5

Figure 65 shows the radiated power by each cell step averaged over 360 s. Since the load of each cell is the same, as expected, the radiated power is almost the same, as also shown in Table 13. The power ripple is due to the different time position and type of service of each user. The averaged radiated power by each cell, over 360 s time interval, is always below 10% of the configured power; the reason for that is the cells are never radiating full power for the whole averaging time; this is a quite expected behaviour in real deployments due to the statistic of the traffic requirements.

Figure 66 shows the CDF of the radiated power averaged over 360 s period. Figure 67 shows the simulated time users' distribution.

¹⁷ Since the Incident Energy Density for the specified example is much far away from the limit, equivalent tables are not reported for all the other tests.

Figure 68a) shows the electric field in the most exposed point by each cell averaged over 360 s^{18,19}. The computed E-field values, averaged over 360 s, in the conditions considered in this test, are included in the interval 0.05 V/m to 0.5 V/m for all the cells. The E-field time profile follows the cell load conditions even if there is larger spread with respect to the behaviour of the radiated power and a higher level of ripple. That is due to the following reasons:

- the different positions of the point with respect to the cell, due to the different heights and positions of the buildings.
- the position and activity of the users, served by the specific cell; in the case there is more than one user active at the same time, the radiated power is shared among all the active users on specific beams.
- the position and activity of the users, served by all the other cells.

Figure 68b) shows the averaged electric field over 360 s period by using a rolling average process. As can be noted exposure values are as in Figure 68a) except for the different ripple due to the different low pass filtering effects due to the different averaging processes.

For comparison, the exposure thresholds for reference levels defined in international guidelines are:

- ICNIRP1998: 61 V/m averaged over 6 minutes period for whole-body exposure.
- ICNIRP2020: 10 W/m² averaged over 30 minutes for whole-body exposure, corresponding to 61.4 V/m in far field.
- ICNIRP2020: 40 W/m², averaged over 6 minutes for local exposure, corresponding to 122.8 V/m in far field.

The following considerations need to be taken into account, when analysing exposure from base stations:

- The exposure is defined at a specific point in space.
- The exposure is influenced by the activity of the cell and by the scenario; a transmitter with the same characteristics generates different exposure levels in different scenarios; all the points where population can stay must have an exposure below the limits established by authorities.
- Whole body exposure is different by local exposure, reference levels for whole body exposure are lower than reference levels for local exposure.
- Links between reference levels and basic restrictions are indicated in the international guidelines.
- Reference levels are expressed in terms on incident or unperturbed field. Basic restrictions are defined inside a lossy medium and measured in terms of SAR or SA.

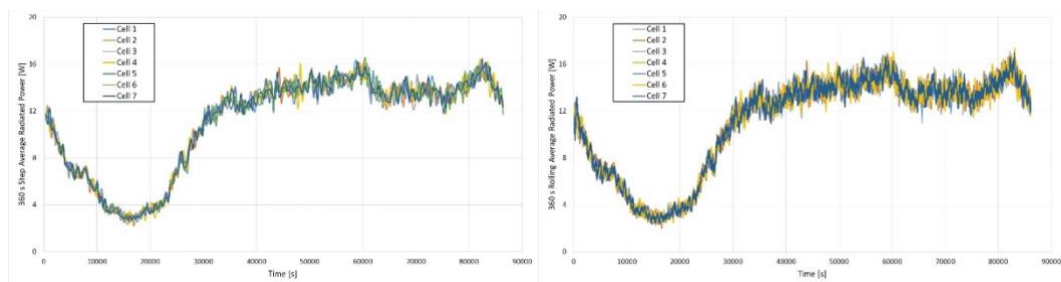


Figure 65: 360 s Averaged Radiated Power

¹⁸ For most exposed point for each cell is intended the point where the cell generates the higher exposure considering the configured power and beam set available to the antenna.

¹⁹ Exposure has been evaluated even in the other 26 Points of Control, randomly located on the streets or over the buildings; in all the cases the exposure in these points is always lower than the exposure shown in figures and have the same time behavior, so have not been reported in the results.

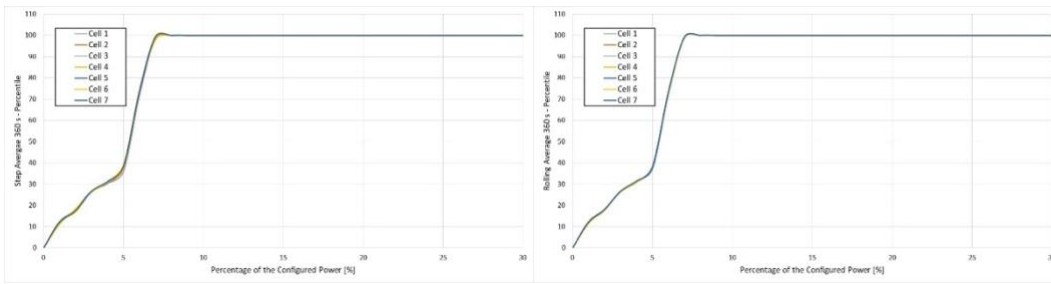


Figure 66: CDF of the 360s Averaged Radiated Power.

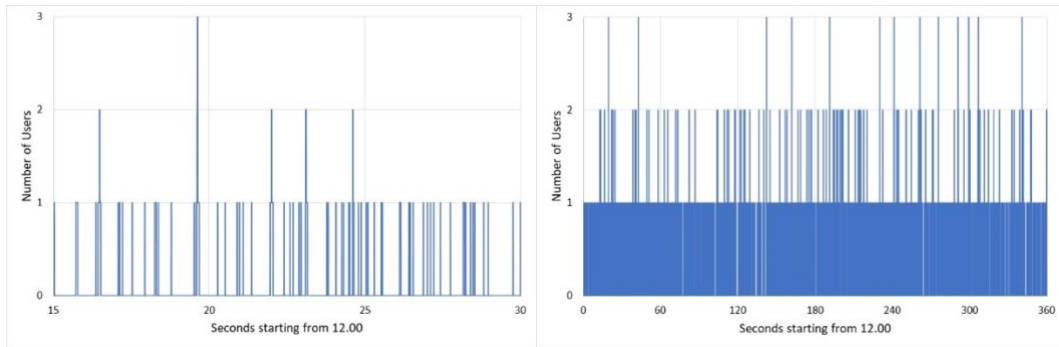


Figure 67: Example of Users distribution in time.

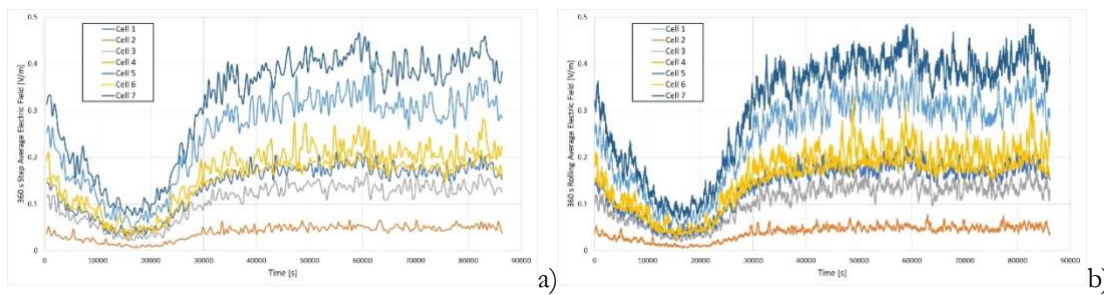


Figure 68: 360 s Averaged Electric Field in the most exposed point for each cell. a) step average, b) rolling average

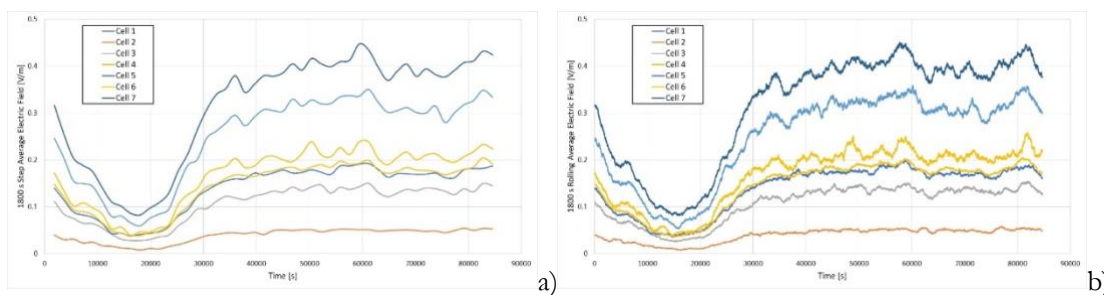


Figure 69: 1800 s Averaged Electric Field in the most exposed point for each cell. a) step average, b) rolling average

Figure 70²⁰ shows the time evolution of the exposure in the scenario. The movie has been generated by showing one frame (TTI) out of 1000 and it represents the E-field distribution over the building or over the streets (maximum value in each point), in the specific TTI, by an observer looking at the scenario from the top. It shows the time variable exposure generated by the MaMIMO antennas when turning on one more beams to serve user requiring service randomly located in the scenario.

²⁰ The time representation of the exposure will not be reported for the other test cases present in this report.

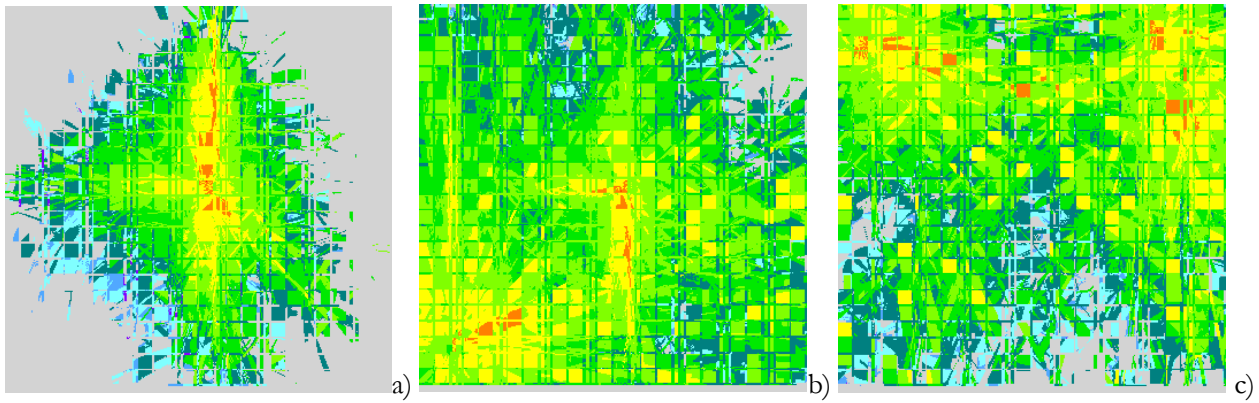


Figure 70: Time evolution of the exposure in the scenario. a) interval 1, b) interval 2, c) interval 3

Since there are not sensible differences in exposure by using the step or rolling average, except for a low pass filter effect of the rolling average removing ripple, results from now on will be reported only in terms of step average.

9.2.1.2 MMGS Scenario Test2: Users located in streets and buildings

In this Test, differently from Test1, users are located both on the streets and on the buildings. Results show not a big difference in exposure in the most exposed PoC; that is due to the statistics of the process in which, almost, the available beams are uniformly used.

Table 15: Cell Radiated Power

			Cell1	Cell2	Cell3	Cell4	Cell5	Cell6	Cell7
Step Average 360s	Min	[W]	2.6	2.6	2.7	2.7	2.5	2.6	2.7
	Max	[W]	16.4	16.2	17.3	17.2	16.2	16.7	16.2
	Mean	[W]	11.1	11.1	11.1	11.1	11.1	11.1	11.1
	StdDev	[W]	4.1	4.1	4.1	4.1	4.1	4.1	4.1
Step Average 1800s	Min	[W]	3	3	3	3	3	3	3
	Max	[W]	15.4	15.4	15.4	15.4	15.4	15.4	15.4
	Mean	[W]	11.1	11.1	11.1	11.1	11.1	11.1	11.1
	StdDev	[W]	4.1	4.1	4.1	4.1	4.1	4.1	4.1

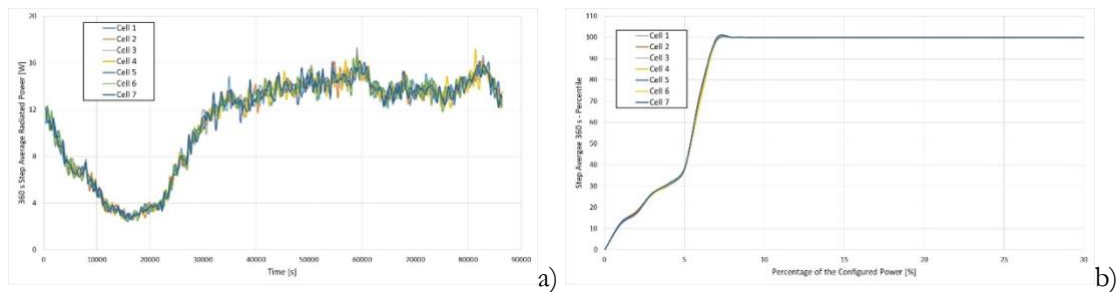


Figure 71: a) 360 s Averaged Radiated Power; b) CDF of the 360s Averaged Radiated Power

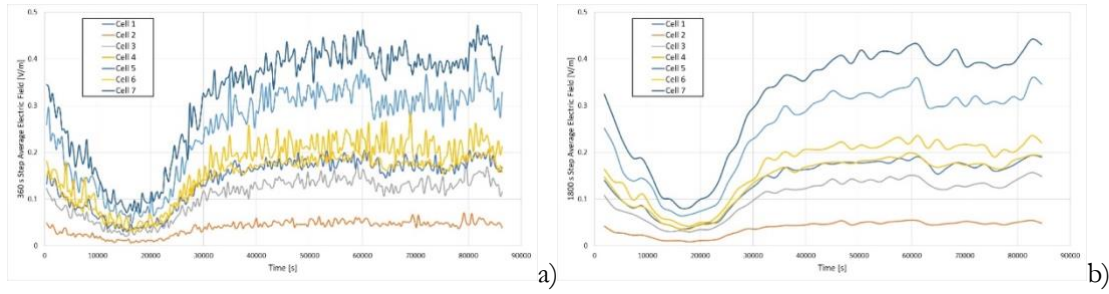


Figure 72: 360 s Averaged Electric Field in the most exposed point for each cell. a) 360 s step average, b) 1800 s step average

9.2.1.3 MMGS Scenario Test 3: Effect of the number of simultaneously served users (3)

In this test, differently than Test1, 3 users are served simultaneously; it means that a maximum of 3 beams are activated simultaneously by each cell. All the other users present at the same time are in a waiting-to-be-served list. The averaged radiated power remains almost unchanged while the exposure is a little bit lower with respect to Test1 due to lower permanence of the beam serving the user at a position.

Table 16: Cell Radiated Power

			Cell1	Cell2	Cell3	Cell4	Cell5	Cell6	Cell7
Step Average 360s	Min	[W]	2.6	2.7	2.5	2.6	2.6	2.6	2.6
	Max	[W]	16.1	16.5	16	16.7	16.6	16.2	16.2
	Mean	[W]	11.1	11.1	11.1	11.1	11.1	11.1	11.1
	StdDev	[W]	4.1	4.1	4.1	4.1	4.1	4.1	4.1
Step Average 1800s	Min	[W]	3	3	3	3	3	3	3
	Max	[W]	15.4	15.4	15.4	15.4	15.4	15.4	15.4
	Mean	[W]	11.1	11.1	11.1	11.1	11.1	11.1	11.1
	StdDev	[W]	4.1	4.1	4.1	4.1	4.1	4.1	4.1

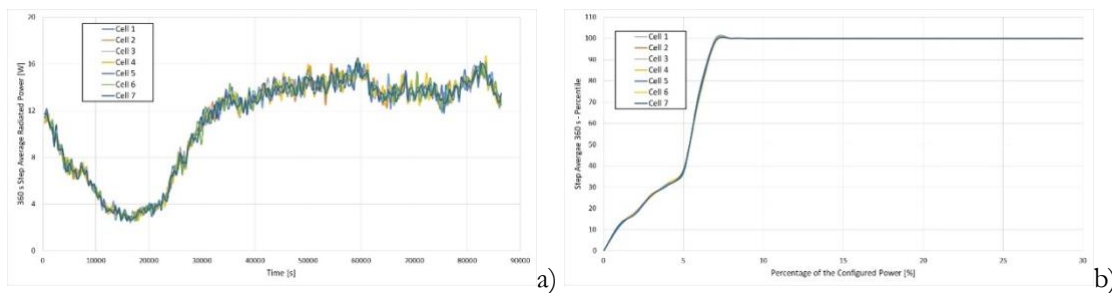


Figure 73: a) 360 s Averaged Radiated Power; b) CDF of the 360s Averaged Radiated Power

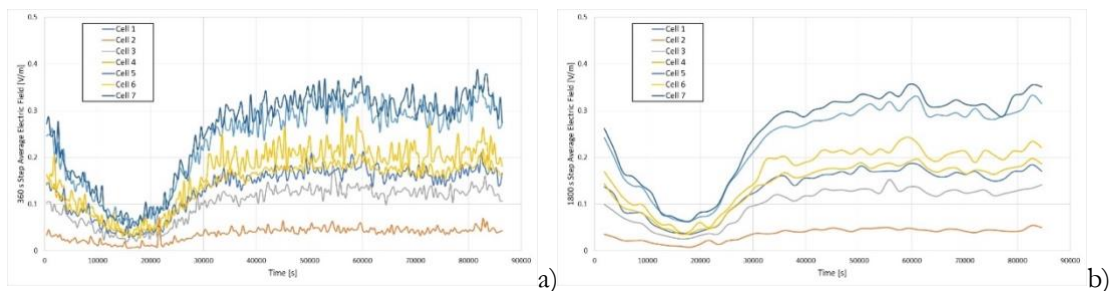


Figure 74: 360 s Averaged Electric Field in the most exposed point for each cell. a) 360 s step average, b) 1800 s step average

9.2.1.4 MMGS Scenario Test 4: Effect of the number of simultaneously served users (10)

In this test, differently from Test1, 10 users are served simultaneously; it means that a maximum of 10 beams are activated simultaneously by each cell. All the other users present at the same time are in a waiting to be served list. The averaged radiated power remains almost unchanged while the exposure is a little bit higher with respect to Test1 due to higher permanence of the beam serving the user at a position.

Table 17: Cell Radiated Power

			Cell1	Cell2	Cell3	Cell4	Cell5	Cell6	Cell7
Step Average 360s	Min	[W]	2.5	2.7	2.7	2.6	2.4	2.7	2.7
	Max	[W]	16.4	16.2	16	16.2	17.3	16.7	16.8
	Mean	[W]	11.1	11.1	11.1	11.1	11.1	11.1	11.1
	StdDev	[W]	4.1	4.1	4.1	4.1	4.1	4.1	4.1
Step Average 1800s	Min	[W]	3	3	3	3	3	3	3
	Max	[W]	15.4	15.4	15.4	15.4	15.4	15.4	15.4
	Mean	[W]	11.1	11.1	11.1	11.1	11.1	11.1	11.1
	StdDev	[W]	4.1	4.1	4.1	4.1	4.1	4.1	4.1

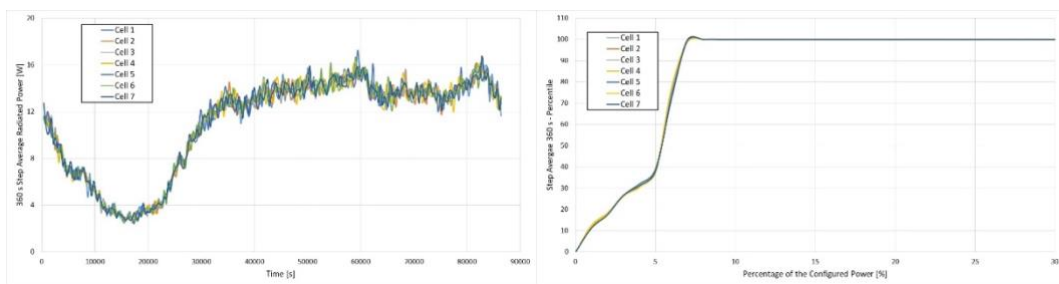


Figure 75: a) 360 s Averaged Radiated Power; b) CDF of the 360s Averaged Radiated Power

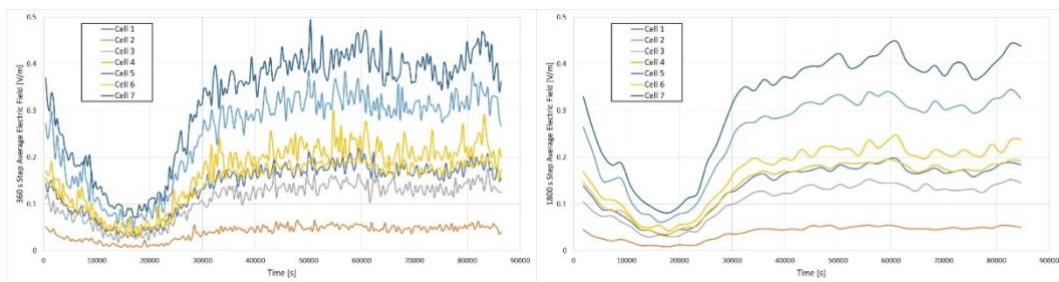


Figure 76: 360 s Averaged Electric Field in the most exposed point for each cell. a) 360 s step average, b) 1800 s step average

9.2.1.5 MMGS Scenario Test 5: Traffic extrapolated to 2026

Due to a higher cell load with respect to Test1, the averaged radiated power is about 13%, at 100-percentile of the configured power; the CDF is shifted toward right due to the increase in radiated power.

Figure 78a) shows the electric field in the most exposed point for each cell averaged over 360 s. The E-field time profile follows the cell load conditions; higher cell load causes higher power radiated by antennas and, consequently, higher field values in the point, and the averaged Electric Field is higher than in Test1.

Table 18: Cell Radiated Power

			Cell1	Cell2	Cell3	Cell4	Cell5	Cell6	Cell7
Step Average 360s	Min	[W]	4	4.1	4.1	4	4	3.9	4.1
	Max	[W]	25.2	25.5	26	25.7	25.9	25.5	25.6
	Mean	[W]	17.5	17.5	17.5	17.5	17.5	17.5	17.5
	StdDev	[W]	6.5	6.5	6.5	6.5	6.5	6.5	6.5
Step Average 1800s	Min	[W]	4.7	4.6	4.7	4.6	4.7	4.7	4.7
	Max	[W]	24.2	24.2	24.2	24.2	24.1	24.2	24.2
	Mean	[W]	17.4	17.4	17.4	17.4	17.4	17.4	17.4
	StdDev	[W]	6.5	6.5	6.5	6.5	6.5	6.5	6.5

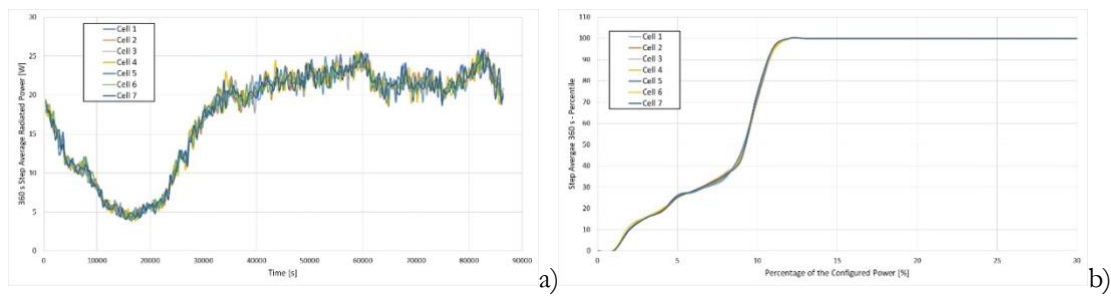


Figure 77: a) 360 s Averaged Radiated Power; b) CDF of the 360s Averaged Radiated Power

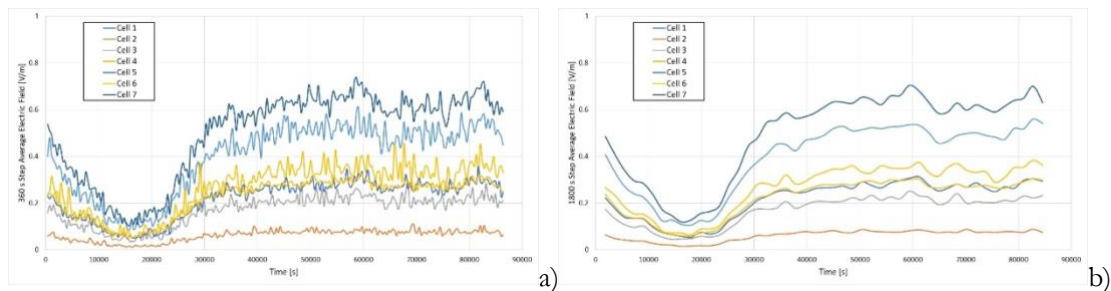


Figure 78: 360 s Averaged Electric Field in the most exposed point for each cell. a) 360 s step average, b) 1800 s step average

9.2.1.6 MMGS Scenario Test 6: Traffic extrapolated to 2029

Same considerations as in 9.2.1.5 hold.

Table 19: Cell Radiated Power

			Cell1	Cell2	Cell3	Cell4	Cell5	Cell6	Cell7
Step Average 360s	Min	[W]	6.1	6.2	5.8	5.9	5.9	5.9	6.1
	Max	[W]	37.9	37.4	37.6	39.4	38.7	37.8	38.6
	Mean	[W]	25.8	25.8	25.8	25.8	25.8	25.8	25.8
	StdDev	[W]	9.5	9.5	9.5	9.5	9.5	9.5	9.5
Step Average 1800s	Min	[W]	6.9	6.8	6.9	6.8	6.9	6.9	6.9
	Max	[W]	35.7	35.7	35.8	35.7	35.8	35.7	35.7
	Mean	[W]	25.7	25.7	25.7	25.7	25.7	25.7	25.7
	StdDev	[W]	9.5	9.5	9.5	9.5	9.5	9.5	9.5

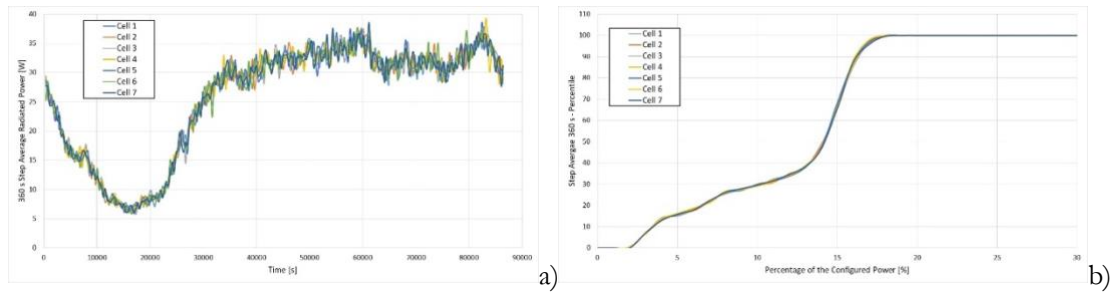


Figure 79: a) 360 s Averaged Radiated Power; b) CDF of the 360s Averaged Radiated Power

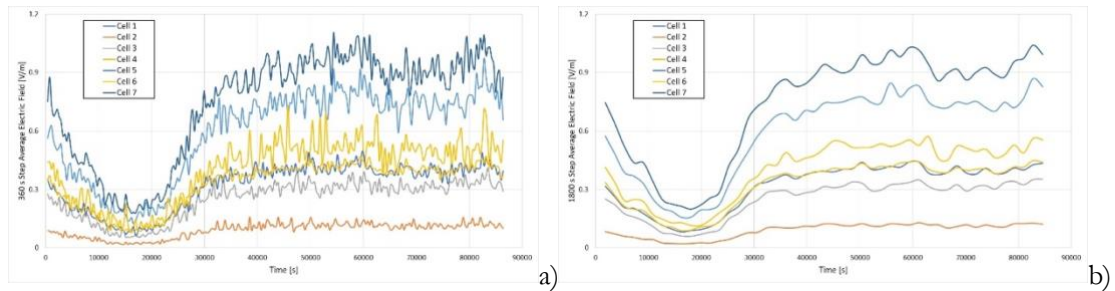


Figure 80: 360 s Averaged Electric Field in the most exposed point for each cell. a) 360 s step average, b) 1800 s step average

9.2.1.7 MMGS Scenario Test 7: Effect of the traffic typology – Voice

In this test the traffic has been considered as only voice, influencing the single service duration and number of served or in waiting list users. No sensible difference can be noted with respect to Section 9.2.1.1 since the total traffic load is kept constant but only TTI distribution changes.

Table 20: Cell Radiated Power

		Cell1	Cell2	Cell3	Cell4	Cell5	Cell6	Cell7	
Step Average 360s	Min	[W]	2.9	3	3.1	3	3	3	
	Max	[W]	16.9	17.1	17	16.9	17	17.1	17.2
	Mean	[W]	12	12	12	12	12	12	12
	StdDev	[W]	4.4	4.4	4.4	4.4	4.4	4.4	4.4
Step Average 1800s	Min	[W]	3.2	3.2	3.2	3.2	3.2	3.2	3.2
	Max	[W]	16.6	16.6	16.6	16.6	16.6	16.6	16.6
	Mean	[W]	11.9	11.9	11.9	11.9	11.9	11.9	11.9
	StdDev	[W]	4.4	4.4	4.4	4.4	4.4	4.4	4.4

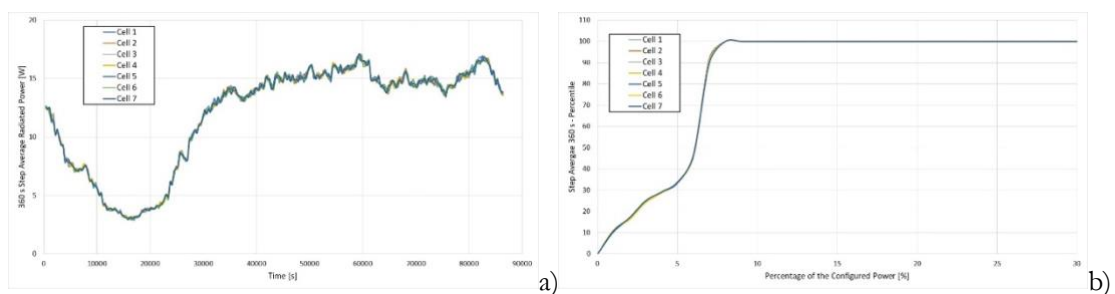


Figure 81: a) 360 s Averaged Radiated Power; b) CDF of the 360s Averaged Radiated Power

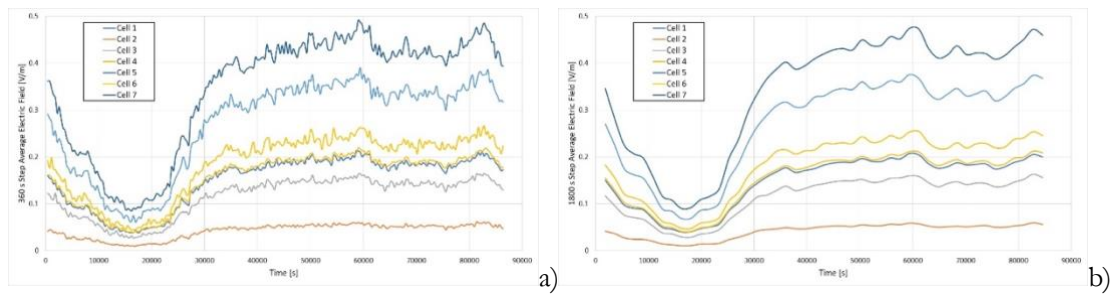


Figure 82: 360 s Averaged Electric Field in the most exposed point for each cell. a) 360 s step average, b) 1800 s step average

9.2.1.8 MMGS Scenario - Test 8: Effect of traffic typology – Web surfing

This test is similar to Test7 and also in this case to substantial differences in exposure are found due to change only in number of served or in waiting list users and TTI active distribution.

Table 21: Cell Radiated Power

		Cell1	Cell2	Cell3	Cell4	Cell5	Cell6	Cell7	
Step Average 360s	Min	[W]	2.4	2.6	2.5	2.3	2.5	2.5	2.5
	Max	[W]	16.5	16.5	16.3	15.6	15.9	15.9	16.2
	Mean	[W]	10.9	10.9	10.9	10.9	10.9	10.9	10.9
	StdDev	[W]	4	4	4	4	4	4.1	4
Step Average 1800s	Min	[W]	2.9	2.9	2.9	2.9	2.9	2.9	2.9
	Max	[W]	15.1	15.1	15.1	15.1	15.1	15.1	15.1
	Mean	[W]	10.8	10.8	10.8	10.8	10.8	10.8	10.8
	StdDev	[W]	4	4	4	4	4	4	4

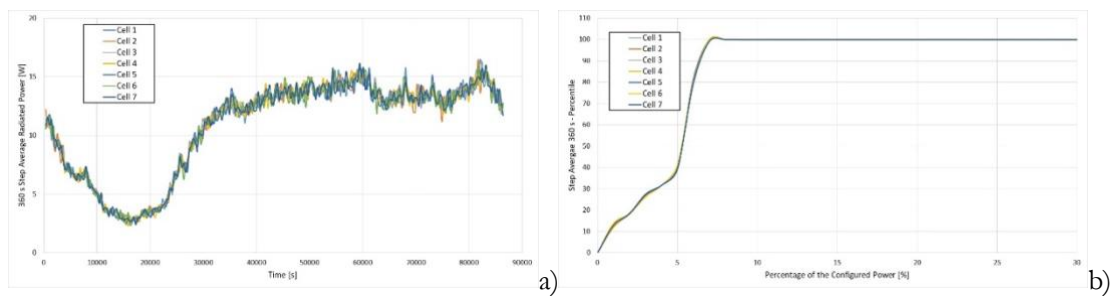


Figure 83: a) 360 s Averaged Radiated Power; b) CDF of the 360s Averaged Radiated Power

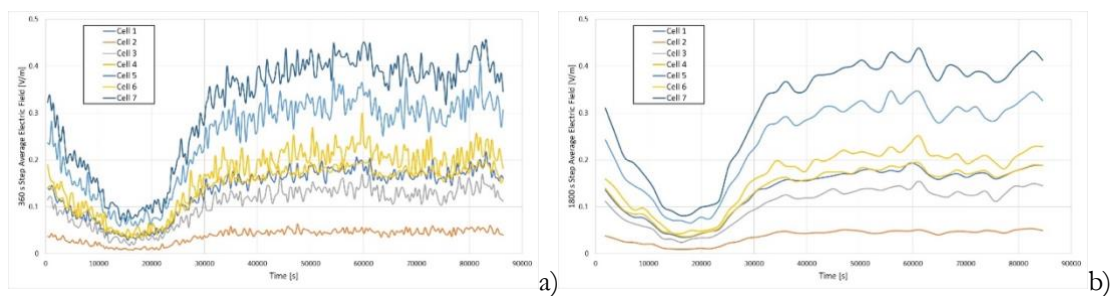


Figure 84: 360 s Averaged Electric Field in the most exposed point for each cell. a) 360 s step average, b) 1800 s step average

9.2.1.9 MMGS Scenario Test 9: Effect of the traffic typology – Huge Download

Same considerations as in Test8 hold.

Table 22: Cell Radiated Power. StdDev = standard deviation.

			Cell1	Cell2	Cell3	Cell4	Cell5	Cell6	Cell7
Step Average 360s	Min	[W]	2	2.1	2.2	2.1	1.7	2.1	1.6
	Max	[W]	18.1	16.6	17	17.6	16.8	16.3	17.2
	Mean	[W]	10.8	10.8	10.8	10.8	10.8	10.8	10.8
	StdDev	[W]	4.1	4.1	4.1	4.1	4.1	4.1	4.1
Step Average 1800s	Min	[W]	2.9	2.9	2.9	2.9	2.9	2.9	2.9
	Max	[W]	15	15	15	15	15	14.9	15
	Mean	[W]	10.8	10.8	10.8	10.8	10.8	10.8	10.8
	StdDev	[W]	4	4	4	4	4	4	4

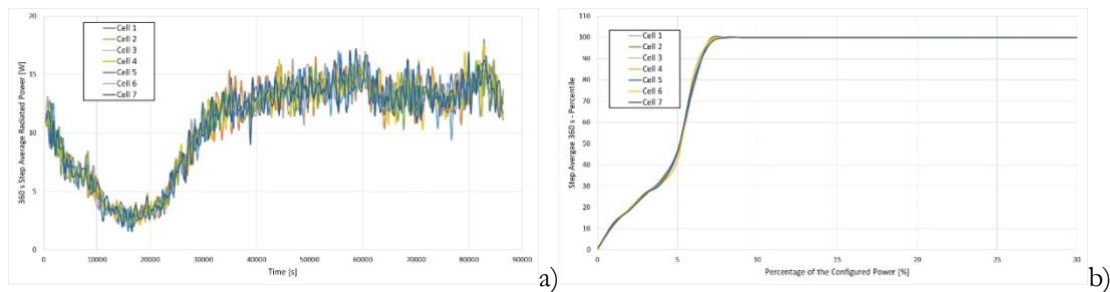


Figure 85: a) 360 s Averaged Radiated Power; b) CDF of the 360s Averaged Radiated Power

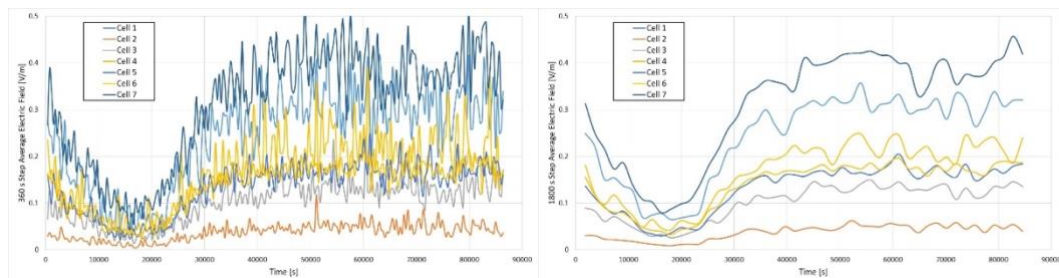


Figure 86: 360 s Averaged Electric Field in the most exposed point for each cell. a) 360 s step average, b) 1800 s step average

9.2.2 Simulations in Real Town Scenario

Simulations are based on the same assumptions as in Section 9.2.1; only differences are reported here.

- The real town scenario consists of an area 3.5 x 2.5 km² wide.
- 7 MaMIMO antennas have been considered, 1 antenna for each corner, 3 antennas in the centre of the scenario for which each antenna is 120 degs from the other:
 - Antenna 1: position x=1544m, y=1166m, z=28m, pan 0 degs, mechanical tilt 0 degs
 - Antenna 2: position x=1544m, y=1166m, z=28m, pan 120 degs, mechanical tilt 0 degs
 - Antenna 3: position x=1544m, y=1166m, z=28m, pan 240 degs, mechanical tilt 0 degs
 - Antenna 4: position x=2439m, y=319m, z=21m, pan 315 degs, mechanical tilt 0 degs
 - Antenna 5: position x=237m, y=404m, z=19m, pan 30 degs, mechanical tilt 0 degs
 - Antenna 6: position x=683m, y=2261m, z=19m, pan 135 degs, mechanical tilt 0 degs
 - Antenna 7: position x=2420m, y=2415m, z=29m, pan 190 degs, mechanical tilt 0 degs

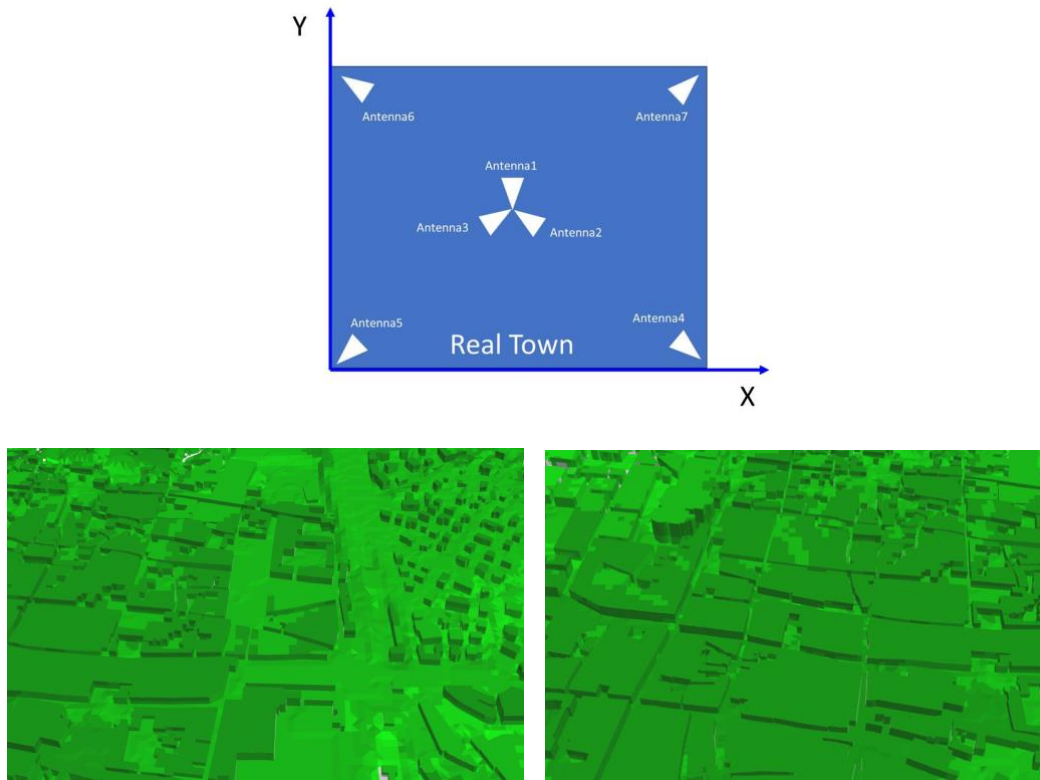


Figure 87: Real town scenario and coverage

Table 23: Service distribution per test

Test	User Position	Max Simultaneous Served Users	Payload per User per Month [10]	Service Distribution
			[GB]	
Test1	Everywhere	5	27	20%Voice 10%Huge 70%Download
Test2	Everywhere	5	64	20%Voice 10%Huge 70%Download
Test3	Everywhere	5	27	100%Voice
Test4	Everywhere	5	64	100%Voice
Test5	Everywhere	5	27	100% Web Surfing
Test6	Everywhere	5	64	100% Web Surfing
Test7	Streets	5	27	20%Voice 10%Huge 70%Download
Test8	Everywhere	2	27	20%Voice 10%Huge 70%Download
Test9	Everywhere	2	64	20%Voice 10%Huge 70%Download

Since results observed in Section 9.2.1, in which there are no substantial differences in exposure by using rolling average or step average, only step average results will be reported in this section.

9.2.2.1 Real Town Scenario Test 1: Reference

This is the reference test, changes in parametrization for all the other test for the town scenario, are referred to this test.

Figure 88 shows the radiated power by each cell step averaged over 360 s. Since the load of each cell is the same, as expected, the radiated power is almost the same for each cell. The power ripple is caused by the different time positions of each user due to different service conditions. The averaged radiated power by each cell, over 360 s

time interval, is always less than 10% of the configured power; as expected, the antenna does not always radiate the configured power in the time.

The exposure shown in Figure 89 appears to be a little bit lower with respect to the exposure shown in Figure 68 and Figure 69 due to the lower height of the buildings. Even in this test, the effect of the average time interval is a sort of low pass filter on the time shape of the exposure.

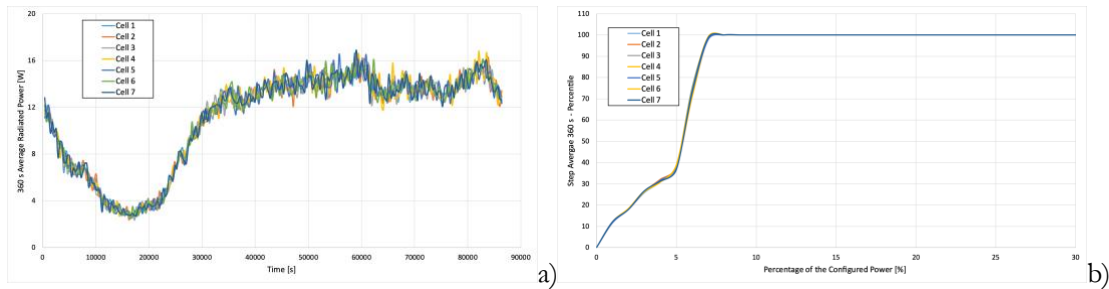


Figure 88: a) 360 s Averaged Radiated Power; b) CDF of the 360s Averaged Radiated Power

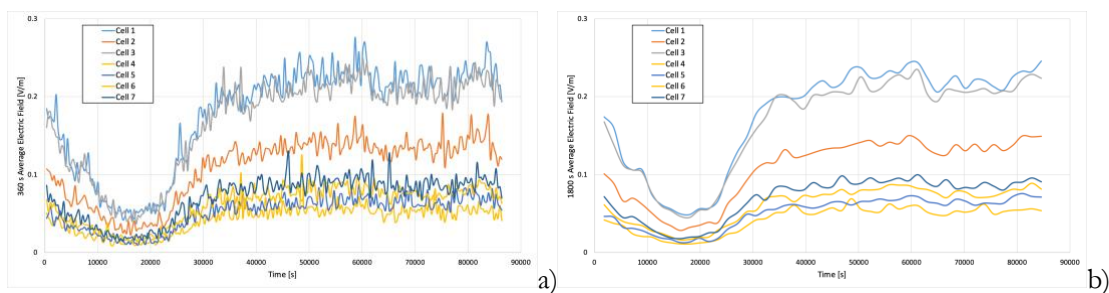


Figure 89: 360 s Averaged Electric Field in the most exposed point for each cell. a) 360 s step average, b) 1800 s step average.

9.2.2.2 Real Town Scenario Test 2: Traffic extrapolated to 2029

Due to a higher cell load with respect to Test1, see Figure 90, the averaged radiated power is about 18%, at 100 percent of the configured power; the CDF is shifted toward the right due to the increase in radiated power.

Figure 91a) shows the electric field in the most exposed point by each cell averaged over 360 s. The E-field time profile follows the cell load conditions; higher cell load causes high power radiated by antennas and, consequently, higher field values, so the averaged Electric Field is higher than the previous test.

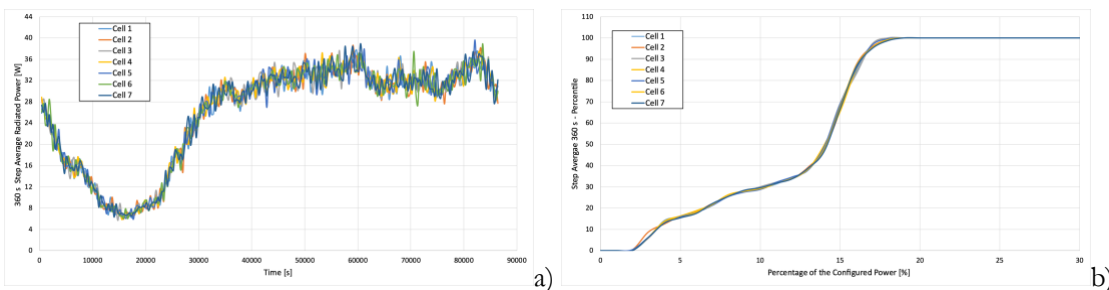


Figure 90: a) 360 s Averaged Radiated Power; b) CDF of the 360s Averaged Radiated Power

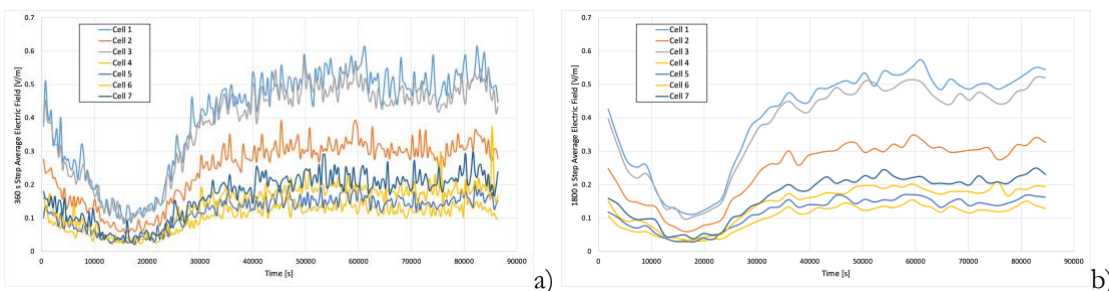


Figure 91: 360 s Averaged Electric Field in the most exposed point for each cell. a) 360 s step average, b) 1800 s step average.

9.2.2.3 Real Town Scenario Test 3: Effect of the traffic typology - Voice

In this test, the traffic has been considered as only voice, influencing the single service duration and number of served or on waiting list users. No sensible difference can be noted with respect to Section 9.2.2.1 since the total traffic load is kept constant, but only TTI distribution changes.

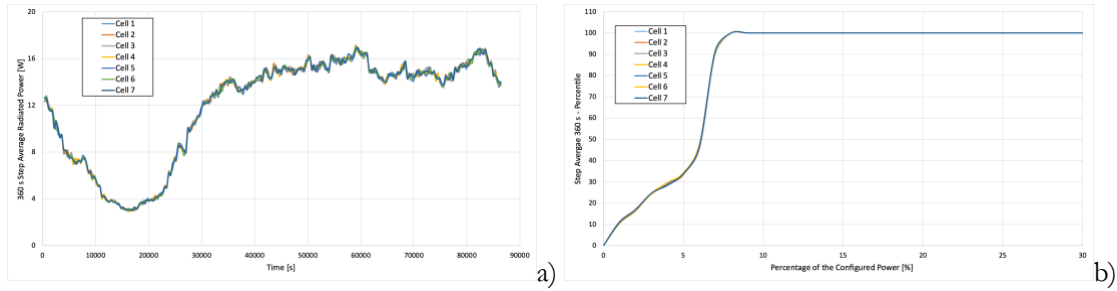


Figure 92: a) 360 s Averaged Radiated Power; b) CDF of the 360s Averaged Radiated Power

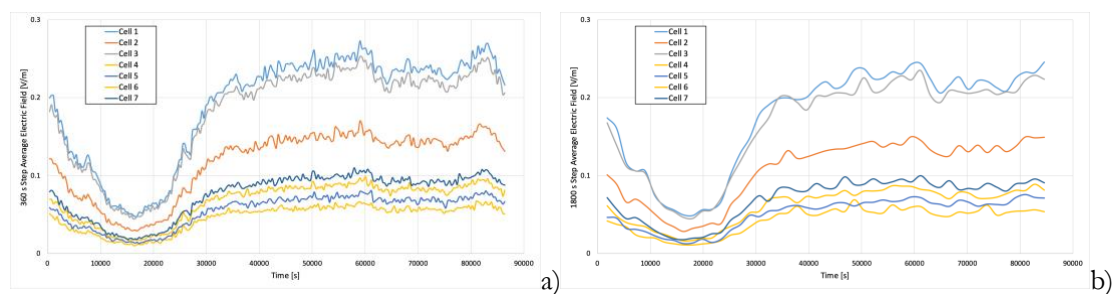


Figure 93: 360 s Averaged Electric Field in the most exposed point for each cell. a) 360 s step average, b) 1800 s step average.

9.2.2.4 Real Town Scenario Test 4: As Test 3 extrapolated to 2029

Same considerations as in 9.2.2.2 can be drawn.

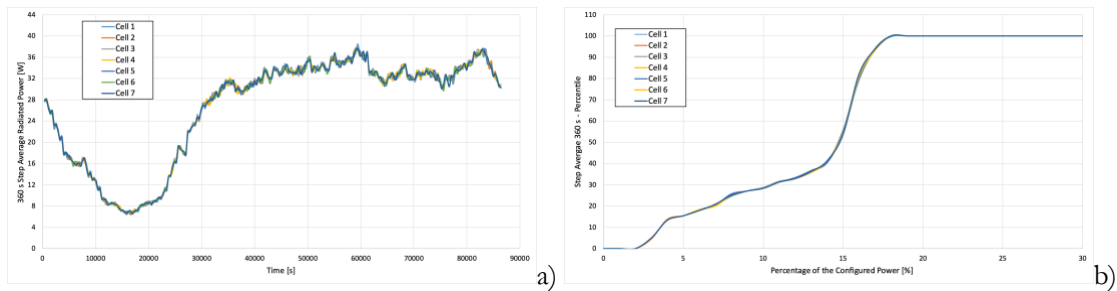


Figure 94: a) 360 s Averaged Radiated Power; b) CDF of the 360s Averaged Radiated Power

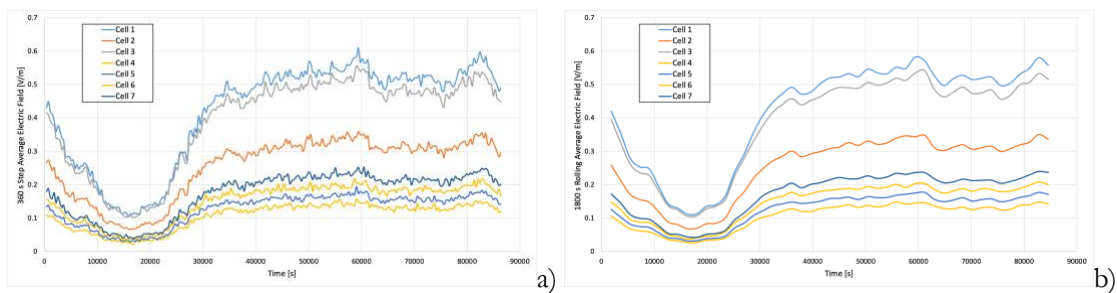


Figure 95: 360 s Averaged Electric Field in the most exposed point for each cell. a) 360 s step average, b) 1800 s step average.

9.2.2.5 Real Town Scenario Test 5: Effect of the traffic typology – Web surfing

This test is similar to Test3 and also in this case the substantial differences in exposure are found due to changes only in number of served or in waiting list users and TTI active distribution.

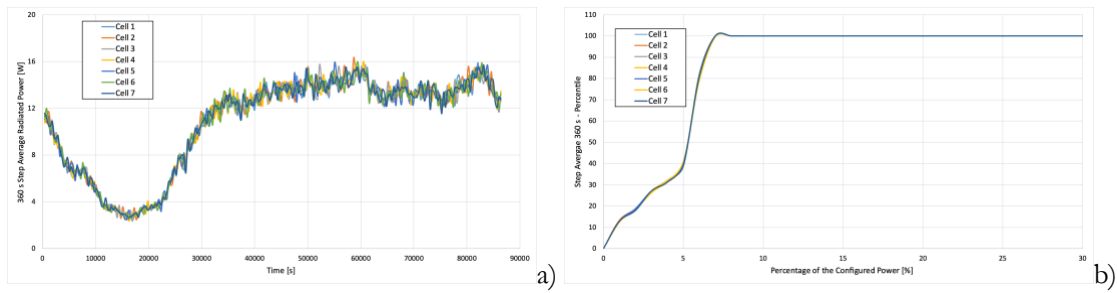


Figure 96: a) 360 s Averaged Radiated Power; b) CDF of the 360s Averaged Radiated Power

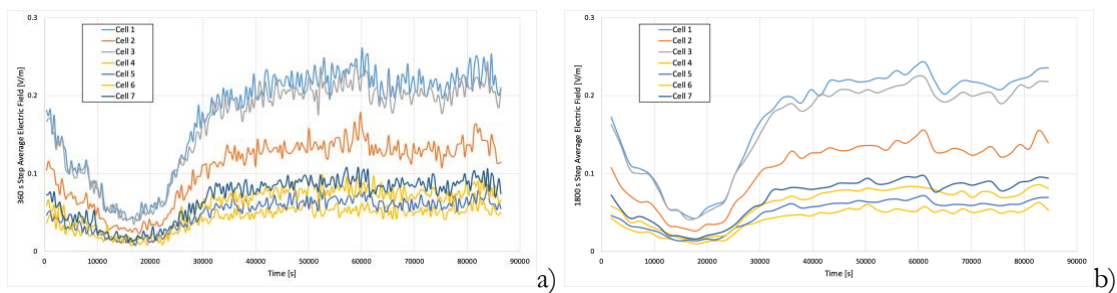


Figure 97: 360 s Averaged Electric Field in the most exposed point for each cell. a) 360 s step average, b) 1800 s step average.

9.2.2.6 Real Town Scenario Test 6: As Test 5 extrapolated to 2029

Even in this case an increase of the exposure is obtained due to the increase of the traffic for each cell.

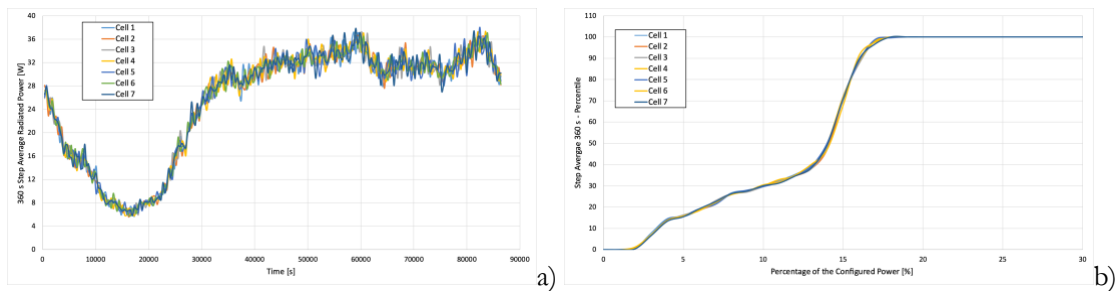


Figure 98: a) 360 s Averaged Radiated Power; b) CDF of the 360s Averaged Radiated Power

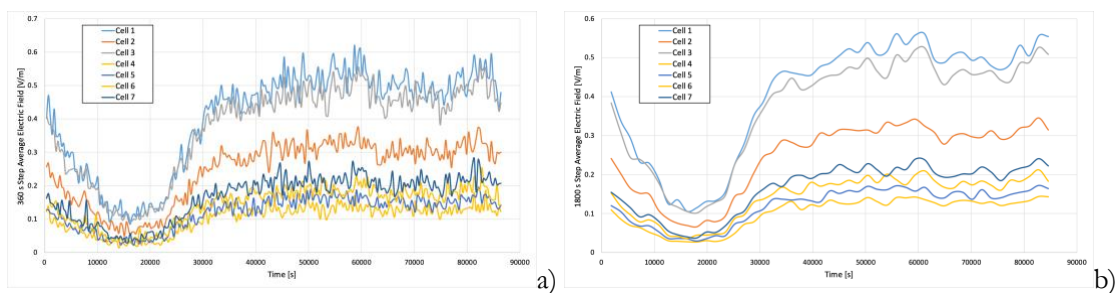


Figure 99: 360 s Averaged Electric Field in the most exposed point for each cell. a) 360 s step average, b) 1800 s step average.

9.2.2.7 Real Town Scenario Test 7: Users located only on the streets

In this test users are located only on the streets and not on the buildings: Exposure in the most radiated PoC for each cell appears to have a very limited or imperceptible effect due to each beam shape and direction with respect to the PoC.

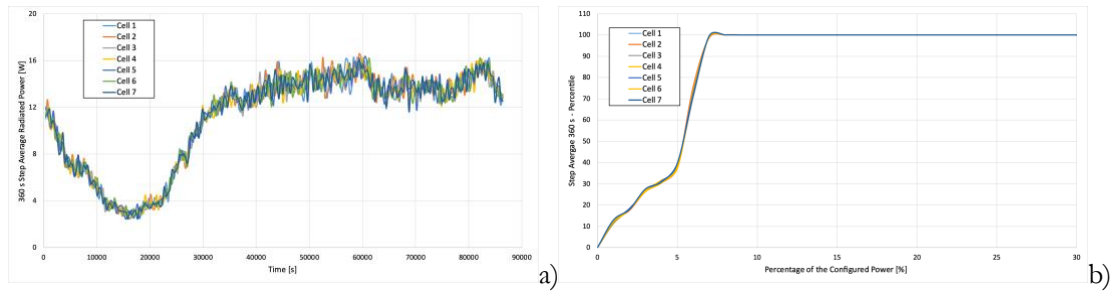


Figure 100: a) 360 s Averaged Radiated Power; b) CDF of the 360s Averaged Radiated Power

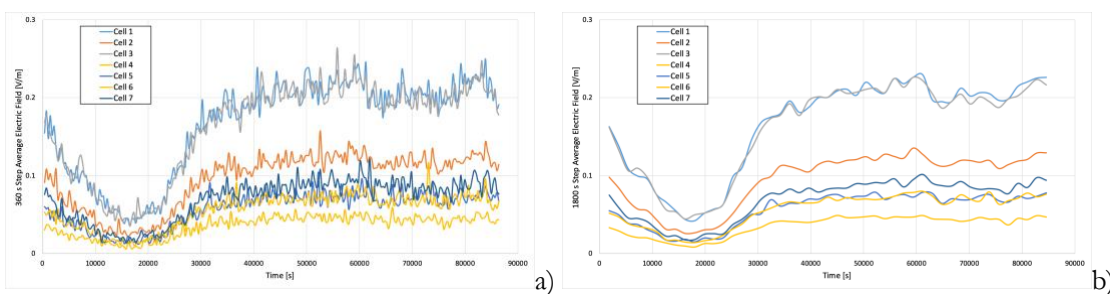


Figure 101: 360 s Averaged Electric Field in the most exposed point for each cell. a) 360 s step average, b) 1800 s step average.

9.2.2.8 Real Town Scenario Test 8: Effect of the number of simultaneously served users

In this test, differently from Test1, 2 users are served simultaneously; it means that a maximum of 2 beams are activated simultaneously by each cell. The averaged radiated power remains almost unchanged while the exposure is a little bit lower with respect to Test1 due to lower permanence of the beam serving the user at a position.

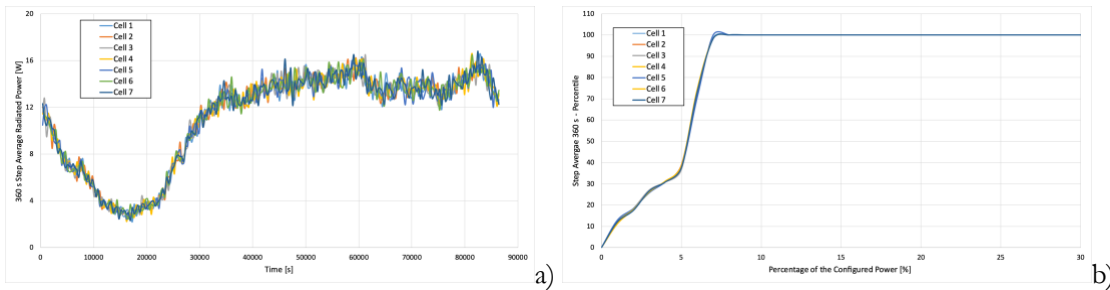


Figure 102: a) 360 s Averaged Radiated Power; b) CDF of the 360s Averaged Radiated Power

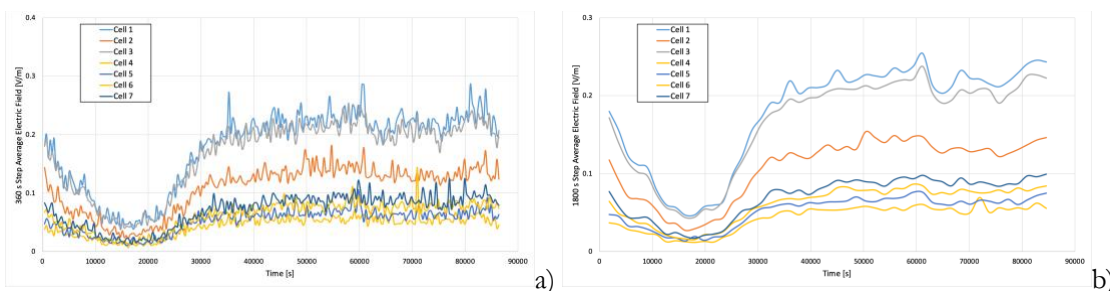


Figure 103: 360 s Averaged Electric Field in the most exposed point for each cell. a) 360 s step average, b) 1800 s step average.

9.2.2.9 Real Town Scenario Test 9: As Test8 extrapolated to 2029

As in the other equivalent cases an increase of exposure occurs.

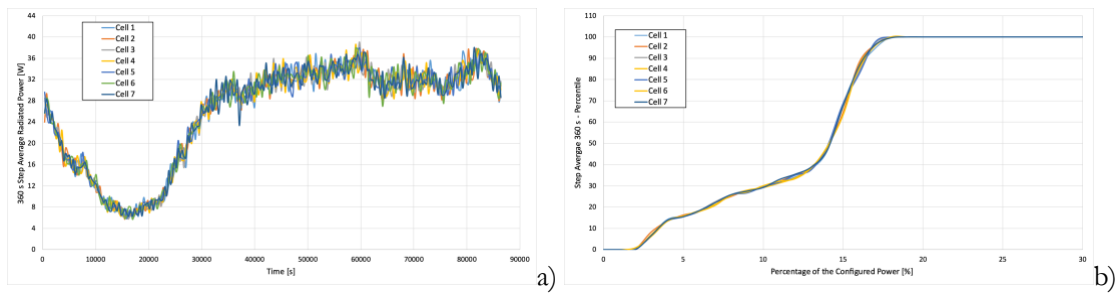


Figure 104: a) 360 s Averaged Radiated Power; b) CDF of the 360s Averaged Radiated Power

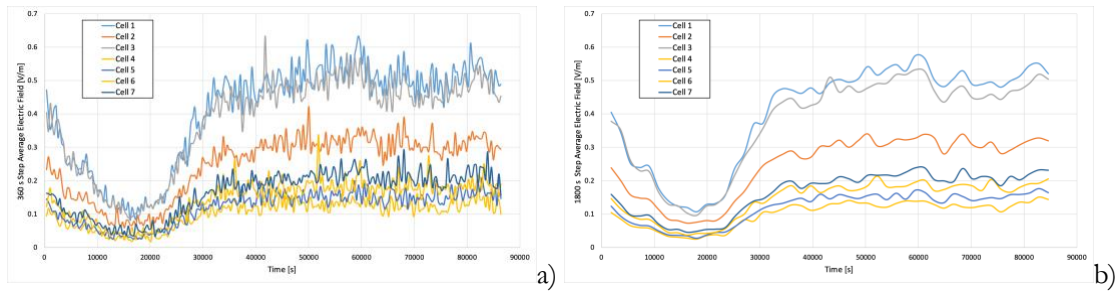


Figure 105: 360 s Averaged Electric Field in the most exposed point for each cell. a) 360 s step average, b) 1800 s step average.

9.2.3 Simulations in Indoor Office (IO) Scenario

The indoor scenario is described in Section 6.1.4. Simulation parameters are as follows:

- IO Scenario consist of an area 14 x 18 m, ceiling height 3 m;
- 2 MaMIMO antennas have been considered, installed at the scenario corner.
 - Antenna 1: position x=1 m, y=17 m, z=2.6 m, pan 140 degs, mechanical tilt 0 degs
 - Antenna 2: position x=13 m,y=1 m, z=2.6 m, pan 320 degs, mechanical tilt 0 degs

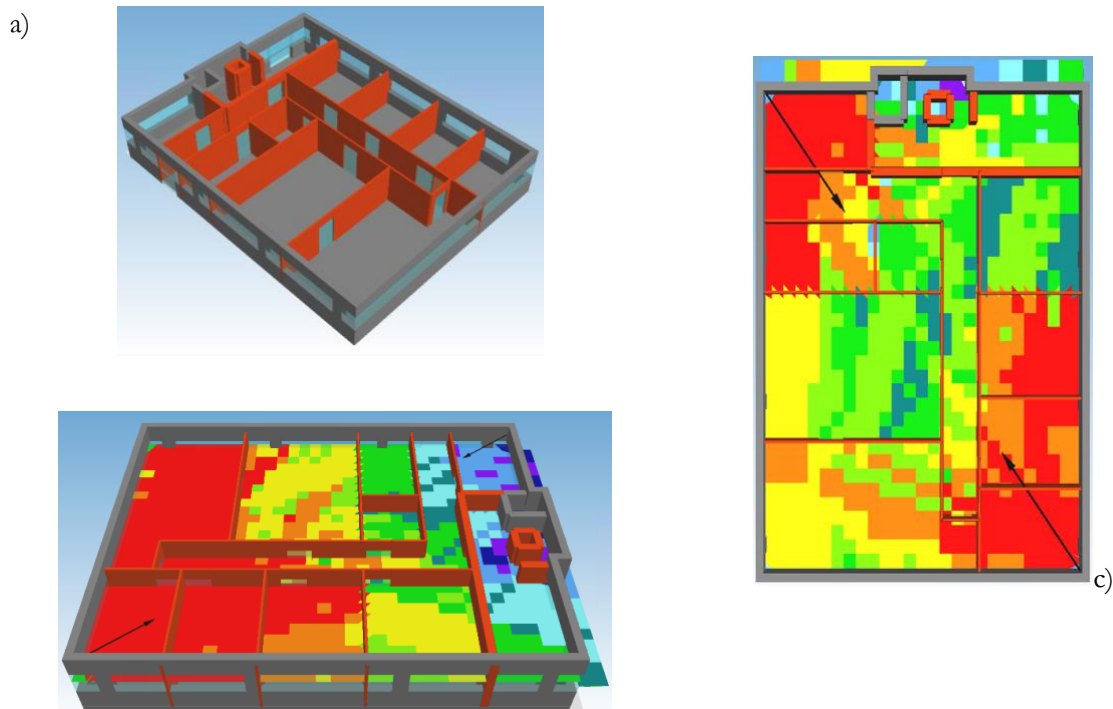


Figure 106: a) the 3D view of the scenario and b) and c) an example of coverage of the MaMIMO antenna.

- Each antenna is equipped with a set of 4 beams, 0 degrees tilted, located on a single layer; the layer covers 120 degs in azimuth.
- The antenna characteristics are described in Section 6.2.4

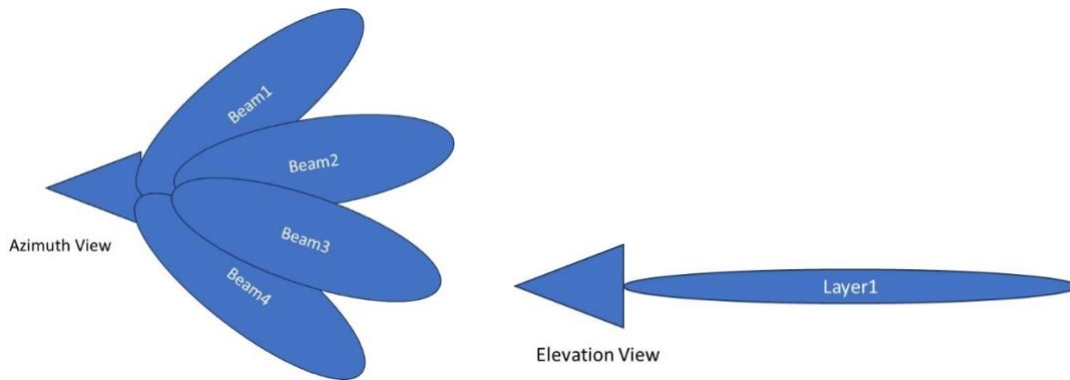


Figure 107: Arrangement of the antenna beams for the Indoor Hangar Industrial Scenario

- Each antenna has 0.1 W configured power
- An 8-2 TDD pattern has been adopted, DDDDDDDDUU, see 9.2.1
- Observation period is eight hours’ time interval to cover the working day hours, discretized in steps of 1 ms, consisting in 28.8 million iterations.
- Within the office, 13 static users and 5 dynamic users are supposed. 2 static users per room have been located in the scenario, 3 in the larger room.
- For each user, since there are not available data for describing the payload in IO Scenario, the payload has been deducted taking data in [14] and some estimation based on internal experience, as shown in Table 24;

Table 24: Services considered in IO simulations and their characteristics

Service	Throughput	Payload per service	Minimum duration	Maximum Duration
	[Mbps]	[MB]	[s]	[s]
VoIP	0.17		300	600
Video Call	2.85		2400	3600
Web Surfing	0.01		900	1800
Video Streaming	3.64		1200	3000
Cloud		300		
Mail		2		

- The load conditions for the traffic are obtained by using the service profile shown in Table 25.

Table 25: Description of the service load per hour of the day per user

Hour	Max allowed Mail	Max allowed VoIP	Max allowed Video calls
1	20	10	1
2	15	10	2
3	15	5	2
4	15	5	2
5	2	1	0
6	10	5	2
7	15	5	2
8	10	10	1

Web Surfing, Video Streaming and Cloud Services are randomly generated during the working hours of the day and associated only to users, in fixed positions or in movement.

- The cell capacity is assumed to be 500 Mbps or 1.5 Gbps depending on the Test.
- For each TTI the SINR at user locations has been evaluated, see section 8.1.3
- Throughput is based on the Ofcom link curve, see section 8.1.3
- Service Time duration is taken from the payload divided by the throughput, since the payload has been randomized for each service then the service time duration for each user is variable.
- User position in time is uniformly random distributed.
- User position in space is randomly distributed over the allowed spaces in the scenario for the dynamic users, while the position is fixed for the statics users.
- From the amount of data per user and cell capacity, the number of simultaneous users requiring services is determined.
- Power has been equally divided among all active beams per each TTI
- Point of Controls are the static users' positions
- Since the load profile depends on random functions, each simulation is repeated 5 times and values have been taken as averages among all simulations performed. On the base of previous simulation experience, only step average is considered.
- Results have been generated in terms of:
 - Time distribution of time-averaged cell power for each cell:
 - 360 and 1800 s time average has been considered as indicated in [1] and [2];
 - CDF of the averaged power.
 - Time distribution of the averaged electric field for the observation points:
 - 360 and 1800 s time average has been considered as indicated in [1] and [2];
 - CDF of the averaged electric field.
- General parameters
 - 5G NR Band: 100 MHz
 - External Temperature: 25.0 Celsius
 - TTI Duration: 1 ms
 - Receiver Gain: 0 dBi
 - Receiver Noise Figure: 3.0 dB
 - Frequency: 3600.0 MHz

The following tests have been performed:

- Test 1: corresponding to a Cell capacity of 1.5 Gbps;
- Test 2, corresponding to a cell capacity of 500 Mbps.

9.2.3.1 IO Scenario Test 1

Since three services, Web Surfing, Streaming Video, and Cloud Services are completely random, a set of five simulations have been performed for each test; then radiated power and exposure have been averaged among the computed data from the pool of simulations. The fall of power and exposure in the middle of the observed period corresponds to a lower request of service due to the lunch break. Average power and exposure assume very low values since the amount of data for the service profile used in the simulations is downloaded in a very short time, in comparison to the cell capacity.

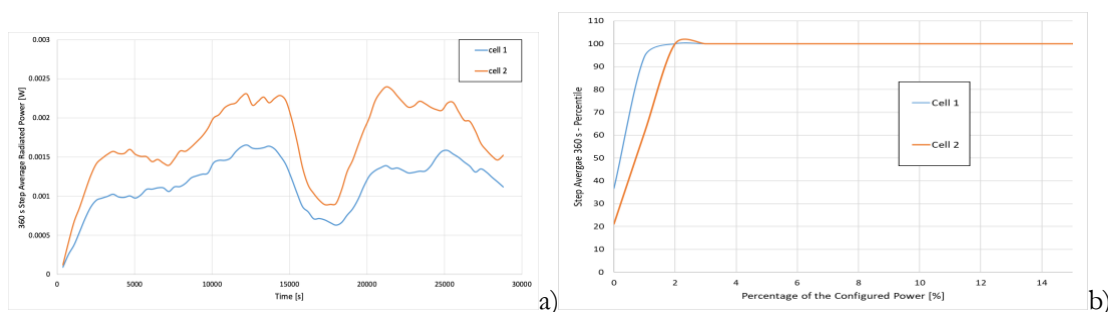


Figure 108: a) 360 s Averaged Radiated Power; b) CDF of the 360s Averaged Radiated Power

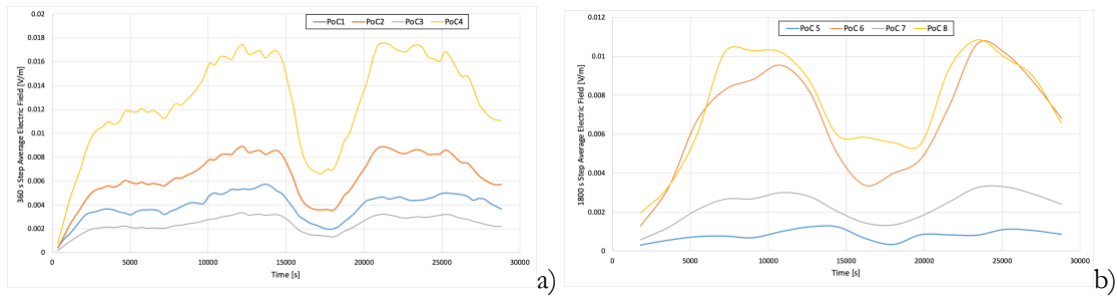


Figure 109: Step Averaged Electric Field in PoCs. a) 360 s average, b) 1800 s average

9.2.3.2 IO Scenario Test 2

Similar considerations as done in test 1 can be drawn for this test except for an increase of the exposure and of the averaged radiated power due to the lower capacity of the cell, requiring more TTIs to download the same amount of data.

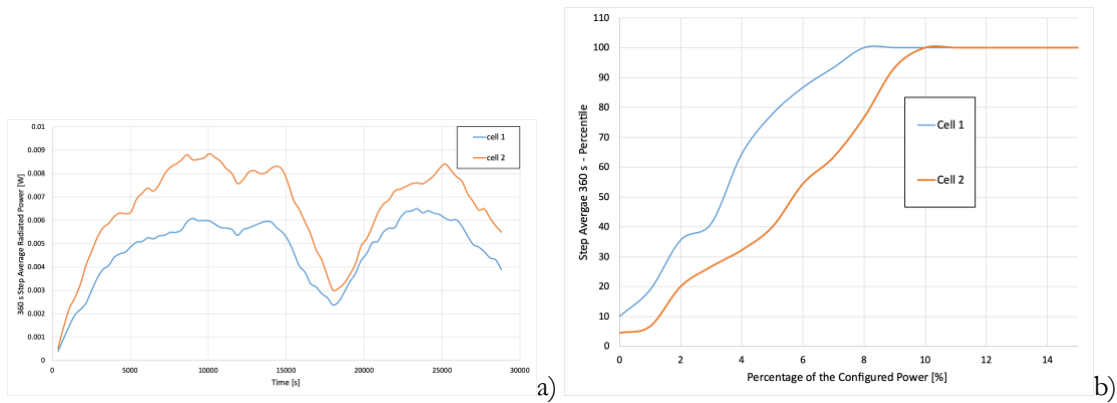


Figure 110: a) 360 s Averaged Radiated Power; b) CDF of the 360s Averaged Radiated Power

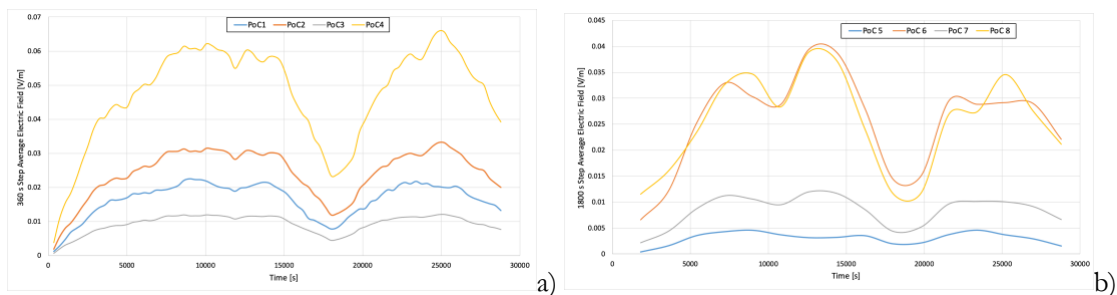


Figure 111: Step Averaged Electric Field in PoCs. a) 360 s average, b) 1800 s average

9.2.4 Simulations in Indoor Industrial Hangar (IIH) Scenario

The IIHS Scenario is described in Section 6.1.4. Parameters for simulations are as follows:

- The scenario consists of an area 160 m x 56 m wide, ceiling height 6 m.
- 2 MaMIMO antennas have been considered, installed at the scenario corners, see Figure 112.
 - Antenna 1: position $x=2m$, $y= 55m$, $z= 5.8$, pan 110 degs, mechanical tilt 0 degs
 - Antenna 2: position $x=158m$, $y= 1m$, $z=5.8$, pan 290 degs, mechanical tilt 0 degs



Figure 112: The industrial hangar scenario and the positions of the radiating points

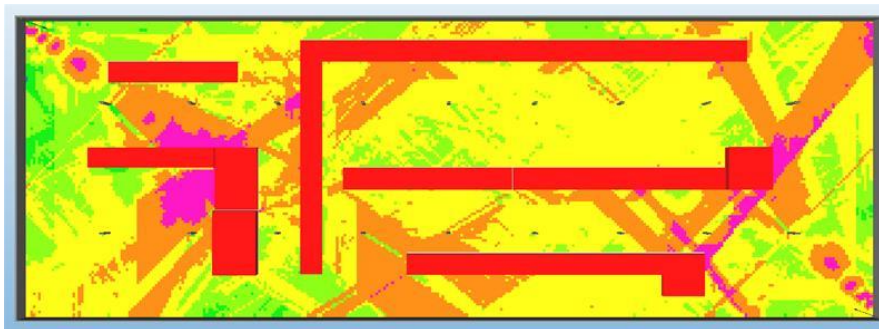


Figure 113: An example of coverage in the IHH scenario for one of the available beams on the cell.

- Each antenna is equipped with a set of 4 beams, 0 degrees tilted, located on a single layer; the layer covers 120 degs in azimuth
- The antenna characteristics are described in Section 6.2.4

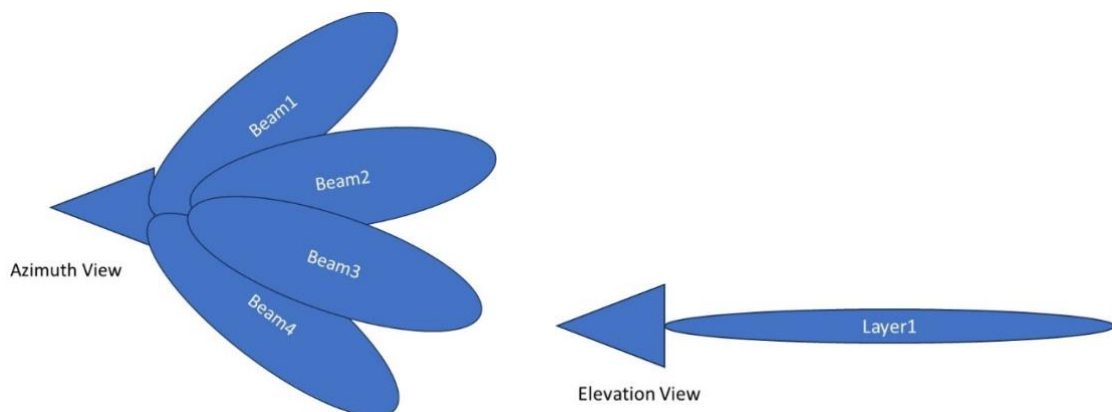


Figure 114: Arrangement of the antenna beams for the Indoor Hangar Industrial Scenario

- Each antenna has 0.1 W configured power.
- An 8-2 TDD pattern scheme has been adopted, DDDDDDDDUU, see Section 9.2.1.
- Observation period is a whole day, discretized in steps of 1 ms, consisting in 86.4 million iterations.
- Within the IHH, there are:

- 38 RX points fixed in positions representing machinery receivers, the yellow dots in Figure 112
- 15 static users, representing workers in fixed positions during the working hours, the green dots in Figure 112
- 10 moving users during working hours, not represented in Figure 112
- For each user, since there are not available data for describing the payload in IIIH Scenario, it has been deducted taken data in [14] and some estimation based on internal experience, as shown in Table 26.
- Ten types of services have been supposed, typical of this type of environment during a working day. Services are characterized in terms of throughput required then randomized in time include in an interval defined by a minimum and maximum or by amount of data to be transmitted, see Table 26.

Table 26: Services considered in IIIH simulations their characteristics

Service	Throughput	Payload	Minimum duration	Maximum duration
	Mbps	MB	s	s
VoIP	0.17		60	600
Video call	2.85		600	3600
Mail		2		
Video Streaming	3.64		900	3000
Cloud		200		
Web Surfing	0.01		600	2400
Remote Control	100		5	15
Digital Twin update	250		5	15
Monitoring/Telemetry	250		1	3

- The load conditions for the traffic are obtained by using the service profile shown in Table 27.

Table 27: Description of the service load per hour of the day per user

Hour	Max allowed Mail	Max allowed VoIP	Max allowed Video calls	Max Allowed Remote Control	Video Control	Digital Twin Update	Monitoring Telemetry
1	0	0	0	60	40	60	240
2	0	0	0	60	40	60	240
3	0	0	0	60	40	60	240
4	0	0	0	60	40	60	240
5	0	0	0	60	40	60	240
6	0	0	0	60	40	60	240
7	0	0	0	60	40	60	240
8	20	10	1	60	40	60	240
9	20	10	1	60	40	60	240
10	15	10	1	60	40	60	240
11	10	5	2	60	40	60	240
12	10	5	2	60	40	60	240
13	2	1	0	60	40	60	240
14	5	5	2	60	40	60	240
15	10	5	2	60	40	60	240
16	10	10	1	60	40	60	240
17	20	10	1	60	40	60	240
18	20	10	1	60	40	60	240
19	15	10	1	60	40	60	240
20	2	1	0	60	40	60	240
21	0	2	0	60	40	60	240
22	0	2	0	60	40	60	240
23	0	0	0	60	40	60	240
24	0	0	0	60	40	60	240

Web Surfing, Streaming Video and Cloud Services are randomly generated during the working hours of the day and associated only to users, in fixed positions or in movement.

- The cell capacity is assumed to be 500 Mbps or 1.5 Gbps.
- For each TTI the SINR at user locations has been evaluated, see section 8.1.3.
- Throughput is based on the Ofcom link curve, see section 8.1.3.
- Service Time duration is taken from the payload divided by the throughput, since the payload has been randomized for each service then the service time duration for each user is variable.
- User position in time is uniformly random distributed.
- User position in space is randomly distributed over the allowed spaces in the scenario for the dynamic users, while position is fixed for the statics users.
- From the amount of data per each user and cell capacity, the number of simultaneous users requiring services is determined.
- Simulations have been performed with a different number of active users served simultaneously.
- Power has been equally divided among all active beams per each TTI
- Point of Controls are the machineries' positions (PoC1) and users' positions (PoC2).
- Since the load profile depends on random functions, each simulation is repeated 5 times and values have been taken as averages among all simulations performed. On the base of previous simulation experience, only step average is considered.
- Results have been generated in terms of:
 - Time distribution of time averaged cell power for each cell:
 - 360 and 1800 s time average has been considered as indicated in [1] and [2];
 - CDF of the averaged power
 - Time distribution of the averaged electric field for the observation points:
 - 360 and 1800 s time average has been considered as indicated in [1] and [2];
 - CDF of the averaged electric field
- General parameters
 - 5G NR Band: 100 MHz
 - External Temperature: 25.0 Celsius
 - TTI Duration: 1 ms
 - Receiver Gain: 0 dBi
 - Receiver Noise Figure: 3.0 dB
 - Frequency: 3600.0 MHz

The following tests have been performed:

- Test 1: corresponding to a Cell capacity of 1.5 Gbps;
- Test 2, corresponding to a cell capacity of 500 Mbps.

9.2.4.1 IIIH Scenario Test1

Figure 115a) shows the averaged radiated power by each cell, it can be noted that it is about 60 mW corresponding to 75% of maximum possible radiated power for each cell as can be noted even in Figure 115b) at 100-percentile.

Figure 116 shows the averaged electric field over 360 s for Points of Control corresponding to machinery receivers or user's position, see Figure 112, as well as Figure 117 for exposure averaged over 1800 s. in both cases the field level is very low compared to limits. From pictures it is also possible to note that the major contribution is due to machinery operations, since the service profiles indicated, with a very slight increase of traffic during working hours. Power, and consequently exposure, is almost flat due to the continuous operations of the MaMIMO antenna due to the service profile adopted in this test.

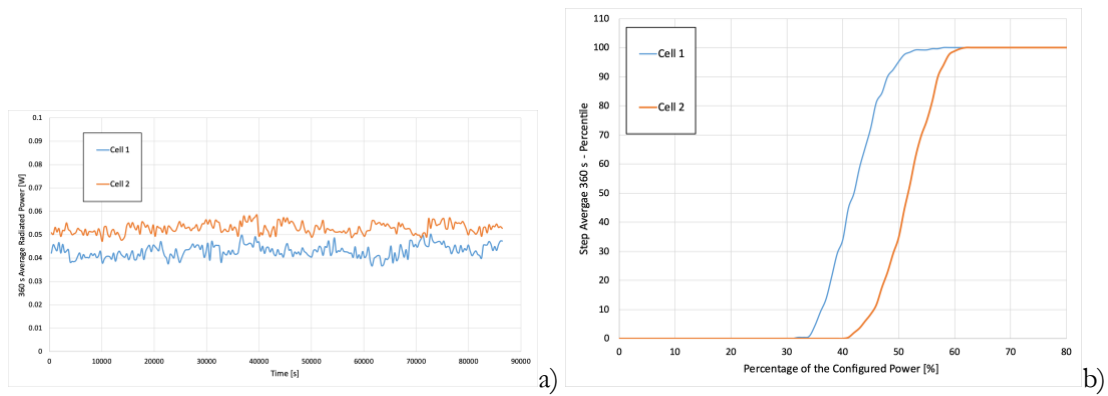


Figure 115: a) 360 s Averaged Radiated Power; b) CDF of the 360s Averaged Radiated Power

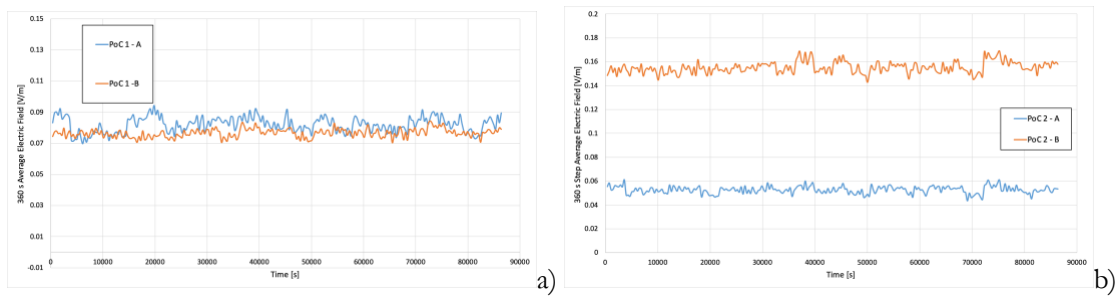


Figure 116: 360 s Step Averaged Electric Field PoCs. a) PoC1, b) PoC2

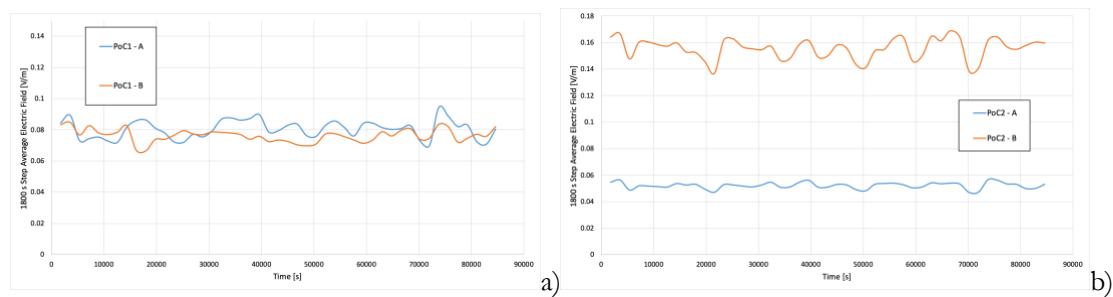


Figure 117: 1800 s Averaged Electric Field in the PoCs. a) PoC1, b) PoC2

9.2.4.2 ITH Scenario Test2

In this case, the reduced cell capacity requires the usage of more TTIs to deliver the same payload, so saturating the cell capacity. Figure 118 indicates the power is constantly radiated at 100% by each cell reaching 80% of the configured power, on the base of the TDD schema adopted. The exposure in the PoCs, see Figure 119 and Figure 120, in average have a ripple around a flat average value, fluctuations are due to the beams' activity serving receivers in different locations.

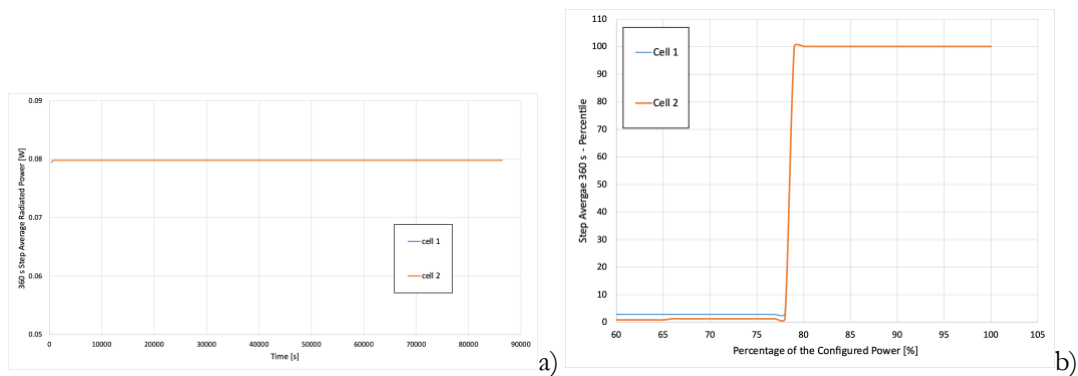


Figure 118: a) 360 s Averaged Radiated Power; b) CDF of the 360s Averaged Radiated Power

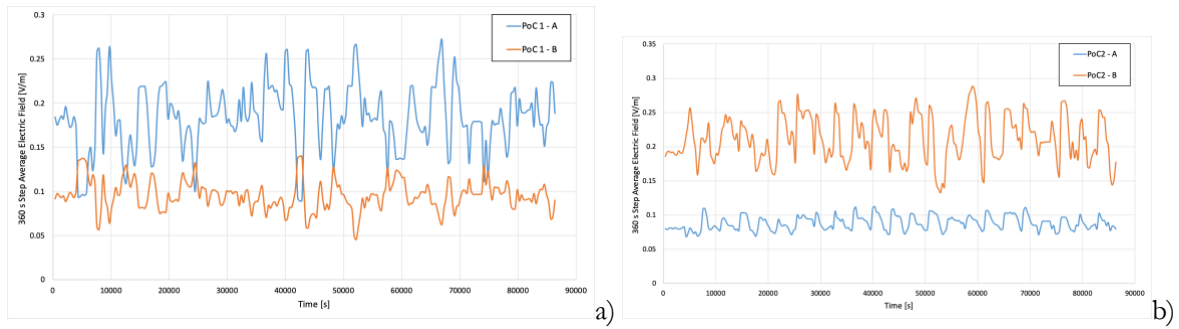


Figure 119: 360 s Step Averaged Electric Field PoCs. a) PoC1, b) PoC2

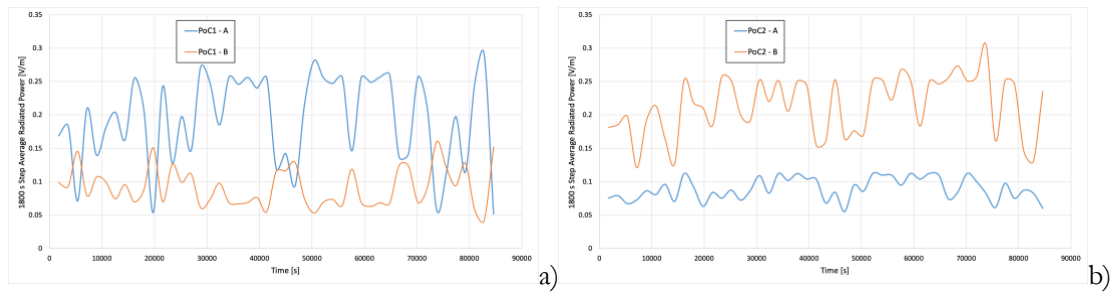


Figure 120: 1800 s Averaged Electric Field in the PoCs. a) PoC1, b) PoC2

9.2.5 Simulations in FR2 reduced MMGS scenario

Simulations in FR2 have been performed in a portion of MMGS consisting of three basic tiles, see Section 6.1.2, as shown in Figure 121.

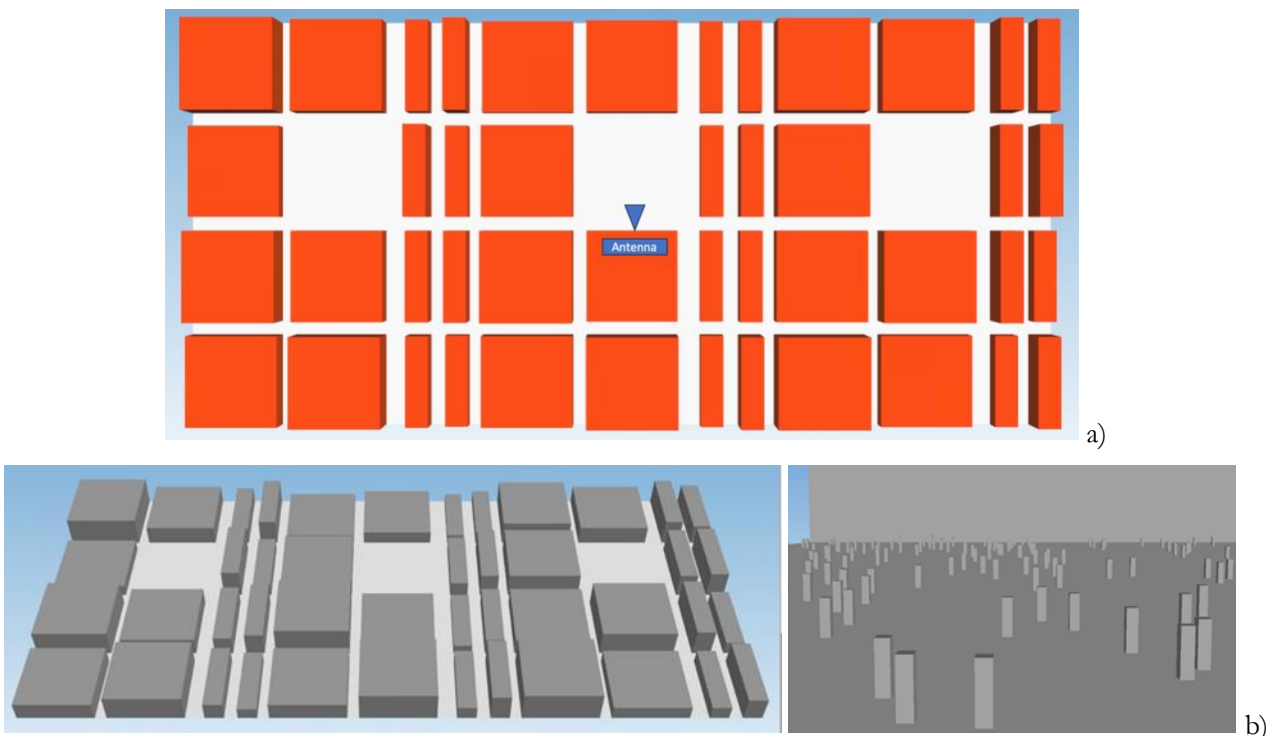


Figure 121: The reduced MMGS scenario used for FR2 simulations. a) the position of antenna. b) 3D scenario and details on users' model.

Four tests have been performed, each one having a different number of elements simulating users in the area of the main plaza, see Figure 121, namely:

- Test 1: no users.
- Test 2: 50 users randomly distributed.

- Test 3: 200 users randomly distributed.
- Test 4: 500 users randomly distributed.

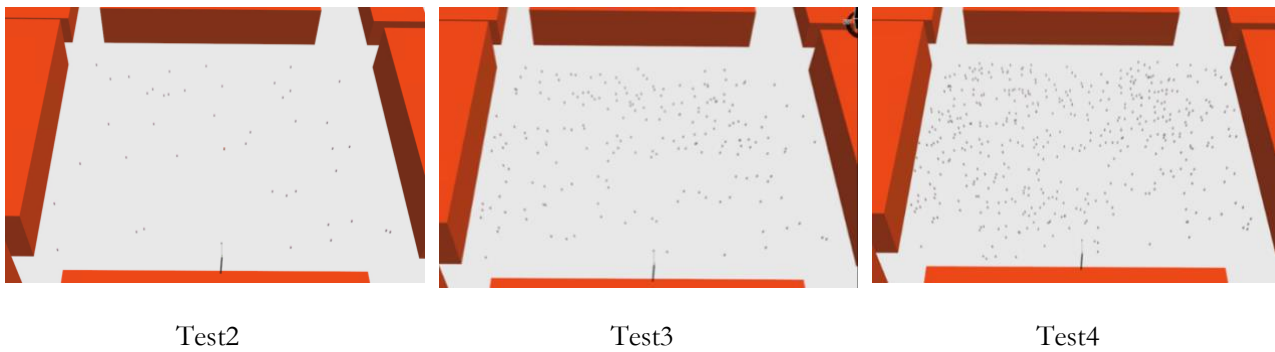


Figure 122: The main plaza with the presence of users.

Each user has been represented as a parallelepiped 50x50x200 cm size, while the electromagnetic characteristics used to simulate the body are listed in Section 6.1.2.2.

The following approach has been used for simulations in reduced MMGS:

- Reduced MMGS scenario consist of an area 1160m x 552 m wide; the coverage has been computed over the central tile of the scenario.
- 1 MaMIMO antennas has been considered, located as shown in Figure 121
 - Antenna 1: position $x=595\text{m}$, $y=266\text{m}$, $z=33\text{m}$, pan 0 degs, mechanical tilt 0 degs
- The antenna is equipped with a single layer, made of 13 beams, 2 degs tilted and covers 120 degs in azimuth: a subset of a beam set generated by UNICAS.

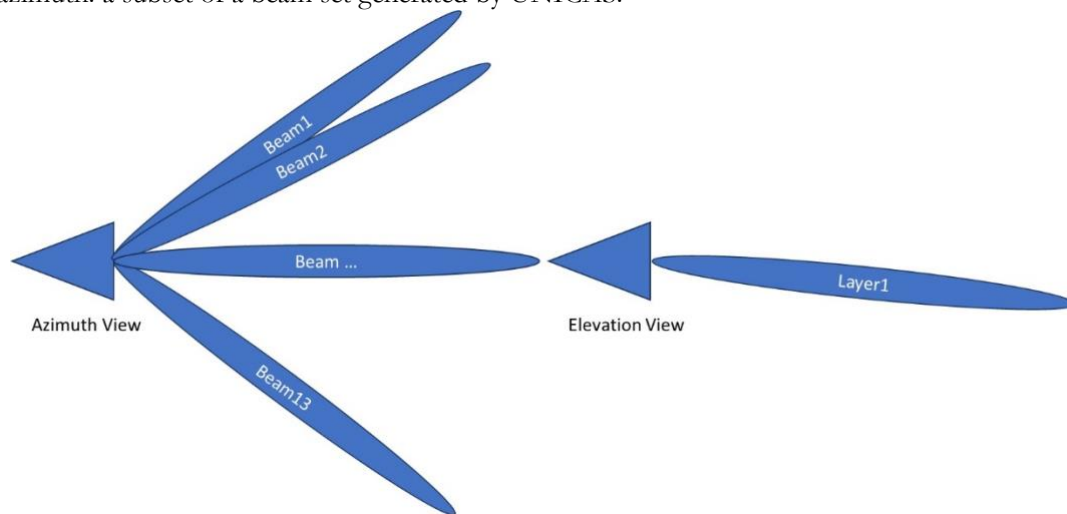


Figure 123: Schematic representation of the beams each MaMIMO antenna can generate in azimuth and elevation

- Point of Controls are randomly distributed over the central part of the scenario, near the users.
- The General parameters
 - Frequency: 26000.0 MHz
 - Power: 1 W
 - Receiver Gain: 0 dBi
 - Receiver Noise Figure: 3.0 dB
- Simulations have been performed fixed in time, reporting:
 - The maximum field in the point
 - No time average is considered
 - Field is evaluated considering a power reduction factor $F_{\text{TDC}} = 0.75$ due to the TDD scheme.

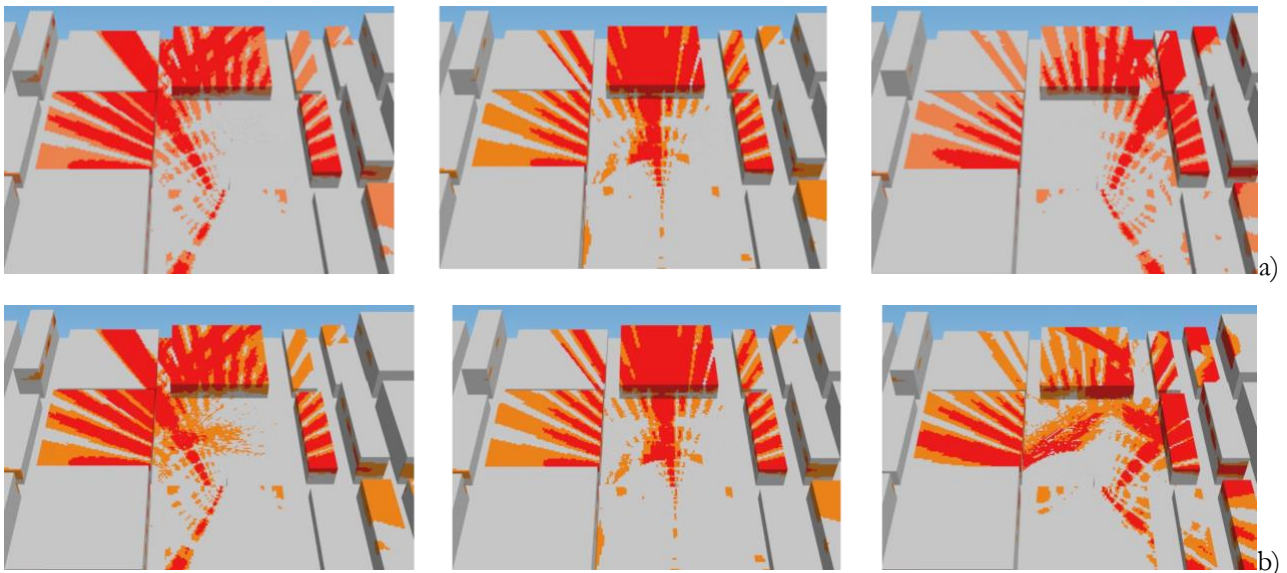


Figure 124: field distribution in the scenario generated by 3 different beams. a) Test1, b) Test4

Table 28: Maximum Electric field computed in PoC, the term F_{TDC} included in the field value.

	Test 1	Test 2	Test 3	Test 4
	[mV/m]	[mV/m]	[mV/m]	[mV/m]
	Leftmost beam			
PoC1	40.3	33.9	8.8	7.7
PoC2	5.2	4.1	7.5	11.1
PoC3	80.4	80.4	4.5	3.8
	Central beam			
PoC4	9.2	8.8	2.9	8.8
PoC5	19.1	18.6	2.3	4.7
PoC6	93.3	92.3	24.0	92.3
	Rightmost beam			
PoC7	18.8	18.8	40.7	18.8
PoC8	47.9	47.9	79.4	47.9
PoC9	6.8	5.4	5.8	6.0

Table 28 shows that the field at position is influenced by the presence of the users, and in general, depending on the positions of the users in the context of the test, the field is lower as much as the density of persons increases; that is due to the blockage effect in mmW bands at the location.

10 Conclusion

The scope of deliverable 3.4 is the description of the simulation parameters as agreed during the preparation phase of the activities planned in task T3.4. As a result of this activity, the following data have been shared on the NextGEM repository available to task T3.4 partners:

- The data file containing the Modified Madrid Grid Scenario for an area of 3 by 3 km to be used for outdoor simulations in FR1, as described in section 6.1.2.
- The data file for three Modified Madrid Grid tiles to be used for outdoor simulation in FR2, as described in section 6.1.5.
- For partners intending to perform indoor simulations, the data file of the scenario is described in section 6.1.4, on request.
- The electromagnetic properties of the materials present in the scenario, section 6.1.2.2,
- The complete set of radiation pattern data files for the description of the MaMIMO antenna, both for FR1 and FR2, as described in section 6.2.4.
- The data file containing the load profile for each transmitter, as described in section 8.1.2.
- The SINR-Throughput function, as defined in [11].
- The data usage per UE as defined in [10].

Additions and/or changes to settings as defined in this deliverable can be applied by each task T3.4 partner depending on the evolution of the simulations. This deliverable contains all the information required to perform a full set of simulations for computing exposure levels in a large-scale area scenario. .

In Deliverable D3.8, the results of the simulations performed on the basis of the parametrizations described are included.

Three reference antennas have been synthesized, and their Grid-of-Beam patterns have been calculated and made available in the repository for all the project partners in T3.4; in particular, the antenna synthesized are:

- An FR1 antenna designed for outdoor applications;
- An FR2 antenna designed for outdoor applications;
- An FR1 antenna designed for indoor applications.

The three antennas are vendor-independent but provide a performance level and radiation characteristics compatible with the antennas currently sold by manufacturers, allowing to perform reasonable simulations.

A detailed analysis has been performed in FR1 by considering:

- different types of scenarios:
 - a simulated town
 - a real town
 - an indoor office scenario
 - an indoor industrial hangar scenario
- different types of services, depending on the scenario, accounting for users' activity
- users' distribution depends on the scenario. In the case of outdoor simulations, the number of users depends on the activity of the cell and the typology of service required.
- time evolution of the exposure considering different load profiles in the time
- exposure extrapolation to 2026 and 2029.
- A detailed analysis of the exposure has been performed, as required by exposure guidelines.

Simulations have been performed in FR2 in a reduced MMGS, considering different densities of persons present in the scenario.

In general, exposure levels in real conditions of exposure in scenarios with base stations located over the roofs are low in the observed points with respect to the relevant exposure limits expressed in terms of Reference Levels.

Whole-body exposure should not be compared nor confused with local exposure since the different limits and dosimetry quantities used to evaluate the exposure are indicated by international guidelines.

Employing the ray launching simulator developed at UCAS, we have been able to assess the variations in terms of radiated power by the antennas with different beamforming schemes employed. In particular, we have shown that:

- the use of grid-of-beam can produce a satisfactory bound for the evaluation of power level: since a strong line-of-sight component is almost always present, the use of eigen-beamforming schemes has a minor impact on the possible reduction of radiated power that in most cases is below 1dB;
- the use of eigen-beamforming schemes seems to be much more appealing for the increase of multiplexing capability of systems, i.e., the ability for the base station antenna to activate quality contemporary connection with multiple users at the time;
- since the eigen-beamforming is not limited to specific directions and is able to focus a beam in any direction, the difference in field levels may be significant in points close to the antenna, which are not covered by the Grid-of-Beams (GoB).

In general, the simulations performed with the ray launching tool at UCAS confirm the validity of the results evaluated by other partners for GoB, also as a preliminary estimation when sophisticated beamforming technologies are used.

References

- [1] <https://www.icnirp.org/cms/upload/publications/ICNIRPrfgdl2020.pdf>
- [2] <https://www.icnirp.org/cms/upload/publications/ICNIRPemfgdl.pdf>
- [3] NGMN Alliance, Basta, Recommendation on base station active antenna system standards v3.0
- [4] IEC TR 62669:2019, Case studies supporting IEC 62232 - Determination of RF field strength, power density and SAR in the vicinity of radiocommunication base stations for the purpose of evaluating human exposure
- [5] IEC 62232:2023, Determination of RF field strength, power density and SAR in the vicinity of base stations for the purpose of evaluating human exposure
- [6] ICT-317669-METIS/D6.1
- [7] Recommendation ITU-R P.2040-3 (08/2023), «Effects of building materials and structures on radio wave propagation above about 100 MHz».
- [8] https://www.3gpp.org/ftp/Specs/archive/38_series/38.101-1/38101-1-i10.zip
- [9] NGMN Alliance, Basta, Recommendation on base station active antenna system standards v2.0
- [10] Ericsson Mobility Report, November 2023 (<https://www.ericsson.com/en/reports-and-papers/mobility-report/reports/november-2023> - accessed on December 17, 2023)
- [11] Ofcom, “Award of the 700 MHz and 3.6-3.8 GHz spectrum bands Further consultation on modelling and technical matters”, 15 may 2020, <https://www.ofcom.org.uk/consultations-and-statements/category-1/award-700mhz-3.6-3.8ghz-spectrum#:~:text=We%20are%20preparing%20to%20award,latest%20generation%20of%20mobile%20services> – accessed on December 18, 2023
- [12] Pinchera, Daniele, Marco Donald Migliore, and Fulvio Schettino. "A Simple Closed-Form Model for the Pattern of Commercial Massive MIMO Antennas." 2024 IEEE International Symposium on Antennas and Propagation and INC/USNC-URSI Radio Science Meeting (AP-S/INC-USNC-URSI). IEEE, 2024.
- [13] H. Yang and T. L. Marzetta, “Quantized array processing gain in largescale antenna systems”, Bell Labs technical report, September 2011
- [14] www.5gstore.com
- [15] <https://itis.swiss/virtual-population/tissue-properties/database/dielectric-properties>